USGS
science for a changing world

Prepared in cooperation with the Lewis and Clark, Lower Elkhorn, Lower Loup, Lower Platte North, Lower Niobrara, Middle Niobrara, Upper Elkhorn, and Upper Loup Natural Resources Districts

Simulation of Groundwater Flow, 1895–2010, and Effects of Additional Groundwater Withdrawals on Future Stream Base Flow in the Elkhorn and Loup River Basins, Central Nebraska—Phase Three

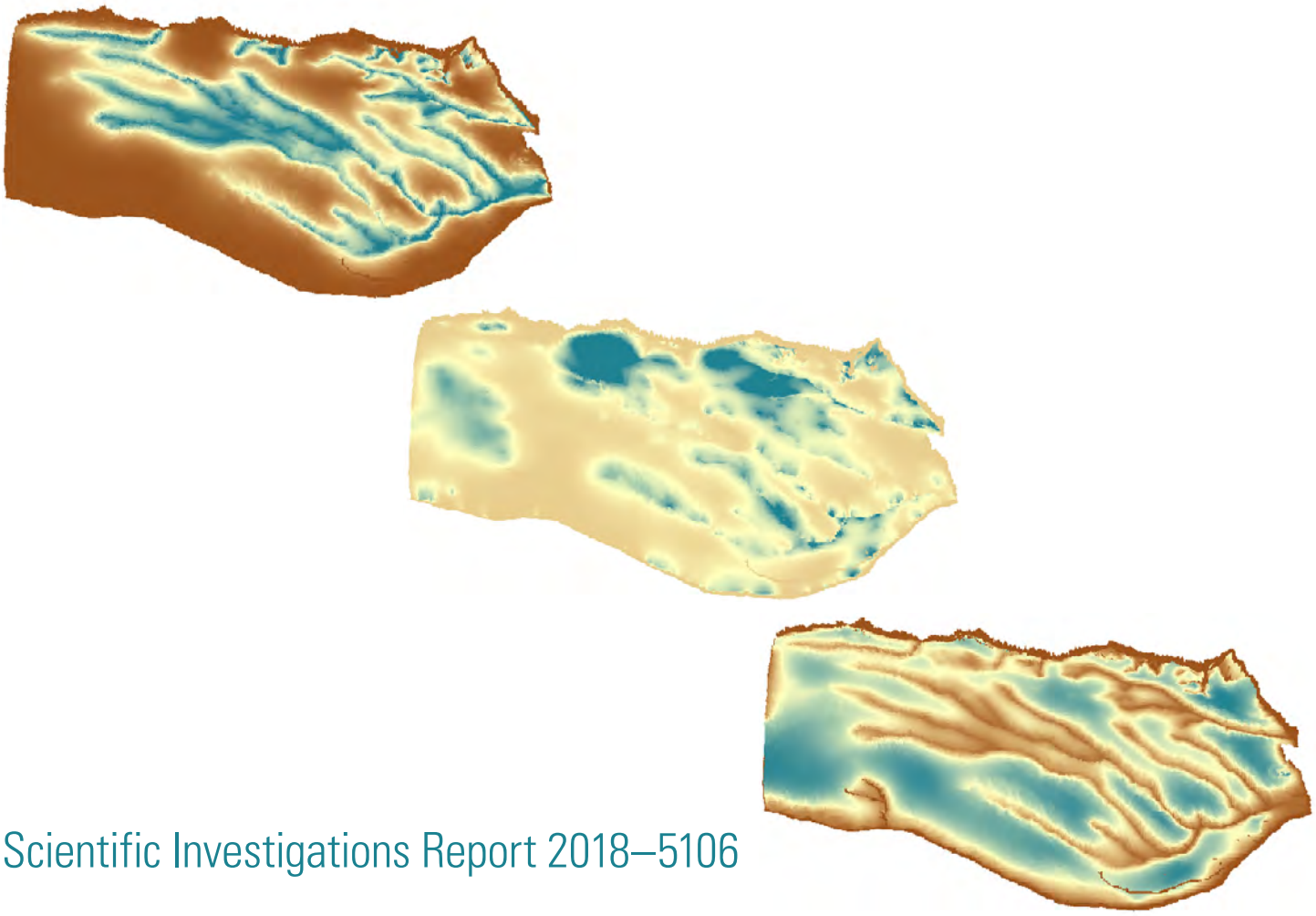

Scientific Investigations Report 2018–5106

U.S. Department of the Interior
U.S. Geological Survey

Cover. Graphics showing simulated future depletions (2011–60) in areas of the Elkhorn-Loup Basins, from top left to lower right: streamflow, evapotranspiration, and storage.

Simulation of Groundwater Flow, 1895–2010, and Effects of Additional Groundwater Withdrawals on Future Stream Base Flow in the Elkhorn and Loup River Basins, Central Nebraska—Phase Three

By Amanda T. Flynn and Jennifer S. Stanton

Prepared in cooperation with the Lewis and Clark, Lower Elkhorn, Lower Loup, Lower Platte North, Lower Niobrara, Middle Niobrara, Upper Elkhorn, and Upper Loup Natural Resources Districts

Scientific Investigations Report 2018–5106

U.S. Department of the Interior
U.S. Geological Survey

U.S. Department of the Interior
RYAN K. ZINKE, Secretary

U.S. Geological Survey
James F. Reilly II, Director

U.S. Geological Survey, Reston, Virginia: 2018

For more information on the USGS—the Federal source for science about the Earth, its natural and living resources, natural hazards, and the environment—visit https://www.usgs.gov or call 1–888–ASK–USGS.

For an overview of USGS information products, including maps, imagery, and publications, visit https://store.usgs.gov.

Suggested citation:
Flynn, A.T., and Stanton, J.S., 2018, Simulation of groundwater flow, 1895–2010, and effects of additional groundwater withdrawals on future stream base flow in the Elkhorn and Loup River Basins, central Nebraska—Phase three: U.S. Geological Survey Scientific Investigations Report 2018–5106, 65 p., https://doi.org/10.3133/sir20185106.

ISSN 2328-0328 (online)

Contents

Figures

Appendix Figures

Tables

Conversion Factors

U.S. customary units to International System of Units

Multiply	By	To obtain
	Length	
inch (in.)	2.54	centimeter (cm)
foot (ft)	0.3048	meter (m)
mile (mi)	1.609	kilometer (km)
	Area	
acre	0.004047	square kilometer (km^2)
square foot (ft^2)	0.09290	square meter (m^2)
square mile (mi^2)	2.590	square kilometer (km^2)
	Volume	
gallon (gal)	3.785	liter (L)
million gallons (Mgal)	3,785	cubic meter (m^3)
cubic foot (ft^3)	0.02832	cubic meter (m^3)
acre-foot (acre-ft)	1,233	cubic meter (m^3)
acre-foot (acre-ft)	0.001233	cubic hectometer (hm^3)
	Flow rate	
acre-foot per year (acre-ft/yr)	1,233	cubic meter per year (m^3/yr)
acre-foot per year (acre-ft/yr)	0.001233	cubic hectometer per year (hm^3/yr)
cubic foot per second (ft^3/s)	0.02832	cubic meter per second (m^3/s)
gallon per minute (gal/min)	0.06309	liter per second (L/s)
gallon per day (gal/d)	0.003785	cubic meter per day (m^3/d)
million gallons per day (Mgal/d)	0.04381	cubic meter per second (m^3/s)
inch per year (in/yr)	25.4	millimeter per year (mm/yr)
inch per month (in/month)	2.12	millimeter per month (mm/month)
	Hydraulic conductivity	
foot per day (ft/d)	0.3048	meter per day (m/d)
	Hydraulic gradient	
foot per mile (ft/mi)	0.1894	meter per kilometer (m/km)

Temperature in degrees Celsius (°C) may be converted to degrees Fahrenheit (°F) as follows:

$$°F = (1.8 \times °C) + 32.$$

Temperature in degrees Fahrenheit (°F) may be converted to degrees Celsius (°C) as follows:

$$°C = (°F - 32) / 1.8.$$

Datum

Vertical coordinate information is referenced to the North American Vertical Datum of 1988 (NAVD 88).

Horizontal coordinate information is referenced to the North American Datum of 1983 (NAD 83).

Altitude, as used in this report, refers to distance above the vertical datum.

Abbreviations

AWC	available-water capacity
BFI	base-flow index
DEM	digital elevation model
ELM	Elkhorn-Loup Model
EVT	Evapotranspiration [package]
GHB	General Head Boundary [package]
GIS	geographic information system
K_h	horizontal hydraulic conductivity
K_v	vertical hydraulic conductivity
LOWESS	Local weighted regression
MODFLOW	modular three-dimensional finite-difference groundwater-flow model software
MODFLOW-NWT	modular three-dimensional finite-difference groundwater-flow model with Newton-Rhapson solver
MODFLOW-2005	modular three-dimensional finite-difference groundwater-flow model software released in 2005
MNW2	Multi-Node Well [program]
NRCS	Natural Resources Conservation Service
NRD	Natural Resources District
PEST	parameter estimation suite of software
RCH	Recharge [package]
SFR2	Streamflow Routing [package used in MODFLOW simulations]
SFR	Streamflow Routing mapping tool
SWB	Soil-Water Balance [model]
UPW	Upstream Weighting [package]
USGS	U.S. Geological Survey
WEL	Well [package]

Acknowledgments

The authors thank the members of the Elkhorn-Loup Model (ELM) technical committee for providing personal knowledge about the ELM study area, assistance with data-collection efforts, and guidance during simulation development.

The authors also thank Steve Westenbroek of the U.S. Geological Survey Wisconsin Water Science Center for providing support for the Soil-Water Balance model. This study was made possible by support provided by the Nebraska Natural Resources Commission and the ELM Natural Resources Districts.

Simulation of Groundwater Flow, 1895–2010, and Effects of Additional Groundwater Withdrawals on Future Stream Base Flow in the Elkhorn and Loup River Basins, Central Nebraska—Phase Three

By Amanda T. Flynn and Jennifer S. Stanton

Abstract

The U.S. Geological Survey, in cooperation with the Lewis and Clark, Lower Elkhorn, Lower Loup, Lower Platte North, Lower Niobrara, Middle Niobrara, Upper Elkhorn, and the Upper Loup Natural Resources Districts, designed a study to refine the spatial and temporal discretization of a previously modeled area. This updated study focused on a 30,000-square-mile area of the High Plains aquifer and constructed regional groundwater-flow models to evaluate the effects of groundwater withdrawal on stream base flow in the Elkhorn and Loup River Basins, Nebraska. The model was calibrated to match groundwater-level and base-flow data from the stream-aquifer system from pre-1940 through 2010 (including predevelopment [pre-1895], early development [1895–1940], and historical development [1940 through 2010] conditions) using an automated parameter-estimation method. The calibrated model then was used to simulate hypothetical development conditions (2011 through 2060). Predicted changes to stream base flow based on simulated changes to groundwater withdrawal will aid in developing strategies for management of hydrologically connected water supplies.

Additional wells were simulated throughout the model domain and pumped for 50 years to assess the effect of wells on aquifer depletions, including stream base flow. The percentage of withdrawal for each well after 50 years, which was compensated by aquifer reductions to stream base flow, storage, or evapotranspiration, was computed and mapped. These depletions are influenced by aquifer properties, time, and distance from the well. Stream base-flow depletion results showed that the closer the added well was to a stream, the greatest the effect on the stream base flow. Areas of stream base-flow depletion percentages greater than 80 percent were generally within 1 mile (mi) from the stream. The distance increased to 6 mi near the confluence of the Dismal and Middle Loup Rivers, and the North Loup and Calamus Rivers. The percentage of stream base-flow depletion decreased as the distance from the stream increased. Areas more than 10 mi from the stream generally had a stream base-flow depletion of 10 percent or less. Evapotranspiration depletion was largest in areas closest to streams, specifically in the Elkhorn River watershed. It was also larger in areas of interdunal wetlands within the Sand Hills. Evapotranspiration depletion was negligible in areas greater than 5 mi from a stream, with the exception of interdunal areas in Cherry, Grant, and Arthur Counties. The storage depletion percentage increased as the distance from a stream increased. Storage depletion was largest in areas between streams. Areas experiencing the smallest amount of storage depletion were adjacent to streams. Calibrated model outputs and streamflow depletion analysis are publicly available online.

Accuracy of the simulations is affected by input data limitations, system simplifications, assumptions, and resources available at the time of the simulation construction and calibration. Most of the important limitations relate either to data used as simulation inputs or to data used to estimate simulation inputs. Development of the regional simulations focused on generalized hydrogeologic characteristics within the study area and did not attempt to describe variations important to local-scale conditions. These simulations are most appropriate for analyzing groundwater-management scenarios for large areas and during long periods and are not suitable for analysis of small areas or short periods.

Introduction

Hydrologically connected groundwater and surface water of central Nebraska provide a vital resource for irrigation, recreation, hydropower production, aquatic life, rural drinking-water wells, and large municipal water systems. Water-resource managers would like to understand the current (2018) and future availability of groundwater, the effect of anthropogenic stresses on the availability and quality of groundwater, and the interaction of groundwater and surface water in the Elkhorn and Loup River Basins.

In 2006, the U.S. Geological Survey (USGS), the Nebraska Department of Natural Resources; the University of Nebraska's Conservation and Survey Division; and the Lewis and Clark, Lower Elkhorn, Lower Loup, Lower Niobrara, Lower Platte North, Middle Niobrara, Upper Elkhorn, and Upper Loup Natural Resources Districts (NRDs, collectively referred to hereinafter as "ELM NRDs") agreed to cooperatively study the water resources of these basins to develop the Elkhorn-Loup Model (ELM) (fig. 1).

The first part of that study, hereinafter referred to as "phase one," was a first step toward understanding long-term average stream-aquifer system conditions and developing strategies for managing hydrologically connected groundwater and surface-water resources in the study area (Peterson and others, 2008). Phase one mainly focused on using preexisting data to develop a regional groundwater-flow model that simulated the effects of groundwater withdrawal from 1940 to 2005 on stream base flow in the Elkhorn and Loup River Basins. The phase one report details the conceptual model and further hydrogeologic and study area information (Peterson and others, 2008).

The second part of that study, hereinafter referred to as "phase two," updated the groundwater-flow model with newly collected data and supporting analyses completed in 2007–08, improved model calibration methods, and incorporated additional approaches for analyzing the effects of groundwater withdrawal for irrigation (Stanton and others, 2010). The newly collected data included revisions to the base-of-aquifer map using test-hole drilling and surface and borehole geophysics (McGuire and Peterson, 2009), synoptic base-flow measurements along stream reaches (Peterson and Strauch, 2007), a runoff-recharge watershed model to estimate long-term patterns of recharge (Strauch and Linard, 2009), and geophysical mapping of resistivity patterns in canals (Teeple and others, 2009). Automated parameter-estimation techniques were used to improve calibration. Other enhancements to the model included refining the grid discretization using time-variable recharge from precipitation, time-variable base-flow estimates, improved estimates of groundwater withdrawals for irrigation, and refined delineation of active evapotranspiration grid cells.

Phase Three Study

A third phase of the study, by the USGS in cooperation with Lewis and Clark, Lower Elkhorn, Lower Loup, Lower Platte North, Lower Niobrara, Middle Niobrara, Upper Elkhorn, and Upper Loup NRDs, was implemented to (1) investigate the sensitivity of the phase two model to a recently developed Soil-Water Balance (SWB) method for estimating aquifer recharge (Stanton and others, 2012); (2) improve understanding of aquifer properties and aquifer base elevations by drilling additional test holes and supplementing traditional test-hole drilling with borehole and surface geophysical data collection (Hobza and others, 2012; Stanton, 2013); and (3) refine the groundwater-flow model inputs spatially and temporally and use the refined model to predict changes to stream base flow that result from groundwater withdrawal. The phase three model is a linked transient model with multiple stress periods: a predevelopment (pre-1895) and early development (1895–1940) model and a historical development (1940 through 2010) model. A separate future development (2011–60) model was constructed using calibrated geophysical properties and water-level outputs from the 1940–2010 model.

Previous models covering the area, including Peterson and others (2008 and 2016) and Stanton and others (2010), were single-layer models. In phase three, the model was refined and divided into two layers. Well logs from both the Nebraska Department of Natural Resources (2012) and the University of Nebraska Testhole Database (University of Nebraska, 2017) were studied to determine the contact between the Plio-Pleistocene and Tertiary sediments. This boundary became the bottom of layer 1 in the phase three model (Stanton, 2013). The well logs analyzed in determining the base then were used to estimate hydraulic conductivity and specific yield in the model layers. This process, also used in Peterson and others (2016), is described in the "Aquifer Properties" section.

Purpose and Scope

The purpose of this report is to present the refined phase three groundwater-flow models for the Elkhorn and Loup River Basins of central Nebraska (fig. 1), to describe the construction and calibration of the simulations for the 1895–1940 and 1940–2010 periods, and to develop a future model for the 2011–60 period to determine the effects of groundwater withdrawal. Effects of groundwater withdrawal by additional hypothetical wells were evaluated using the refined model to simulate the spatial distribution of the percentage of pumped water that causes base-flow, evapotranspiration, and storage depletion at the end of a 50-year period (2011–60).

Study Area Description

The ELM study area covers about 30,000 square miles (mi^2) and extends from the Niobrara River in the north to the Platte River in the south (fig. 1). The western boundary roughly coincides with the western boundaries of the Upper Loup NRD, the Middle Niobrara NRD, and the Twin Platte NRD, and the eastern boundary roughly coincides with the approximate location of the westernmost extent of glacial till in eastern Nebraska (Conservation and Survey Division, University of Nebraska-Lincoln, 2005a). Quaternary-age loess and fine-grained sand; Quaternary-age alluvial silt, sand, and gravel; and Tertiary-age silt, sand, and gravel of the Ogallala Group (Condra and Reed, 1943) constitute the principal hydrogeologic units of the High Plains aquifer in the study area.

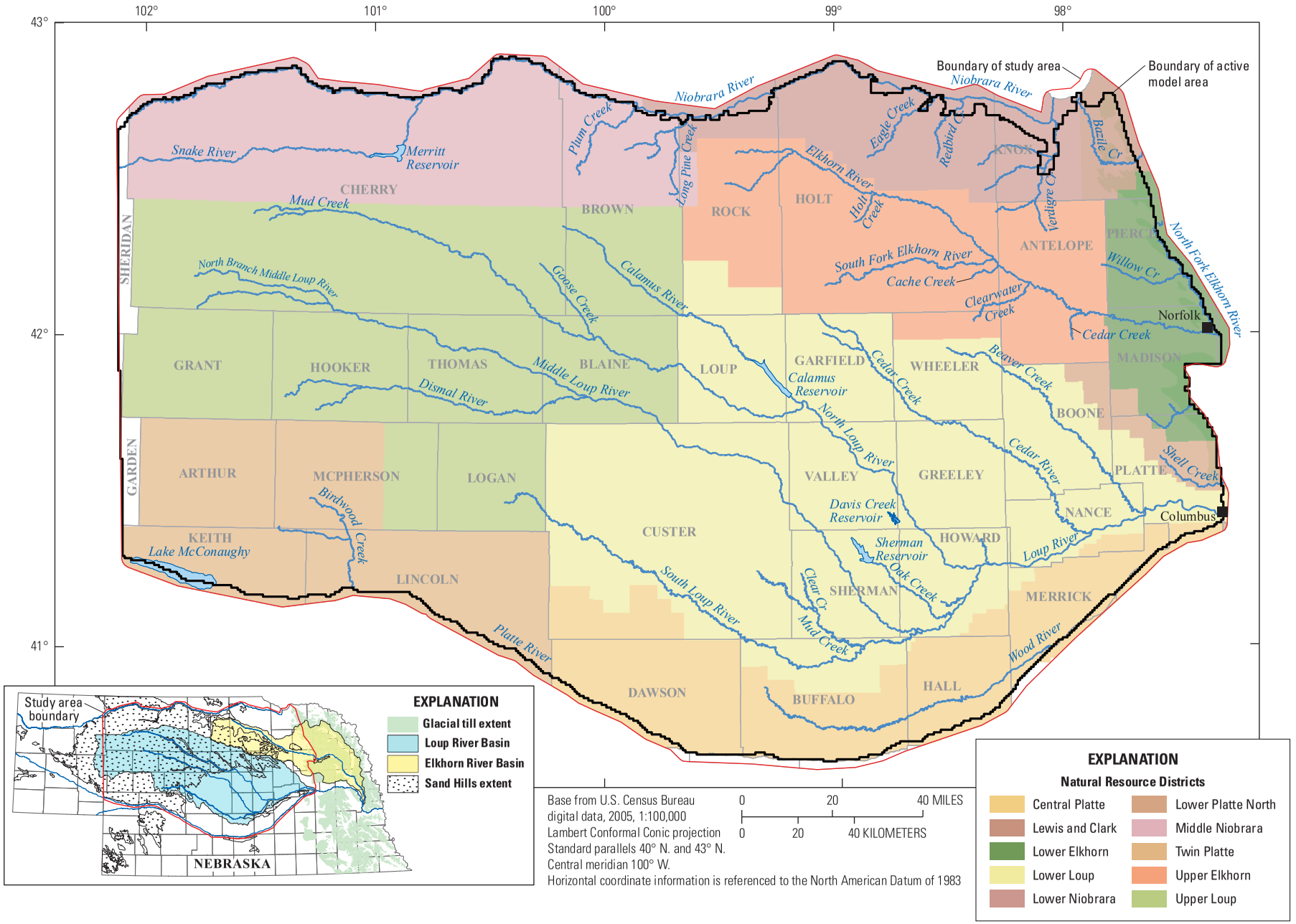

Figure 1. Location of the Elkhorn-Loup Model study area, extent of glacial till (Conservation and Survey Division, University of Nebraska-Lincoln, 2005a), and extent of the Sand Hills (Conservation and Survey Division, University of Nebraska-Lincoln, 2005b) within the State of Nebraska, and the major river basins (Watermolen, 2005), Natural Resources Districts (Nebraska Department of Natural Resources, 2002), and counties (Nebraska Department of Natural Resources, 2003) within the study area, Elkhorn and Loup River Basins, Nebraska.

Groundwater in the ELM area generally flows from west to east and has an average water-table slope of about 10 feet per mile (ft/mi) (Conservation and Survey Division, 2003). The water-table gradient tends to be larger in the Sand Hills, averaging 14 ft/mi, and is less in the rest of the area, averaging 8 to 9 ft/mi. Locally, such as near the Niobrara River, water-table gradients can be in excess of 10 ft/mi and range from 20 to 80 ft/mi because groundwater moves from an upper, gently eastward-sloping plateau toward deeply incised valleys of the Niobrara River and its tributaries (Peterson and others, 2008).

Major streams in the area are the Elkhorn River and its tributaries upstream from Norfolk, Nebr., and the Loup River and its tributaries upstream from Columbus, Nebr. (fig. 1). The Elkhorn River flows from west-northwest to east-southeast, draining wet meadows, plains, and marshy plains east of the Sand Hills (Peterson and others, 2008), and larger tributaries include the North Fork of the Elkhorn River. The Loup River Basin includes numerous large tributary streams that originate in or at the boundary of the Sand Hills, such as the Cedar River, Calamus River, Dismal River, Middle Loup River, North Loup River, and the South Loup River. Tributaries to the Loup River flow from northwest to southeast, draining the Sand Hills and dissected loess plains. The Loup River flows either east or east-northeast through the large river valley region shared with the Platte River to the south (Peterson and others, 2008). Additional streams within the model area are the Snake River, which drains into the Niobrara River in the northwest section of the ELM study area, and Birdwood Creek (and tributaries) and Wood River, which are tributaries to the Platte River. All streams originate within the study area, except the Platte and Niobrara Rivers. Detailed information on the climate, land use, water use and management, and hydrogeology is included in Peterson and others (2008).

Conceptual Model

The conceptual model used for the third phase of the study, the "phase three model," is identical to the phase one and two models. The external boundaries of the model consist of zero-flow, fixed water-level, general head, and stream cells (fig. 2). A zero-flow cell is an inactive cell and is assumed to have no groundwater flow into or out of the cell. Zero-flow cells are not shown on figure 2. Fixed water-level cells are cells along the edge of the model that have groundwater levels that do not change (Stanton and others, 2010). General-head cells have an assigned groundwater level throughout the simulation but also contain a conductance term incorporating thickness, area, and hydraulic conductivity of the bed sediments (Harbaugh, 2005). Stream cells simulate groundwater interaction with streams. Stream cells are controlled by physical characteristics of the streambed and the elevations of the stream stage and groundwater level; the amount of streamflow gain or loss is controlled by the magnitude of difference between stream stage and groundwater-level elevations and streambed characteristics (Niswonger and Prudic, 2005). The streambed represents the boundary between the stream and the underlying aquifer sediments (Stanton and others, 2010).

The lateral external boundaries of the simulation consisted of either a stream boundary or zero-flow boundary along the northern boundary, combined zero-flow boundaries or fixed water-level boundaries for the eastern and western boundaries, and a fixed water-level boundary for most of the southern boundary to simulate the Platte River, except at the western end where, for some simulation periods, it is a general-head boundary (fig. 2). The bottom (vertical) boundary of the simulation is a zero-flow boundary representing the base of the water-table aquifer, and the upper vertical boundary is the water table. Areas that previously had been categorized as having no aquifer present or having a very thin aquifer were not included in the simulation (Peterson and others, 2008). Flow directions near these external boundaries were interpreted from a 1995 water-table contour map (Conservation and Survey Division, 2003).

Stream boundaries were used to simulate perennial reaches of most of the streams in the ELM area (Peterson and others, 2008) and can be an inflow and outflow component of the groundwater system. A general-head boundary was used to simulate reservoirs for their operation periods for the 1940–2010 simulation and is usually an inflow component to the groundwater system. General-head boundaries are similar to fixed water-level boundaries, except that the interaction of the boundary with the simulated groundwater system is controlled by a conductance term. Simulated evapotranspiration was used to represent the sum of transpiration of groundwater by plants and evaporation of groundwater near or at land surface. Evapotranspiration is an outflow of the groundwater system. Recharge, defined as the amount of water that infiltrates land surface and moves downward below the root zone and eventually crosses the regional water table, was simulated for the entire surface of the model area as an inflow to the groundwater system. Additional recharge from canal seepage was applied to cells along canal paths. Recharge from canal seepage was first simulated in the pre-1940 period of the model, mimicking the development of surface-water irrigation across the area. Canal operations started in 1895 and continued to expand within the study area until 1992. Lastly, well withdrawals were simulated for irrigation pumping and municipal water use and are an outflow of the groundwater system. These components are discussed in depth in the "Groundwater-Flow Model Construction" section.

Simulation of Groundwater Flow

The phase three model was developed to simulate groundwater flow, groundwater withdrawals, and stream-aquifer interactions for the Elkhorn and Loup River Basins, Nebr. Hydrogeologic data from numerous sources were compiled as spatially referenced data layers within a geographic information system (GIS) and then assigned to the model at

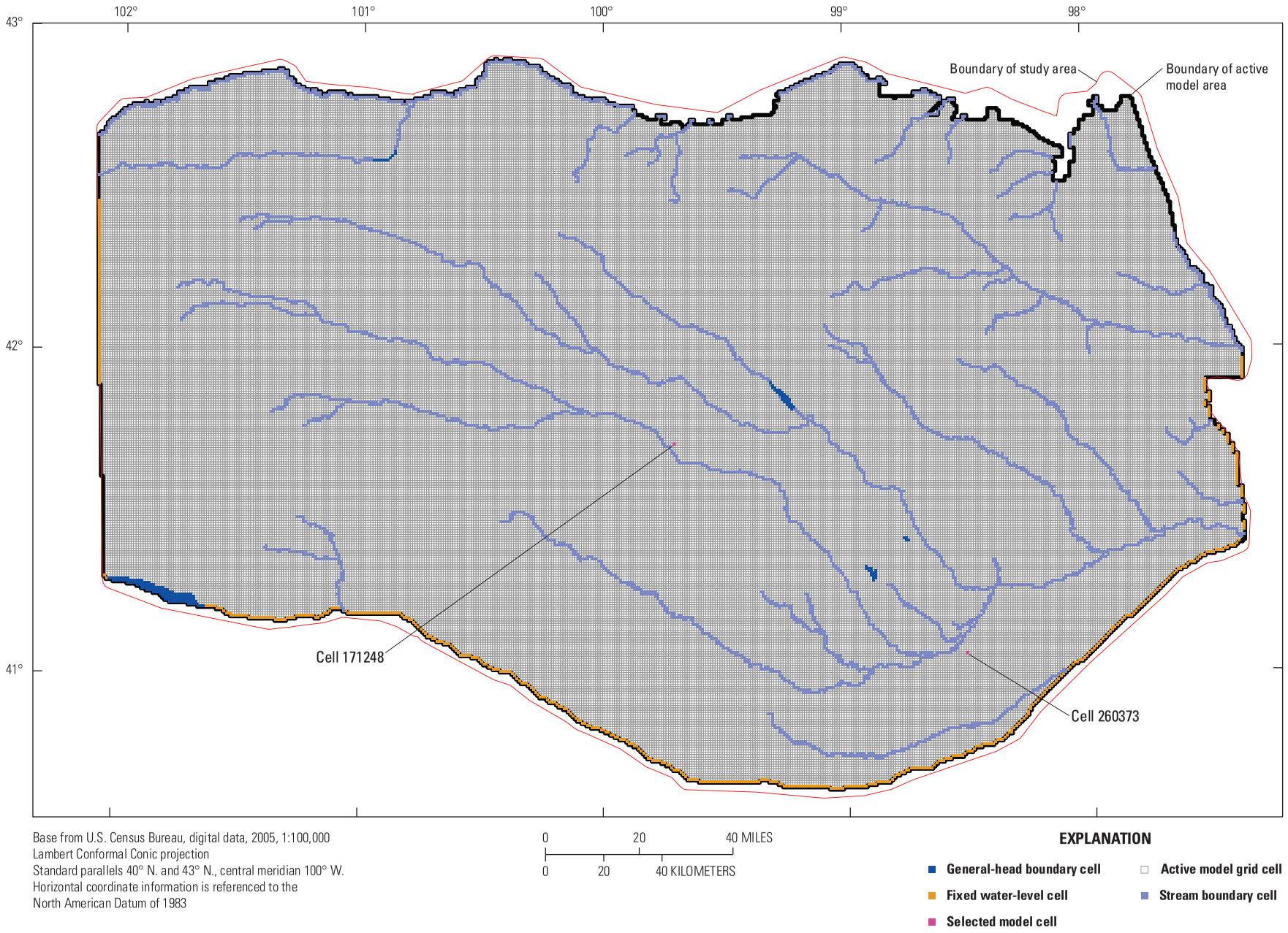

Figure 2. Active model grid and boundary cells of the Elkhorn-Loup Model, phase three, Elkhorn and Loup River Basins, central Nebraska.

discrete intervals in space and time. The model was built using modular three-dimensional finite-difference groundwater-flow model with Newton-Rhapson solver (MODFLOW-NWT) (Niswonger and others, 2011) with assistance from Groundwater Vistas Version 6 software (Environmental Simulations, Inc., 2009).

Selected data groups were adjusted through calibration. The results from the pre-1940 and 1940 to 2010 simulation were compared to measured groundwater levels (U.S. Geological Survey, 2016a; Conservation and Survey Division, University of Nebraska-Lincoln, 2017; Flynn, 2018) and estimated groundwater discharge to streams (hereinafter referred to as "base flow") (Nebraska Department of Natural Resources, 2017).

Groundwater-Flow Model Construction

This study modified the phase two model by adjusting the model grid and stress period discretization. The phase two model was constructed using the 2005 version of modular three-dimensional finite-difference groundwater-flow model software (MODFLOW-2005) (Harbaugh, 2005) and associated model packages; the phase three model was constructed using MODFLOW-NWT (Niswonger and others, 2011) and the associated model packages. This model was simulated using MODFLOW-NWT because it incorporates an improved ability to solve nonlinear unconfined aquifer simulations with wetting and drying of cells by applying the Newton-Rhapson linearization approach to solving the flow equations (Niswonger and others, 2011). The aquifer is thin in some areas and, although cells in the model were not expected to desaturate during the simulation, the use of MODFLOW-NWT prevented removal of desaturated cells from the simulation. This section of the report discusses the construction of the phase three model and differences between the phase three and phase two models. A side-by-side comparison of phase two (Stanton and others, 2010) and phase three model components is shown in table 1.

Spatial and Temporal Discretization

The phase three model was constructed by refining the spatial and temporal discretization of the phase two model. The phase two model was a single layer, consisting of 30,772 active 1-mile (mi) by 1-mi grid cells. The phase three model is two layers of different thicknesses, consisting of 235,643 active half-mile by half-mile grid cells. Phase three incorporated the Scientific Investigations Map generated by Stanton (2013), which defined the base of the Plio-Pleistocene sediments in the study area, creating two model layers. The inclusion of this boundary better represents the aquifer and the connectivity of the layers to one another. The model cells were further divided into half-mile cells to capture discrete changes in the geology and hydrogeologic properties. Additionally, more data, such as water levels, base-flow estimates, and canal seepage estimates, were gathered from data sources to allow the change from annual to monthly stress periods. The boundary conditions of the phase two model are shown in figure 2 of Stanton and others (2010), and the boundary conditions of phase three are shown in figure 2 of this report. A comparison between the two shows the difference in spatial discretization: one cell in the phase two model covers the same area as four cells in the phase three model. Additionally, the fixed water-level cells in the phase three model cover the same spatial length as the those in the phase two model, but the fixed water-level cells in the phase three model only cover one-half of the width because the fixed water-level values were only placed in the cells closest to the active model boundary. The values of the fixed water-level cells in phase three were the same as those used in phase two. The data for the phase three model are available in Flynn and Stanton (2018).

The phase three model was built to simulate the stream-aquifer system from pre-1940 through 2010. As with phase two, the phase three model was split into three models: the pregroundwater development model, which covered pre-1940 (pre-1895, approximated using a 1,000-year transient stress period) and early development (1895–1940, using two transient stress periods modeling the start of surface water canal diversions); historical groundwater development (1940 through 2010, using monthly transient stress periods); and future hypothetical development (2011 through 2060, using a single stress period). The phase two 1940–2005 simulation used annual stress periods for a total of 66 stress periods, whereas the phase three 1940–2010 simulation used monthly stress periods, which resulted in 852 stress periods (table 1).

Aquifer Properties

The aquifer properties horizontal hydraulic conductivity (K_h), specific yield, vertical hydraulic conductivity (K_v), and specific storage were estimated for the model area using the Upstream Weighting (UPW) package, an aquifer property package unique to MODFLOW-NWT (Niswonger and others, 2011). Initially, K_h and specific yield were assigned by analyzing well logs to determine specific properties for each model layer. The well logs (Stanton, 2013) were analyzed using the "GeoParm" macro for lithologic content based on the geologic description and depth interval provided in the well log (Houston and others, 2013). The GeoParm macro was developed for use in the Cooperative Hydrologic Study model in Central Nebraska (Cannia and others, 2006) to read lithologic descriptions by geologists and drillers for depth intervals in wells and to assign a K_h and specific yield to the interval based on keywords in the description. The keywords in the lithologic descriptions were defined and assigned average hydraulic conductivity values by E.C. Reed and R. Piskin, geohydrologists with the University of Nebraska Conservation Survey Division (Cannia and others, 2006). The lithologic sediments for the wells (Stanton, 2013) were assigned to layer 1 or layer 2 based on the base elevation of layer 1 (as defined in Stanton, 2013). The weighted-average K_h and specific yield values for the lithologic intervals in the specified layers then were interpolated

Table 1. Comparison of phase two and phase three model components, Elkhorn and Loup River Basins groundwater-flow model, central Nebraska.

[MODFLOW-2005, modular three-dimensional finite-difference groundwater-flow model software released in 2005; MODFLOW-NWT, modular three-dimensional finite-difference groundwater-flow model with Newton-Rhapson solver; PEST, Parameter estimation; MODFLOW, modular three-dimensional finite-difference groundwater-flow model software; SFR2, streamflow routing package; GIS, geographic information system; SWB, soil-water balance; ET, evapotranspiration]

	Phase two (Appendix 1, Stanton and others, 2010)	Phase three
Software and computer code	Groundwater Vistas, MODFLOW-2005.	Groundwater Vistas, MODFLOW-NWT, PEST.
Grid-cell size	1 mile on one side (total of 30,772 active cells).	Half-mile on each side (total of 235,643 active cells).
Number of layers	One.	Two.
Simulation periods	Pre-1895 (one transient stress period), 1895 to 1940 (two stress periods), 1940 through 2005 (66 annual stress periods), 2006 through 2055 (50 stress periods).	Pre-1895 (one transient stress period), 1895 to 1940 (two stress periods), 1940 through 2010 (852 monthly stress periods), 2011 through 2060 (one stress period).
Streams	All streams in the model represented using MODFLOW Streamflow Routing Package (SFR2).	All streams in the model represented using MODFLOW SFR2.
Streambed characteristics	Streambed conductance was calculated separately for each stream cell using width, length, streambed hydraulic conductivity, and thickness terms. Width was determined from low-flow streamflow measurements. Length was calculated using GIS. Streambed hydraulic conductivity was assigned using aquifer hydraulic conductivity adjacent to simulated stream and then adjusted during the manual trial-and-error calibration to improve simulation results. Thickness was assumed to be 1 foot.	Streambed conductance was calculated separately for each stream cell using width, length, streambed hydraulic conductivity, and thickness terms. Width was determined from low-flow streamflow measurements. Length was calculated using GIS. Streambed hydraulic conductivity was an adjustable parameter based on stream location. Streams were categorized as tributaries or main stems, and further divided into Sand Hills, Elkhorn, Niobrara, or Platte locations. Streambed thickness was assumed to be 1 foot.
Recharge from precipitation	Recharge zones correspond to simplified watershed model regions. Recharge in each zone changed over time.	Calculated in SWB code.
Additional recharge from canal seepage	Calculated from water mass balance when available. Otherwise, estimated as 43 percent of the total water diverted.	Calculated from water mass balance when available. Otherwise, estimated as 43 percent of the total water diverted.
Additional recharge from irrigated cropland	Fixed 1.0 acre-inch/acre per year.	Process simulated by SWB, in inch/month.
Additional recharge on nonirrigated acres	Fixed 0.5 acre-inch/acre per year.	Process simulated by SWB, in inch/month.
Net irrigation pumpage	Initially calculated as the crop irrigation requirement minus growing season effective precipitation and adjusted using measured pumping values for corn. Pumping for all crop types adjusted based on 323 measurements of pumping volume measurements for corn acres in 2005. Most of the measurements were collected from four counties (Antelope, Holt, Nance, and Platte).	Calculated in SWB model.

Table 1. Comparison of phase two and phase three model components, Elkhorn and Loup River Basins groundwater-flow model, central Nebraska.—Continued

[MODFLOW-2005, modular three-dimensional finite-difference groundwater-flow model software released in 2005; MODFLOW-NWT, modular three-dimensional finite-difference groundwater-flow model with Newton-Rhapson solver; PEST, Parameter estimation; MODFLOW, modular three-dimensional finite-difference groundwater-flow model software; SFR2, streamflow routing package; GIS, geographic information system; SWB, soil-water balance; ET, evapotranspiration]

	Phase two (Appendix 1, Stanton and others, 2010)	Phase three
Estimated fraction of measured pumpage (used to adjust crop irrigation requirement) that returns to groundwater	20 percent of pumped water.	Process simulated by SWB.
ET	Active ET cells: determined from wetlands, open water bodies, and riparian land-use categories of the CALMIT 2005 land-cover map (Center for Advanced Land Management Information Technologies, 2007). Maximum ET rate: determined from lake-evaporation contours that were adjusted using measured ET at Odessa, Nebraska. Values were adjusted during manual trial-and-error calibration.	Active ET cells were determined from National Wetland Inventory (U.S. Fish and Wildlife Service, 2017). Maximum ET rate: described in the Northern High Plains modeling report (Peterson and others, 2016). Values not adjusted.
Horizontal hydraulic conductivity	Values assigned to 91 zones. Initial (precalibration) values within zones derived from test-hole data.	Generated initial values from a combination of phase two calibrated values and estimated hydraulic conductivity from test holes and well logs used in Stanton (2013). Initial values assigned to pilot points, which were used as a calibration tool in PEST. Calibrated hydraulic conductivity interpolated from calibrated pilot points.
Bedrock elevation	Adjusted elevations from phase one simulation using data from additional test holes drilled to characterize bedrock elevation in areas with little or no previous information.	Base of layer one is from Stanton (2013). Base of layer 2 is the same as the base of phase two.
Specific yield	Interpolated from points and contours obtained from the Conservation and Survey Division of the University of Nebraska.	Calculated using GeoParm macro, as described in Peterson and others (2016) and Houston and others (2013).
Groundwater levels	506 measurements used for the pre-1940 period.	A total of 1,467 measurements used for the pre-1940 period, and 150,118 measurements used during the 1940 through 2010 period from USGS (2016a), the Conservation and Survey Division, University of Nebraska-Lincoln (2017), and individual NRDs (Flynn, 2018).
Groundwater-level changes	3,259 measurements used from 1940 through 2005.	Not used in the phase three model.
Base flows to streams	Pre-1940 period: 20 base-flow targets were estimated using the annual base-flow targets for the period of record. 1940 through 2005 simulation: base-flow separation (Wahl and Wahl, 2007) provided 1,435 annual base-flow targets at 38 streamgages. Low-flow streamflow measurements provided an additional 165 targets for 2005.	Pre-1940, 38 base-flow targets were estimated using the annual base-flow targets for the first ten years of the record. 1940 through 2010 simulation: base-flow separation (Wahl and Wahl, 2007) provided 22,169 monthly base-flow targets at 51 streamgages. Low-flow streamflow measurements provided an additional 184 targets for 2006 (Peterson and Strauch, 2007).
Calibration method	Manual trial-and-error combined with PEST.	PEST (Doherty, 2016).

between wells using the Gaussian method (variable search radius of 12 points; Johnston and others, 2001). The interpolated values then were extracted to each model cell as the initial K_h or specific yield value. Specific yield ranged from 0.01 to 0.23 and was not adjusted from the initial values estimated by the GeoParm macro. The K_h was assigned to pilot points in layers 1 and 2 and adjusted by parameter estimation, which is discussed in the "Horizontal Hydraulic Conductivity" section. Specific storage was assigned the same value as that used in Stanton and others (2010).

The K_v was defined as a fraction of the K_h and ranged from 5 to 20 feet per day (ft/d). Three areas within layer 1 of the model domain were identified as having thicker lower-conductivity sections; that is, sections of layer 1 contained a thicker confining unit, which has led to isolated localized aquifers within layer 1. Vertical conductivity in these areas was adjusted manually before automated parameter estimation. In the remaining parts of the model domain, K_v was not modified.

Flow Across Lateral Boundaries

Flow across lateral boundaries was simulated as fixed water-level cells in the basic modular three-dimensional finite-difference groundwater-flow model software (MODFLOW) package (Harbaugh, 2005). The fixed water-level cells from phase two were resampled to populate the phase three model grid, as described in the "Spatial and Temporal Discretization" section. The fixed water-level cells were placed in layer 1 of the model. The conductivity between the two layers allowed for the heads in both layers to equilibrate, which negated the need for fixed water levels in layer 2. The zero-flow boundaries in the phase three model were kept the same as those in Stanton and others (2010), with the base of layer 2 being the base of the aquifer and a zero-flow boundary.

Streams

The stream network in the phase three model was the same as used in Stanton and others (2010). The stream shapefile from phase two was intersected with the phase three grid cells. Any cell that overlapped a stream segment by at least 100 feet (ft) was designated as a stream cell. The stream properties width and thickness were retained from the phase two model and used to simulate the streams in the MODFLOW Streamflow Routing (SFR2) (Mehl and Hill, 2010) using the Streamflow Routing (SFR) mapping tool described in Peterson and others (2016). A total of 5,330 cells were designated as stream cells. The Niobrara River was simulated as a stream but was discontinuous through the study area because it intersected areas without an aquifer. The Platte River was simulated as fixed water-level cells, as it was in Stanton and others (2010). Initial streambed conductivity was the same as phase two; however, in phase three, streambed conductivity was designated as a parameter based on the stream system and will be discussed further in the "Calibration" section.

All streams originated within the study area, except the Platte and Niobrara Rivers. Because the Platte River is simulated using fixed water-level cells, an inflow value did not need to be provided for that river. The monthly SFR inflows to the Niobrara River were from monthly base-flow values estimated for the Niobrara River near Gordon (USGS streamgage 06457500; U.S. Geological Survey, 2016b) using the base-flow index (BFI) program (Wahl and Wahl, 2007). Streamflow data for this streamgage were missing for 1940–45 and 1992–2010. For 1940–45, the average base flow for each month was computed for 1946–50, and that specified monthly average was applied as the SFR2 inflows to the Niobrara River for the corresponding months. For 1992–2010, the average base flow for each month was computed for 1982–91, and those averaged base flows were applied as the SFR2 inflows to the Niobrara River for the corresponding months.

Additionally, reservoir releases to streams (U.S. Bureau of Reclamation, 2017) were used as SFR2 inflows to the segment downstream from the reservoir. The average monthly BFI was calculated from the nearest downstream USGS streamgage using the BFI program (Wahl and Wahl, 2007). The BFI percentage was applied to the reservoir outflow to determine the approximate base-flow value of the reservoir outflows. This value then was used as the stream inflow. Before the reservoir was constructed, the SFR2 stream segments were connected to each other through the reservoir area. After the reservoir was constructed, the SFR2 stream segments were separated and the outflow from the upstream segment was routed out of the model.

Recharge

Recharge was separated into two components: recharge from precipitation and recharge from canal seepage. Recharge from precipitation was derived from the SWB code (Westenbroek and others, 2010), which is described in the next section. The SWB code also calculates irrigation seepage applied to agricultural areas, which is included in the recharge from precipitation calculation. Recharge from canal seepage was estimated from canal diversion and delivery records. The process is described in the "Recharge from Canal Seepage" section. The resulting datasets were added together to create a single MODFLOW Recharge (RCH) file (Harbaugh, 2005).

Recharge from Precipitation Using the Soil-Water Balance Code

The amount of water entering the aquifer as recharge was estimated with SWB code that uses a modified Thornthwaite and Mather (1957) soil-water accounting method to track soil water in each grid cell with time (Westenbroek and others, 2010; Stanton and others, 2012). The SWB code uses spatially distributed soil and landscape properties with daily weather data to calculate recharge, runoff, evapotranspiration from the soil profile, crop-water demand, and other components of the soil-water budget. Recharge is represented in the SWB code

by deep percolation and is the amount of water in excess of the storage capacity of the soil. Recharge is calculated for each cell by subtracting the sum of the water outputs from the soil profile (surface runoff and evapotranspiration) from the water inputs to the soil profile (precipitation, snowmelt, irrigation water, and surface runoff from adjacent cells). Soil available-water capacity (AWC), hydrologic soil group (Musgrave, 1955), land use, and direction of surface-water runoff affect the movement of water on and within the soil. The SWB code provides a detailed spatial and temporal distribution of recharge that is based on physical processes.

The SWB code used the same discretization as the phase three groundwater-flow model. Each SWB cell was populated with daily weather data, land cover, soil properties, and direction of surface flow. Daily precipitation and temperature data for 1939 through 2010 were assembled from weather-station data that were within 100 mi of the active model area (National Climatic Data Center, 2012) (fig. 3). Precipitation and temperature values between weather stations were interpolated using an inverse-distance weighted method (with a power of 3 and a variable search radius of 12 points; Johnston and others, 2001).

Hydrologic soil group and AWC were derived from the State Soil Geographic Database (U.S. Department of Agriculture, 2006). Land-use classes included agricultural, urban, forest, and grassland categories (Multi-Resolution Land Characteristics Consortium, 2001). Land-use data were obtained using the same methods that were used for Stanton and others (2010), but data were extended through 2010. Characteristics assigned according to land use, such as the Natural Resources Conservation Service (NRCS) runoff-curve number for estimating the potential for surface runoff, plant-interception values, and root-zone depth, were obtained from the U.S. Department of Agriculture National Engineering Handbook (U.S. Department of Agriculture, 2004; Cronshey and others, 1986; Thornthwaite and Mather, 1957). Surface-water flow directions were derived from digital elevation models (DEMs) (Nebraska Department of Natural Resources, 1998) using the Flow Direction tool in ArcGIS (Esri, 2017).

The SWB code provided estimates of amounts of recharge for different land-use categories such as nonirrigated cropland and irrigated cropland, which were combined with precipitation to form the recharge applied to land surface. Simulated recharge in the phase two model consisted of recharge applied to land surface (from precipitation), additional recharge ascribed to irrigated and nonirrigated agricultural lands, and canal seepage (Stanton and others, 2010).

Recharge from Canal Seepage

The SWB code did not simulate canal seepage (fig. 4, table 2), so that component of recharge was manually calculated and added to the SWB recharge for the phase three model. Multiple agencies provided canal diversion and delivery data and physical canal properties to assist in determining the canal seepage recharge for the model. Canal operation data were collected by the Bureau of Reclamation and provided by NRDs for the Ainsworth and Twin Loups Irrigation Districts (fig. 4, table 2). The Ainsworth Irrigation District operates the Ainsworth Canal; the Twin Loups Irrigation District operates the Mirdan and Fullerton canals (fig. 4, table 2). These data included diversion data from the source, other inputs to the canal, canal waste and losses, and amount delivered to farms or laterals. Individual irrigation districts and NRDs provided diversion and delivery information for the other canals within the model area, including the Farwell, Middle Loup, North Loup, and Sargent canals (fig. 4, table 2). Canals operated along the Platte River, in particular, Gothenburg, Birdwood, Elm Creek, Cozad, Kearney, and Dawson, had diversion data available but no delivery data.

Canal seepage was calculated manually in a multistep process. First, the amount of seepage from each canal system was determined by subtracting canal and lateral losses, canal waste, and delivery from the total amount of water diverted into the canal. Canal systems lacking delivery data used diversion data for canals multiplied by a rate similar to the rates used in the Stanton and others (2010) model. If delivery data were available for only part of the record, an average seepage rate was determined with that delivery data, and that average seepage rate was applied to the rest of the record. This seepage amount was then applied to the corresponding canal model cells. The canal seepage then was added to the SWB recharge to generate a single recharge file for the MODFLOW model.

Phase three model cells were defined as canal seepage cells by intersecting canal shapefile lines with the model grid. A model cell was designated a canal seepage cell if more than 100 ft of the canal intersected the cell. Seepage rates were distributed equally along the canal cells as long as the canal lining was similar along the entire canal. An example of an exception is the Ainsworth Irrigation District, where a part of the canal system is lined with concrete. In this situation, only 10 percent of the calculated seepage was applied to the canal cells where the canal was lined. The remaining 90 percent of seepage was applied to the unlined canal. Canal system information is provided in table 2.

Well Withdrawal

Well withdrawal was estimated for municipal wells and irrigation wells in the phase three model. The municipal well locations, which were described by Stanton and others (2010), were used in the phase three model. The monthly withdrawal amounts for municipal wells for 1940 to 2005, which were assembled by Stanton and others (2010), were used without change in the phase three model, and were used as the monthly withdrawal amounts for 2006–10 in the phase three model. Municipal wells were simulated using the Multi-Node Well (MNW2) package (Konikow and others, 2009) so they could be simulated separately from irrigation wells.

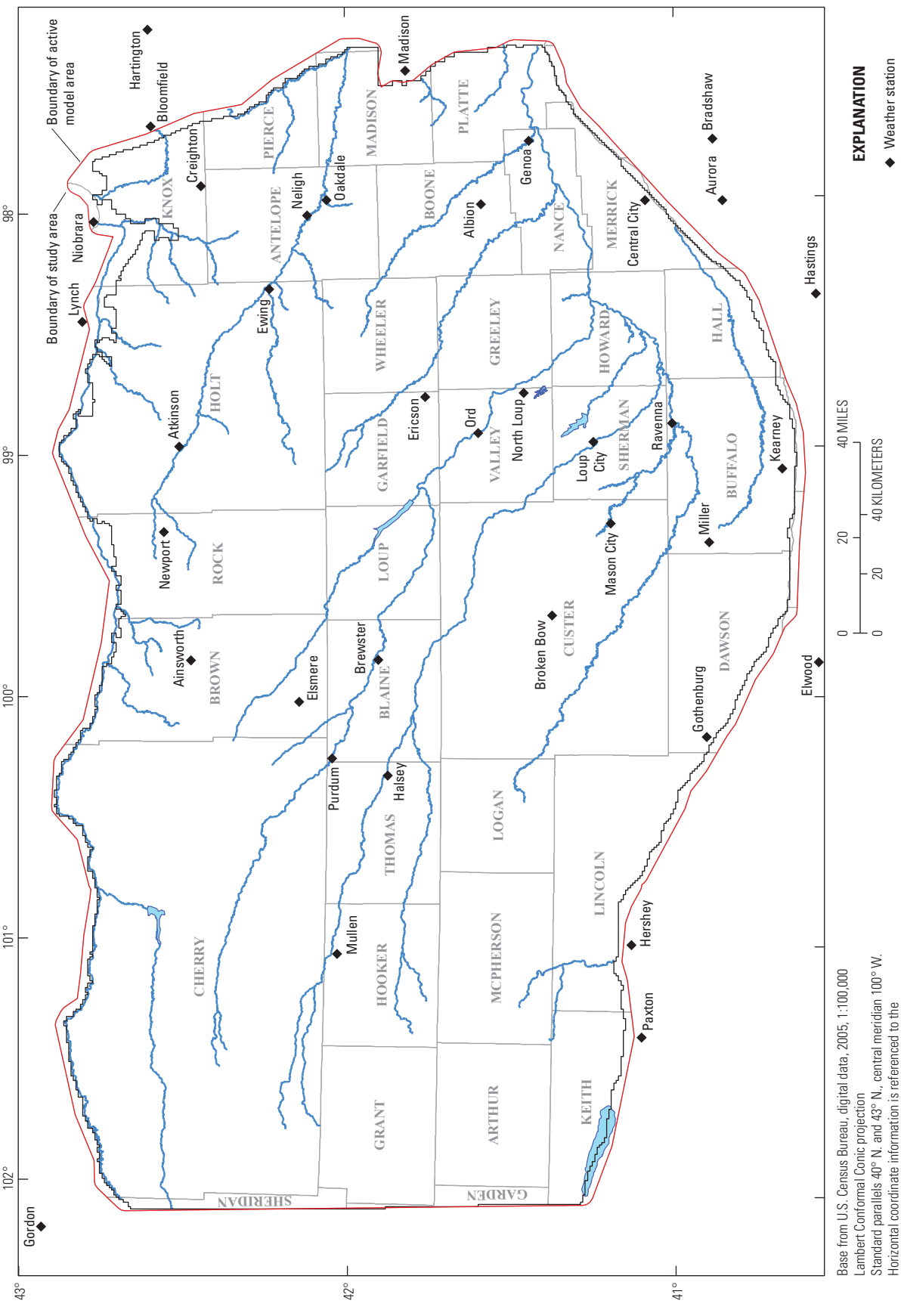

Figure 3. Climate stations used in the Soil-Water Balance code to generate recharge and irrigation pumping used as inputs to the phase three model, 1940–2010, Elkhorn and Loup River Basins, central Nebraska.

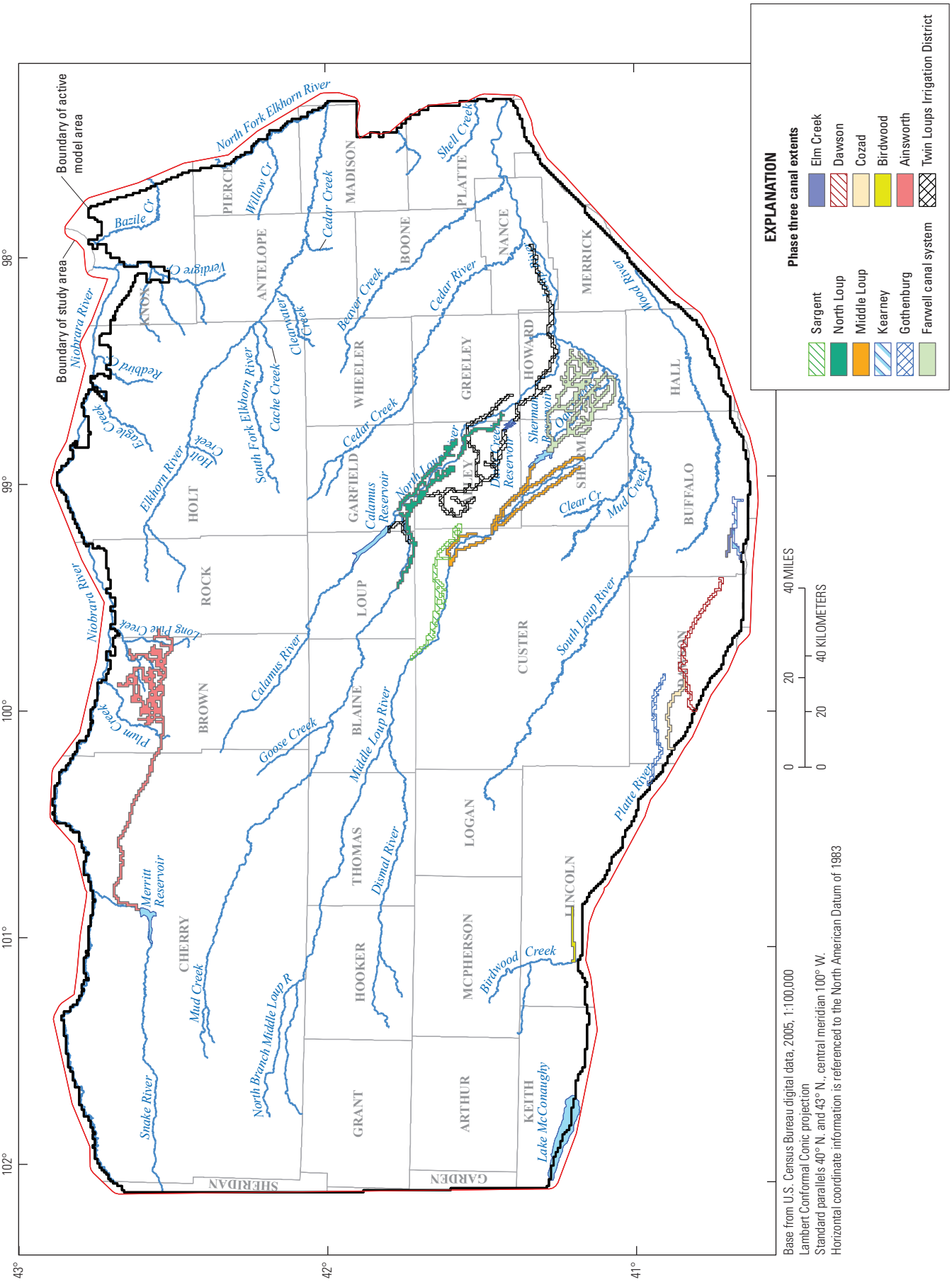

Figure 4. Canals used in the phase three model, shown as extent of canal seepage recharge, 1940–2010, Elkhorn and Loup River Basins, central Nebraska.

Table 2. Canal system information for canals used in phase three, Elkhorn and Loup River Basins groundwater-flow model, central Nebraska.

[No., number]

Irrigation group/ canal system name (fig. 4)	Canal name	Liner description	Canal length, in miles	Total number of model cells used to simulate the canal	Years active	Calibration canal group	Calibration multiplier, in percent	Estimated irrigation season average canal seepage recharge by canal system, 1940–2010, in acre feet per year	Calibrated irrigation season average canal seepage recharge by canal system, 1940–2010, in acre feet per year
Kearney	Kearney	Unlined	18.6	36	1895–present	Platte	14	5,882.4	6,703.2
Gothenburg	Gothenburg	Unlined	29.1	64	1895–present	Platte	14	25,465.6	29,030.4
Dawson	Dawson County	Unlined	41.5	93	1895–present	Platte	14	24,719.4	28,179
Elm Creek	Elm Creek	Unlined	7	15	1929–1962	Platte	14	3,267	3,724.5
Cozad	Cozad	Unlined	21.7	46	1895–present	Platte	14	10,727.2	12,226.8
North Loup	Taylor-Ord Canal	Unlined	59.5	120	1947–present	Loup	−38	8,016	4,974
	Burwell-Sumter Canal	Unlined	32.4	70	1947–present	Loup	−38	4,648	2,880.5
	Ord-North Loup Canal	Unlined	16.9	41	1947–present	Loup	−38	3,767.9	2,336.18
Farwell	Sherman Feeder Canal	Unlined	20.3	47	1963–present	Loup	−38	2,1408.5	13,272.8
	Farwell Main Canal	Unlined	102.6	211	1963–present	Loup	−38	27,057.2*	16,774.08*
	Farwell South Canal	Unlined	65.3	135	1963–present	Loup	−38		
Sargent	Sargent Canal	Unlined	63.7	131	1957–present	Loup	−38	8,842.5	5,478.42
Twin Loups Irrigation District	Mirdan Canal	Lined	18.9	41	1987–present	Loup	−38	188.6	117.26
		Unlined	35.9	78		Loup	−38	4,422.6	2,740.92
	Geranium Canal	Unlined	20.6	44		Loup	−38	13,292.1*	8,244.99*
	Scotia Canal	Unlined	31	66		Loup	−38		
	Fullerton Canal	Unlined	50.4	114		Loup	−38		
	Elba Canal	Unlined	3.4	8		Loup	−38		
	Kent Canal	Lined	3.7	9		Loup	−38		
		Unlined	0.9	2		Loup	−38		

Table 2. Canal system information for canals used in phase three, Elkhorn and Loup River Basins groundwater-flow model, central Nebraska.

[No., number]

Irrigation group/ canal system name (fig. 4)	Canal name	Liner description	Canal length, in miles	Total number of model cells used to simulate the canal	Years active	Calibration canal group	Calibration multiplier, in percent	Estimated irrigation season average canal seepage recharge by canal system, 1940–2010, in acre feet per year	Calibrated irrigation season average canal seepage recharge by canal system, 1940–2010, in acre feet per year
Middle Loup	Middle Loup No. 1 Canal	Unlined	12.3	28	1947–present	Loup	−38	2,346.4	1,454.04
	Middle Loup No. 2 Canal	Unlined	12.2	26	1947–present	Loup	−38	2,490.8	1,544.4
	Middle Loup No. 3 Canal	Unlined	24.9	62	1947–present	Loup	−38	6,553.4	4,062.24
	Middle Loup No. 4 Canal	Unlined	29.6	66	1947–present	Loup	−38	5,860.8	3,631.98
Ainsworth	Ainsworth Canal	Lined	52.5	118	1965–present	Ainsworth	23	436.6	542.8
		Unlined	155.5	301		Ainsworth	23	15,320.9	18,857.65
Birdwood	Birdwood Canal	Unlined	13.7	27	1946–present	Platte	14	2,543.4	2,899.26

*The Farwell canal system and canals downstream from Davis Creek Reservoir in the Twin Loups Irrigation District did not have individual diversion and delivery data for each canal. Seepage was distributed as an equal rate across the canals in the system.

Irrigation well withdrawals were estimated using the SWB code. Well withdrawal determined using this method is an irrigation demand that is specific to crop type and is based on the distribution of irrigated acres and the amount of water available in the soil profile from nonirrigation sources. Crop types are used to assign specific properties related to their water demand throughout the growing season.

Irrigated acres for 1940 through 2002 were defined as irrigated by groundwater or surface water using data from Stanton and others (2010). Irrigated acres for 2003 through 2010 were defined using additional spatial data, such as acreage reports provided by the NRDs, representing surface and groundwater irrigated acres that were developed by the NRDs from 2005 through 2010 (Stanton and others, 2011).

Crop-water use variables used for estimating irrigation demand are unique to each crop or land cover type and include maximum crop coefficient, first-stage crop coefficient, and dates for the start and end of the irrigation season (Westenbroek and others, 2010; Flynn and Stanton, 2018). These variables are used to determine the total water demand of each crop at various growth stages. Then, irrigation-water demand is calculated as the amount of water needed to maintain soil moisture in irrigated areas above the minimum level of soil moisture a crop requires during the growing season. For the purposes of this study, the minimum level of soil moisture in irrigated areas was required to be at least 65 percent of the AWC for the soil (Westenbroek and others, 2010). The volume of water necessary to maintain that minimum level of soil moisture was assumed to be the volume of water entering the soil profile from irrigation and was calculated as equal to the part of crop demand beyond that available from infiltrated precipitation plus stored soil water above the specified minimum level.

Irrigation-water demand was separated into groundwater and surface-water sources for purposes of defining groundwater withdrawal in the phase three model and to, at least partially, account for general differences in the amount of irrigation-return flow associated with gravity- and center-pivot-irrigation methods. Model grid cells in irrigated areas were defined as either 100 percent groundwater (representing center pivot irrigation) or 75 percent surface water and 25 percent groundwater (representing mostly gravity irrigation). Grid cells that were irrigated by groundwater were assigned an irrigation efficiency value of 85 percent, meaning that 85 percent of the irrigation water is available for crop-water demand and the other 15 percent returns to the aquifer as irrigation-return flow. Grid cells that were mostly irrigated with surface water were assigned an irrigation efficiency value of 60 percent. The total groundwater withdrawals for irrigation by county for 2010, in millions of gallons per day, are shown in figure 5. The irrigation-water demand was calculated on a cell-by-cell basis. The water demand for each individual cell was computed by the SWB code for the growing season (May–September) and was output as a single well for the cell. It is worth noting that because the water demand is computed using actual precipitation data and estimated crop coverages, actual pumping values may vary from computed values. This assumption explains why total pumping may differ from rates calculated or recorded outside of this model. This information was compiled into a MODFLOW Well (WEL) package (Niswonger and others, 2011). The model pumping layer designated in the WEL file was determined from registered irrigation wells within the cell (Nebraska Department of Natural Resources, 2012). All registered irrigation wells were assigned a pumping layer based on the screen location of the well. Each model cell was assigned the pumping layer of the closest registered well. When there was more than one registered well in a cell, the cell was assigned the most common pumping layer out of the wells in the cell.

Evapotranspiration from the Saturated Zone

Evapotranspiration from the saturated zone is an important outflow component within this groundwater-flow system (Stanton and others, 2010). Areas of active evapotranspiration vary with climate conditions but are generally around streams, lakes, and wetland areas, where the water table is within a few feet of the land surface (Stanton and others, 2010, 2011). Evapotranspiration from the saturated aquifer was simulated using the EVT (Evapotranspiration) package for MODFLOW (Harbaugh, 2005). This package needs an evapotranspiration rate, surface elevation, and evapotranspiration extinction depth to calculate evapotranspiration from the saturated zone for the model.

Evapotranspiration from the saturated zone was estimated in the phase three model using the methods of Stanton and others (2010). Evapotranspiration cells were selected by overlaying the National Wetlands Inventory (U.S. Fish and Wildlife Service, 2017) and the model cells. If a National Wetlands Inventory cell overlapped a model cell by at least 50 percent, the model cell was coded as an evapotranspiration cell. This process resulted in a difference in evapotranspiration extent compared to the phase two simulation (Stanton and others, 2010, fig. 6). Evapotranspiration rates were determined using the data and approach of Peterson and others (2016), which include an extinction depth of 7 ft and 40 percent of the National Weather Service potential evapotranspiration rate (Stanton and others, 2011) to account for evapotranspiration in the soil horizon (which was accounted for in the SWB code). The evapotranspiration surface was the DEM (Nebraska Department of Natural Resources, 1998). The average yearly rate of evapotranspiration from the saturated zone for assigned evapotranspiration cells ranged from 9 to 16 inches per year (in/yr) (fig. 6).

Reservoir Seepage

A minor component of groundwater inflow within the model area is reservoir seepage (Stanton and others, 2010), which is water that seeps from reservoirs into the groundwater-flow system. In the phase three model, reservoir seepage

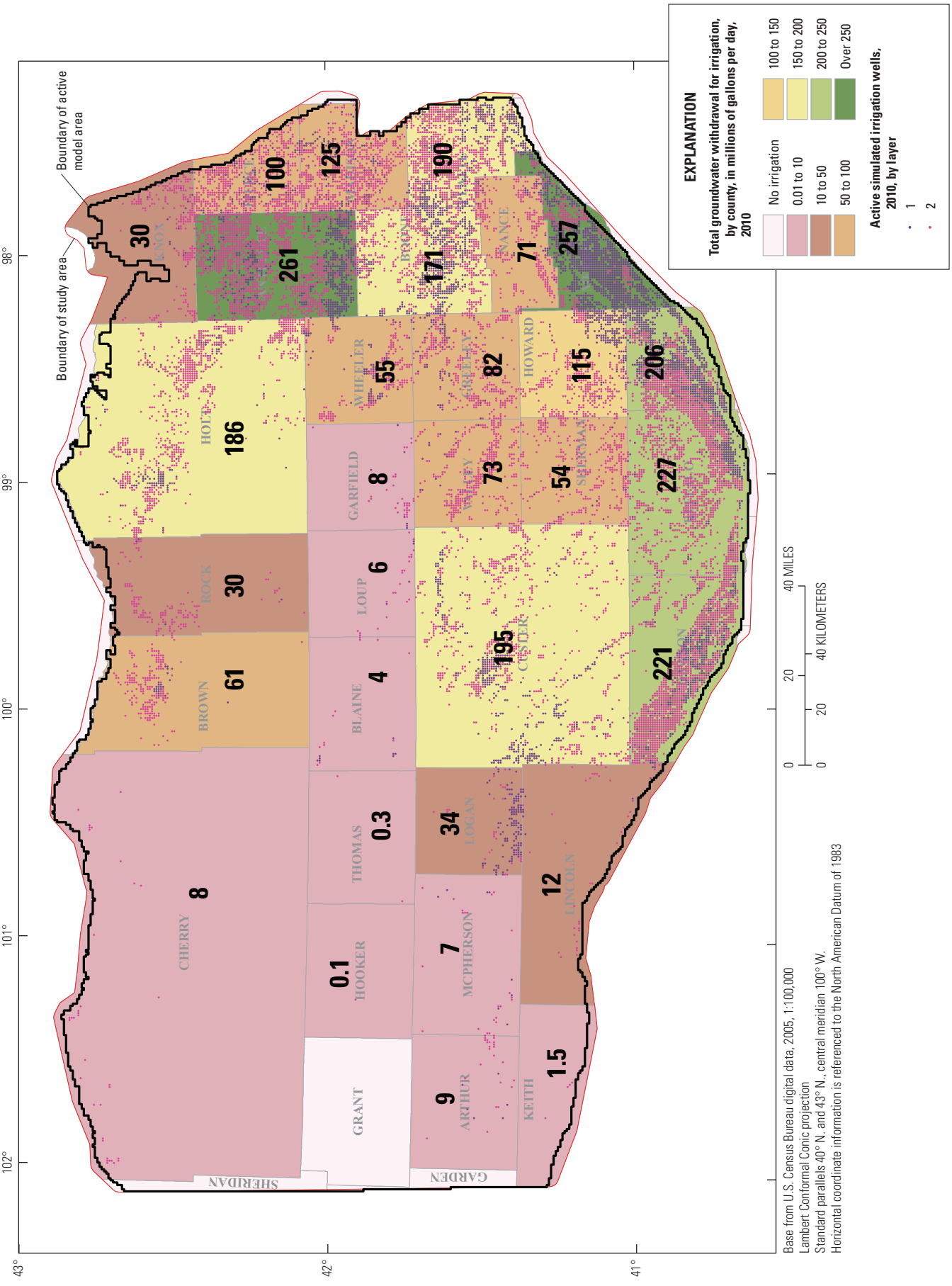

Figure 5. Active simulated irrigation wells by layer and 2010 estimated total groundwater withdrawals for irrigation, by county, Elkhorn and Loup River Basins, central Nebraska.

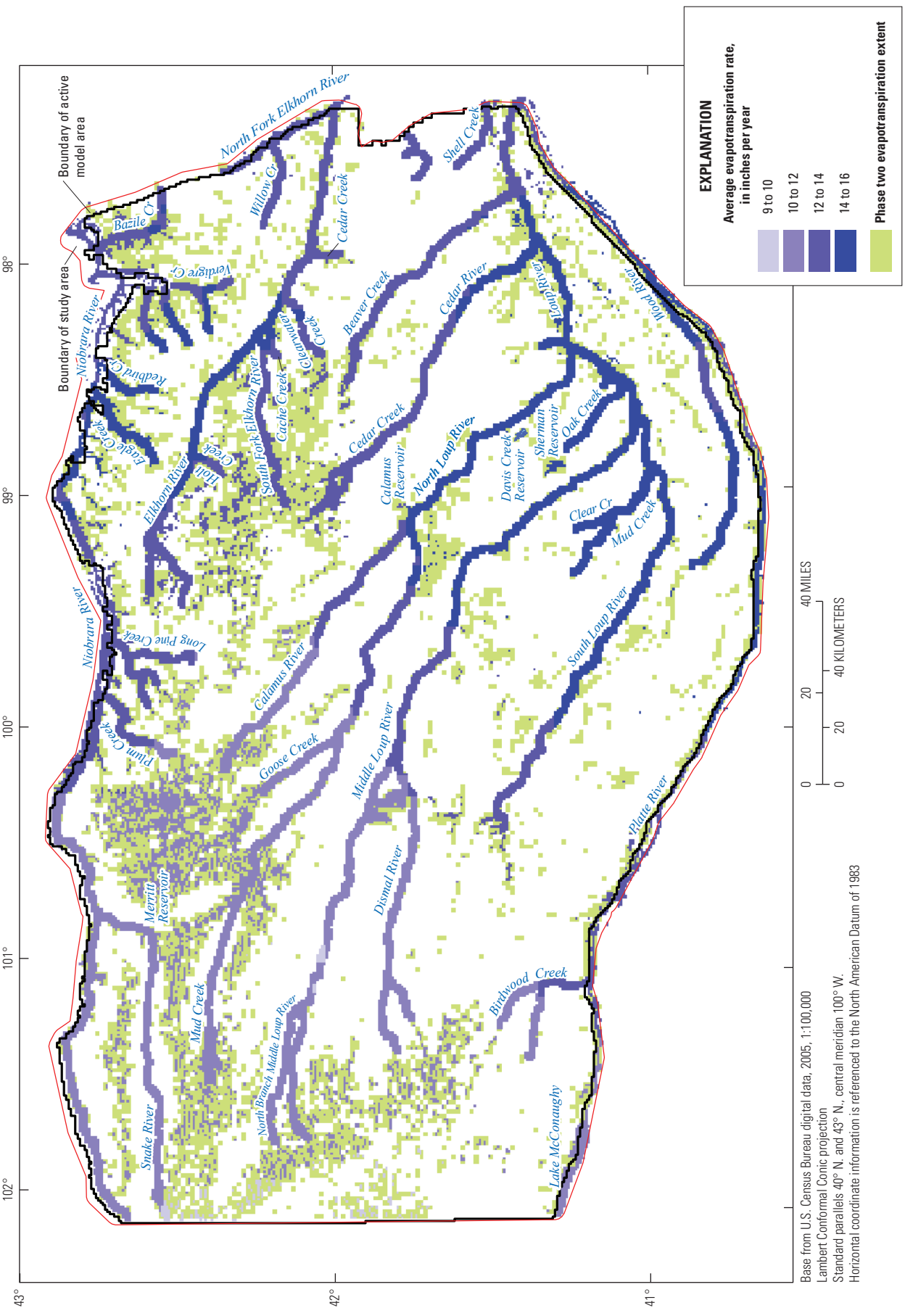

Figure 6. Phase two evapotranspiration extent and the phase three average yearly total evapotranspiration, in inches, from the saturated zone, 1940–2010, Elkhorn and Loup River Basins, central Nebraska.

from Lake McConaughy, Sherman Reservoir, Davis Creek Reservoir, Merritt Reservoir, and Calamus Reservoir (fig. 1) was simulated in layer 1 using the General Head Boundary (GHB) package for MODFLOW (Harbaugh, 2005), whereas only Lake McConaughy was simulated for the phase two model in Stanton and others (2010). The average monthly forebay elevation (the elevation of the water behind the dam) of each reservoir was downloaded from the Reclamation Hydromet web page, which contains reservoir operations data (U.S. Bureau of Reclamation, 2017). The forebay elevation was used as the GHB elevation. Grid cells were assigned as GHB cells for a specific reservoir by overlaying the reservoir area on the grid cells. If a grid cell was more than 50 percent covered by the reservoir area, it was categorized as a GHB cell. The reservoir areas were from Stanton and others (2010) and were overlaid on aerial imagery (Esri, 2018) to verify the extent for the phase three model. The GHB cell conductance ranged from 101 to 202 ft/d per cell when the reservoirs were in operation.

Calibration

The phase three model was calibrated using a parameter estimation suite of software (PEST) (Doherty, 2016). Parameters are specific model inputs that can be adjusted by PEST based on modeled responses to calibration targets. The parameters were adjusted to assist the model in replicating two sets of calibration targets: groundwater levels, in altitude above the North American Vertical Datum of 1988 (NAVD 88), and stream base flows. Both sets of calibration targets were active in the pre-1940 and 1940–2010 simulation periods, resulting in four calibration target groups. The pre-1940 and 1940–2010 period models were calibrated using methods of Peterson and others (2016).

Parameter Groups

Parameters were classified into three parameter groups. The parameter groups in this model were hydraulic conductivity (total of 560 pilot point parameters for layer 1 and layer 2); recharge, both applied to land surface (43 multiplication parameters) and canal seepage (4 multiplication parameters); and streambed conductivity (7 parameters). Each set of parameters was given a calibration range in the PEST control file within which the parameter group could be adjusted to improve the model calibration. The initial and calibrated values are discussed in this section. The recharge parameter discussion has been divided between the two types of recharge: recharge applied to land surface and canal seepage recharge.

Horizontal Hydraulic Conductivity

The K_h was calibrated using the pilot point approach, which is similar to the method used in Peterson and others (2016) and unlike the zone method used by Stanton and others (2010). A pilot point network was developed for each layer of the model. Previous estimates of hydraulic conductivity, apart from those published in the phase one and phase two reports, can also be found in Gutentag and others (1984) and in Houston and others (2013).

Layer 1 contained 292 pilot points for K_h, and layer 2 contained 268 pilot points. At each point, K_h was allowed to adjust from 0 to 500 ft/d and was interpolated between pilot points. The calibrated K_h in layer 1 averaged 57 ft/d and ranged from 11 to 525 ft/d (fig. 7*A*). The calibrated K_h in layer 2 averaged 27 ft/d and ranged from 1 to 306 ft/d (fig. 7*B*). The weighted-average calibrated K_h for both layers was 40 ft/d (fig. 7*C*), which is an increase compared to the phase two model calibrated average K_h of 26 ft/d. The range of K_h for both layers in the phase three model was from 2 to 505 ft/day.

The use of pilot points, smaller grid size, and the additional layer used in the phase three model provided a more detailed interpolation of K_h data than the phase two model, which used 91 K_h zones, a larger grid size, and one layer. This resulted in areas of higher K_h in the calibrated phase three model than the calibrated phase two model. In the calibrated phase three model, K_h is thought to better represent K_h heterogeneity in the study area, as estimated from lithologic descriptions in well logs (Houston and others, 2013).

Recharge Applied to Land Surface

This section focuses on recharge applied to land surface as determined from the SWB code. The recharge value applied to the phase three model includes precipitation and irrigation seepage applied to agricultural areas. The SWB code generated a recharge file for each month from January 1940 to December 2010. These monthly files then were grouped into 5-year nonirrigation season (January, February, March, April, October, November, and December) and irrigation season (May, June, July, August, and September) recharge parameter groups, resulting in a set of 28 parameter groups for PEST calibration. The breakdown of groups into irrigation and nonirrigation seasons allows adjustment of parameters that might vary seasonally. The decision to group recharge into 5-year increments was made to adjust for climatic variations. The PEST software adjusted recharge parameters to a percentage between a 100-percent increase or decrease to improve the model calibration.

The average calibrated recharge from precipitation applied to the simulation during 1940–2010 is shown in figure 8. After calibration, the average adjustment to recharge from the SWB code recharge estimate was an increase of 1.6 percent. The largest increase in recharge (89 percent, average increase of 0.43 in/yr per cell) took place during the 1980–84 irrigation season. This increase coincides with a wet climatic period when rainfall was above average. The largest reduction in recharge (78 percent, average decrease of 0.14 in/yr per cell) took place during the 1965–69 nonirrigation season.

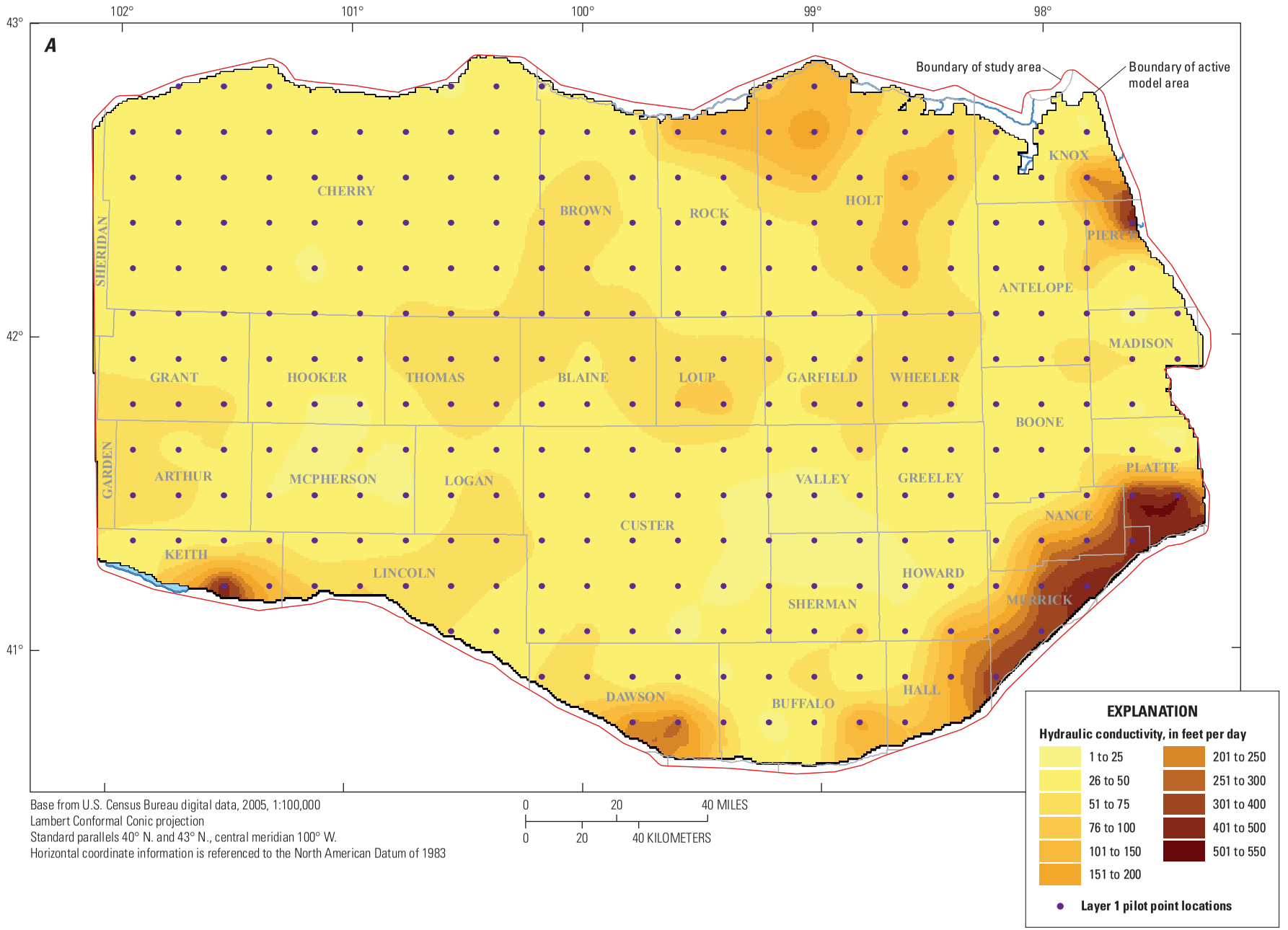

Figure 7. Calibrated horizontal hydraulic conductivity for Elkhorn and Loup River Basins, central Nebraska; *A*, and pilot points for layer 1; *B*, pilot points for layer 2; and *C*, weighted-average calibrated horizontal hydraulic conductivity of layer 1 and layer 2.

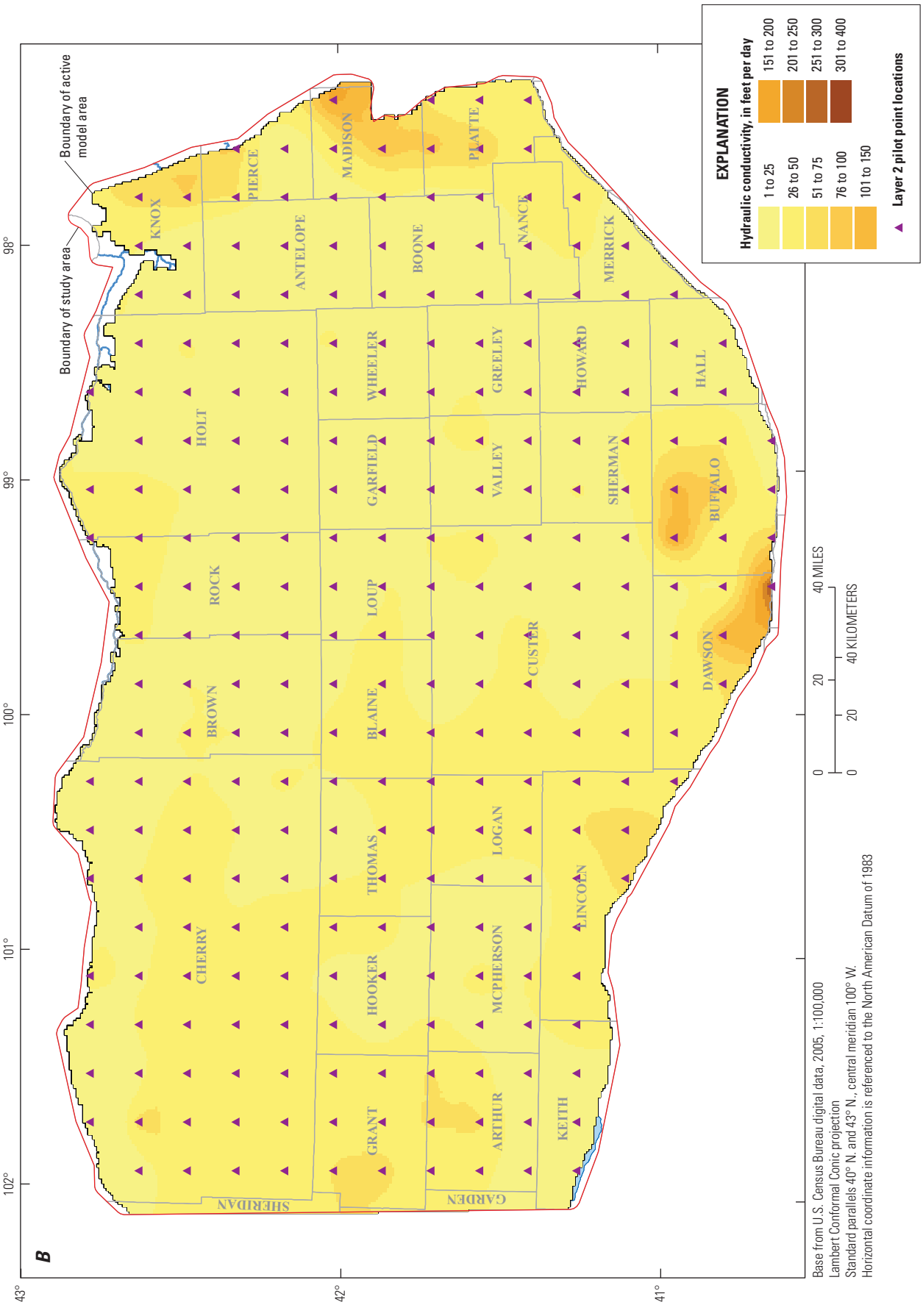

Figure 7. Calibrated horizontal hydraulic conductivity for Elkhorn and Loup River Basins, central Nebraska; *A*, and pilot points for layer 1; *B*, pilot points for layer 2; and *C*, weighted-average calibrated horizontal hydraulic conductivity of layer 1 and layer 2.—Continued

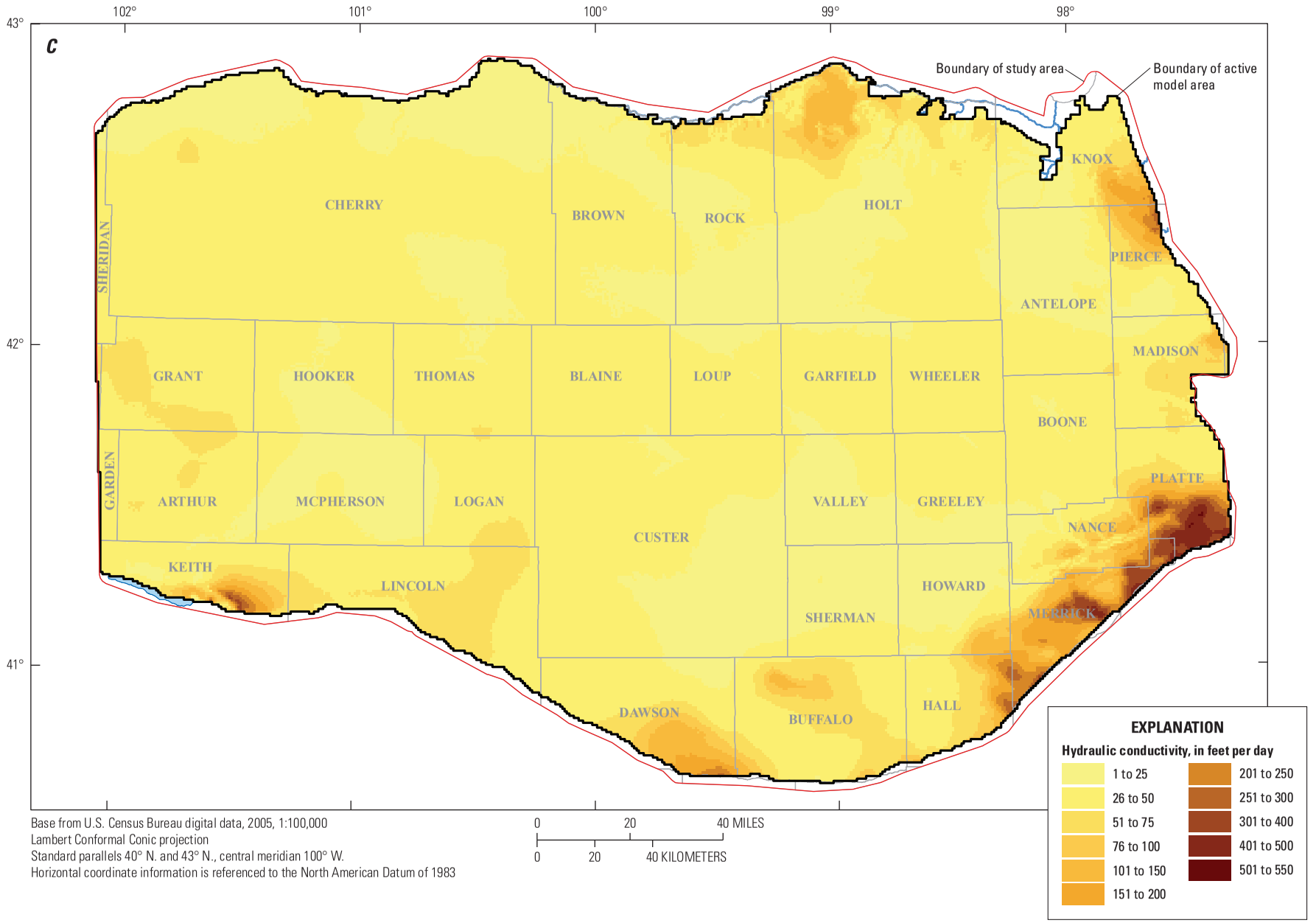

Figure 7. Calibrated horizontal hydraulic conductivity for Elkhorn and Loup River Basins, central Nebraska; *A*, and pilot points for layer 1; *B*, pilot points for layer 2; and *C*, weighted-average calibrated horizontal hydraulic conductivity of layer 1 and layer 2.—Continued

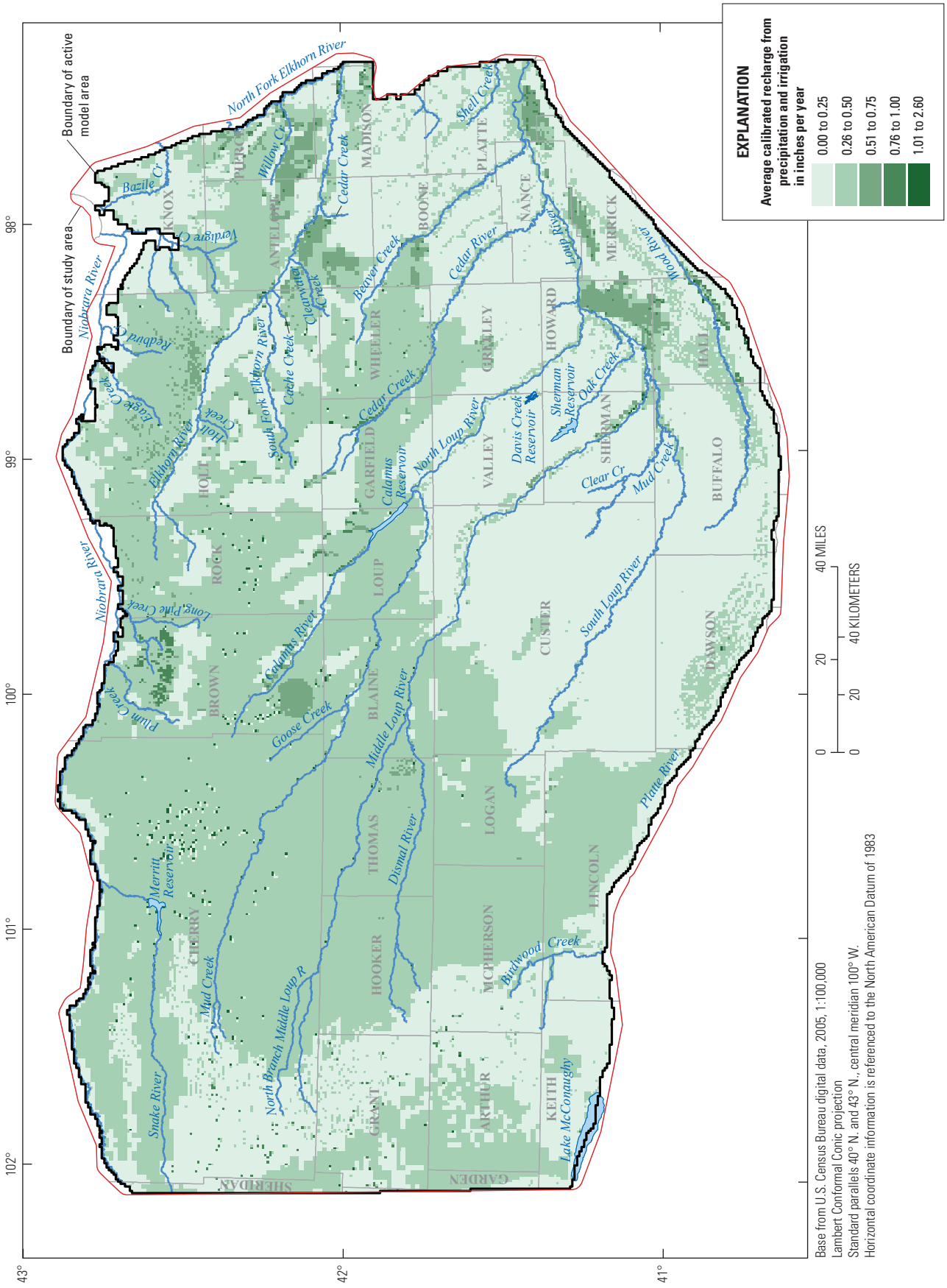

Figure 8. Average calibrated recharge from precipitation and irrigation, 1940–2010, Elkhorn and Loup River Basins, central Nebraska.

Canal Seepage Recharge

Canal seepage is a large component of groundwater inflow into the system (Stanton and others, 2010) in localized areas. The amount of water diverted into the canal systems varied monthly based on surface-water availability. Seepage rates for the model were determined from canal diversion and delivery records, as previously described in the "Recharge" section of this report.

Canal seepage was broken into three parameter groups based on the river system from which the canal received water (fig. 4, table 2). The three canal groups were the Platte System, Loup System, and Ainsworth system (representing the northern canals near the Niobrara River). The canal groups and the active dates of each canal system are shown in table 2.

Canals that were active before 1940 were used as a parameter group for the pre-1940 simulation period of the model. During calibration, the pre-1940 canal group seepage rate was decreased by 48 percent to match the targets. The reduction in seepage recharge was acceptable because of the lack of diversion and delivery data for this period. After calibration, there was a 23 percent increase in seepage recharge from the Ainsworth Canal group, a 38 percent reduction in the Loup Canal group, and a 14 percent increase in the Platte Canal group. These adjustments were considered acceptable for the following reasons: (1) For the Ainsworth Canal group, the estimated canal seepage was divided between lined and unlined canals. Because the date of the lining of the canals was not taken into account in the model, it is possible the canals provided more recharge to the system than what was estimated. (2) For the Loup Canal group, it is possible that the losses estimated from the diversion and delivery records did not all result in canal seepage recharge. Instead, it is possible these losses were gains to other parts of the hydrologic system, such as evaporation or unmeasured return flow to surface water. (3) For the Platte Canal group, the estimated canal seepage recharge was determined from a rate used in a previous modeling report (Stanton and others, 2010). Because no delivery records were available for the Platte Canal group, it is possible the losses to the groundwater system from the canal were greater than estimated. The average canal seepage recharge along each canal system is shown in figure 9.

Streambed Conductivity

Streambed conductivity was divided into seven parameter groups based on location and stream size. Streams first were split into four groups (Niobrara River Basin, Sand Hills, Elkhorn River Basin, and dissected plains) based on location defined by the Nebraska Conservation and Survey Division (Conservation and Survey Division, University of Nebraska-Lincoln, 2005b). The Niobrara, Elkhorn, and dissected plains groups then were split again into the main stem of the river and tributaries (fig. 10). Calibrated streambed-conductivity values ranged from 0.06 ft/d for the dissected plains rivers group to 2.42 ft/d for the Elkhorn River tributaries group. The final streambed conductivity values from Stanton and others (2010), which were manually calibrated, ranged from less than 0.10 ft/d to 6 ft/d, which is comparable to the calibrated phase three values.

Calibration Targets and Results

Measured groundwater levels and estimated stream base flows were used as calibration targets for the phase three model. Weights were assigned to each calibration target following the same approach used in Peterson and others (2016), which was based on an error-based weighting method (Hill and Tiedeman, 2007). Weights were used to adjust for different magnitudes of the different types of measurements and to account for certainty of the observation or estimation of the target. The target weight for water levels was assigned as the inverse of 1.96 (the 95-percent confidence interval) multiplied by the estimated uncertainty associated with the measurement. For water levels in the pre-1940 and 1940–2010 periods, the uncertainty was assumed to be 5 ft. The weight of the estimated base-flow values was the inverse of the average estimated base flow multiplied by 1.96 (in line with the 95-percent confidence interval). Some water-level and base-flow targets were zero weighted. These targets were monitored during calibration but did not affect the calibration results and will be discussed further in the corresponding target sections.

Parameters were subjected to Tikhonov regularization in the parameter estimation process, which prevents overfitting and spurious parameter estimates by imposing a numerical penalty on the objective function for deviations from the initial estimates (Doherty, 2016). The objective function is affected by the number of targets in each group, the residual of each target, and the weight assigned to each target.

In this report, the difference between observed and simulated values for water levels and stream base-flow targets is called a residual. The residual is calculated by subtracting the simulated value from the observed value; therefore, a positive residual means that a simulated water level or stream base-flow value is less than the observed value. A negative residual means the simulated water level or stream base-flow value is greater than the observed value.

Groundwater Levels

Groundwater-level measurements were collected from multiple agencies, including the USGS (2016a); the Conservation and Survey Division, University of Nebraska (2017); and individual NRDs (Flynn, 2018). More than 260,300 water levels were collected at 7,330 wells. Pre-1940 groundwater-level calibration included 1,462 water levels at 1,462 wells. The 1940–2010 groundwater-level calibration used 149,902 water levels at 6,845 wells. Many factors were considered when determining if a water level was an appropriate calibration target. Water levels without a date or only a month and year were not included as calibration targets. Pre-1940 water levels must have been measured from 1930

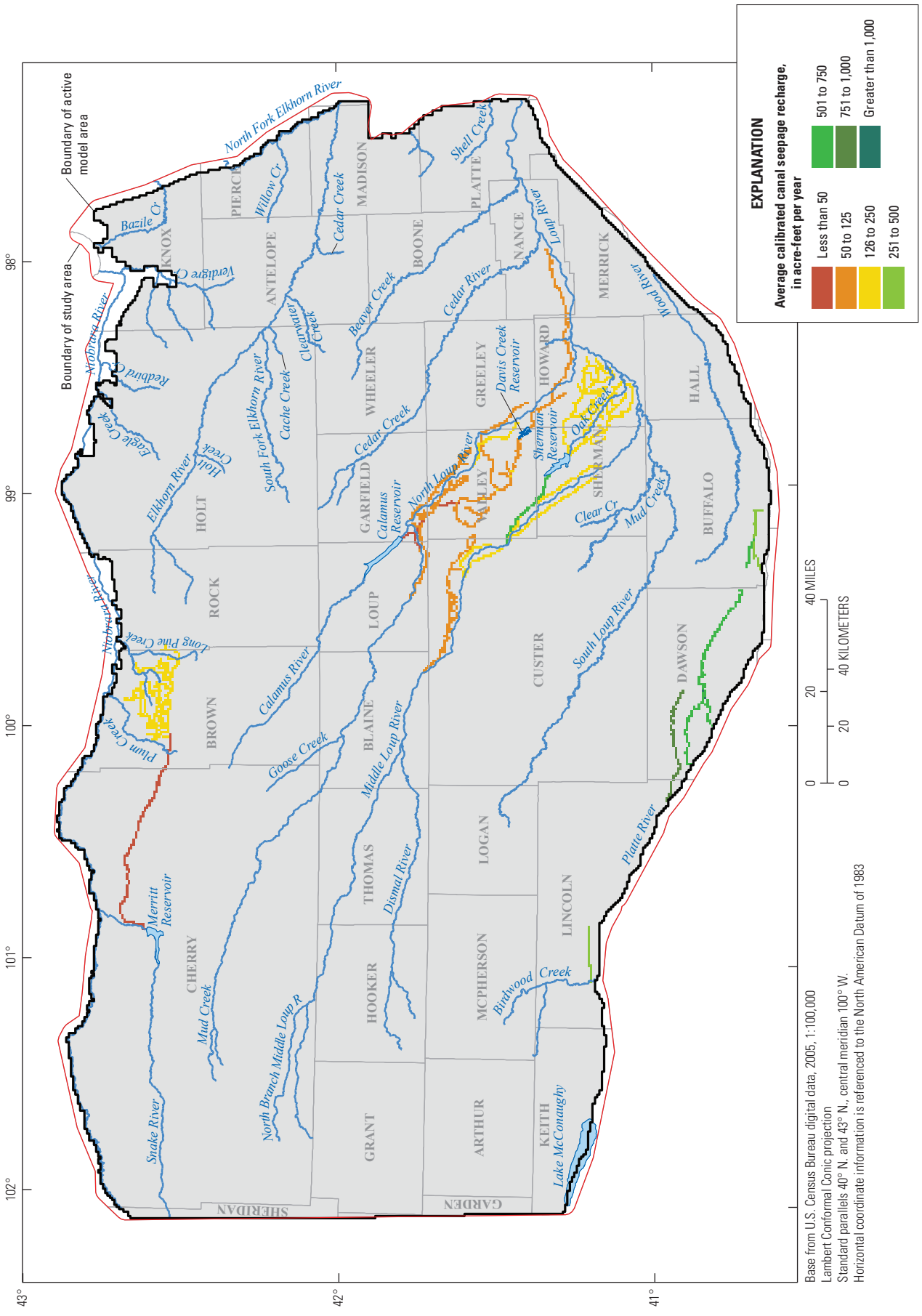

Figure 9. Average calibrated canal seepage recharge values in acre-feet per year, 1940–2010, Elkhorn and Loup River Basins, central Nebraska.

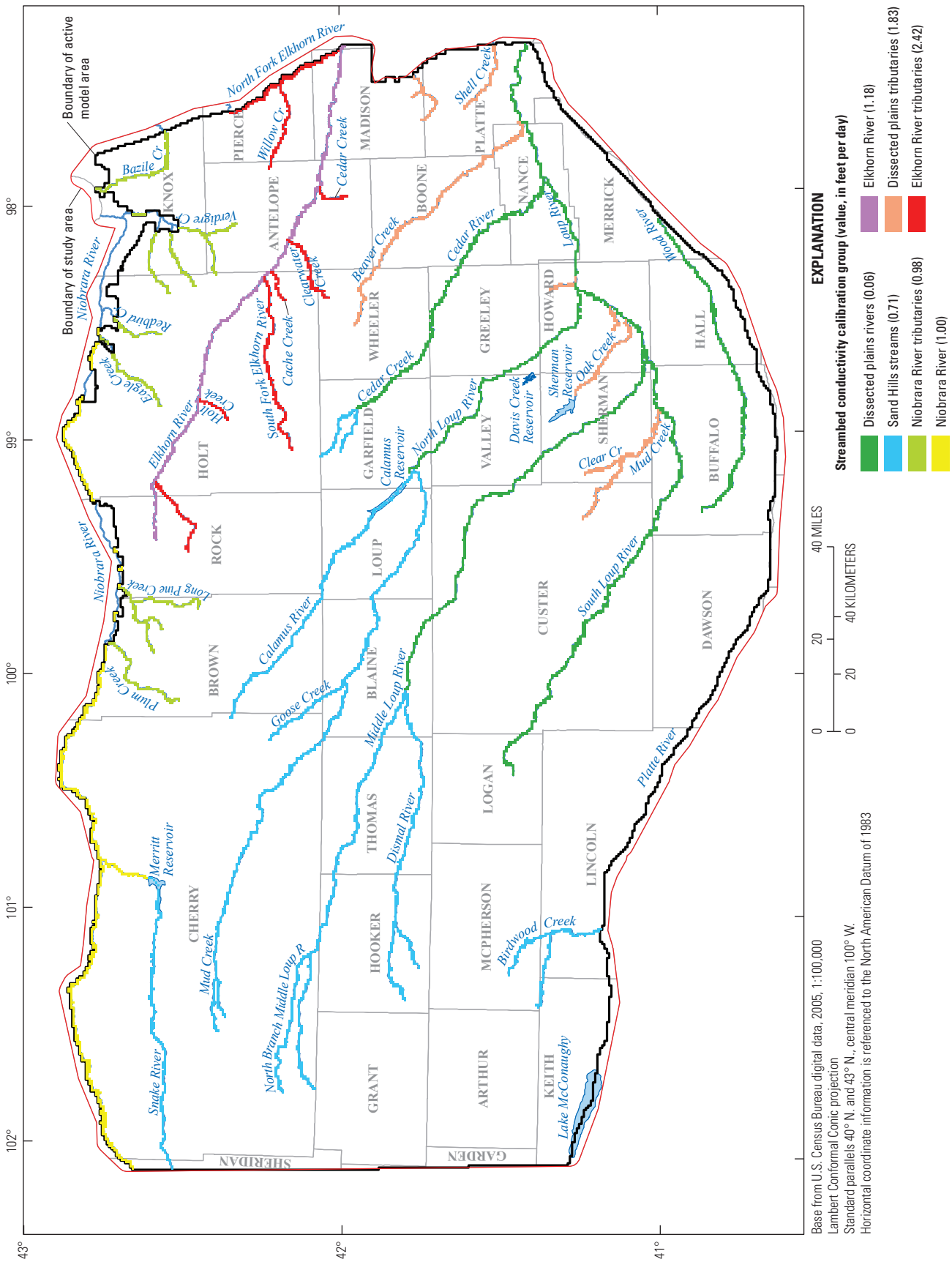

Figure 10. Calibrated streambed conductivity calibration group and value, Elkhorn and Loup River Basins, central Nebraska.

through 1940. The 1940–2010 water levels must have been measured during the simulation period (January 1, 1940, through December 31, 2010). The altitude of the water level was computed using the land-surface altitude supplied by the reporting agency, if available, or extracted from a DEM (Nebraska Department of Natural Resources, 1998). Wells with many water-level measurements were reviewed to determine if the first recorded static water levels were more than 10 ft from the mean altitude of the water table before the well was drilled (Nebraska Department of Natural Resources, 2012). If such measurements could not be verified, they were not used as calibration targets for 1940–2010. An additional check compared well locations in selected areas with aerial images to verify the location of the wells. Water levels that were measured within 1 mi of the model boundaries were not included as calibration targets because the zero-flow boundary in the model could affect the simulated water level and, therefore, affect the model calibration.

The pre-1940 period had 1,462 groundwater levels as calibration targets; none were zero-weighted. The mean residual for pre-1940 was −7.86 ft, the median was −11.26 ft, and the standard deviation was 22.28 ft (table 3, fig. 11). The range of residuals for pre-1940 was from −63.01 ft to 263.65 ft. Of the simulated groundwater levels, 83 percent were within 30 ft of the measured groundwater levels, compared to the phase two model, where 81 percent of the of the residuals were within 30 ft of the measured groundwater levels (Stanton and others, 2010). The location of each pre-1940 water level and the residual range are shown in figure 12*A*. The pre-1940 period had fewer targets than the 1940–2010 period. Also, there was greater uncertainty in the measured groundwater levels in pre-1940 than in 1940–2010 period because the accuracy of the groundwater-level values was not recorded for many of the measurements. In spite of this uncertainty, the group weights for the groundwater levels in the pre-1940 period were kept equal to those in the 1940–2010 period.

Of the 149,902 groundwater levels used as calibration targets in the 1940–2010 period, 199 were zero weighted because of their proximity to the model boundary. The mean residual for the 1940–2010 simulation was −2.52 ft, the median was −3.42 ft, and the standard deviation was 16.37 ft (table 3). The range of residuals was from −199.5 ft to 269.3 ft. The larger residuals were outliers for the simulation in that they were single measurements that did not indicate continued bias in the modeled area. Of the simulated water levels, 75 percent were within 15 ft of the observed value. A decadal breakdown of the groundwater-level residuals is shown in table 3, and the average residual for the 1940–2010 groundwater level for each well is shown in figure 12*B*. Although these mean residuals (table 3) indicate the simulated water level has been consistently higher than the measured water levels, the mean residual decreased steadily through the 1940–2010 period, indicating a smaller residual and better match for the most recent water levels. A direct comparison of the phase two and phase three water-level residuals is not possible as the phase two simulation was calibrated to decadal water-level change targets (Stanton and others, 2010), and the phase three simulation was calibrated to monthly water-level targets.

Stream Base Flows

Stream base flows were estimated at 235 locations across the model area for calibration targets. Of these locations (appendix, fig. 1.1, table 4), 51 coincide with streamgages operated by the USGS or the Nebraska Department of Natural Resources and streamflow records for these stations were collected. The estimated base-flow values at these 51 locations were determined using the daily mean streamflow values (Nebraska Department of Natural Resources, 2017; U.S. Geological Survey, 2016b) from the original record and analyzed using the BFI program (Wahl and Wahl, 2007), which also was used in Stanton and others (2010) and in the Northern High Plains model (Houston and others, 2013; Peterson and others, 2016). The other 184 measurements were estimated from measured low-flow values during a November 2006 seepage run (Peterson and Strauch, 2007). These low-flow values were collected when evapotranspiration was negligible, diversions were absent, and no major precipitation events happened in

Table 3. Statistical summary of calibration of water levels, pre-1940–2010, Elkhorn and Loup River Basins, central Nebraska.

Time period	Mean difference, in feet	Minimum difference, in feet	Maximum difference, in feet	Median difference, in feet	Standard deviation, in feet	Root mean square, in feet	Number of measurements
pre-1940s	−7.86	−63.01	263.65	−11.26	22.28	23.63	1,462
1940s	−6	−113.7	151.5	−6.14	15.04	16.19	12,594
1950s	−3.14	−107.8	180	−3.51	13.61	13.96	16,657
1960s	−4.14	−76.9	88	−4.3	11.45	12.17	21,555
1970s	−2.92	−115.9	146.7	−3.81	14.81	15.09	24,507
1980s	−2.24	−128.1	109.8	−2.57	16.83	16.97	26,508
1990s	−1.57	−199.5	143.5	−1.97	17.07	17.15	24,023
2000s	0.31	−148.9	269.3	−2.06	21.49	21.49	24,058
1940–2010	−2.52	−199.5	269.3	−3.42	16.37	16.57	149,902

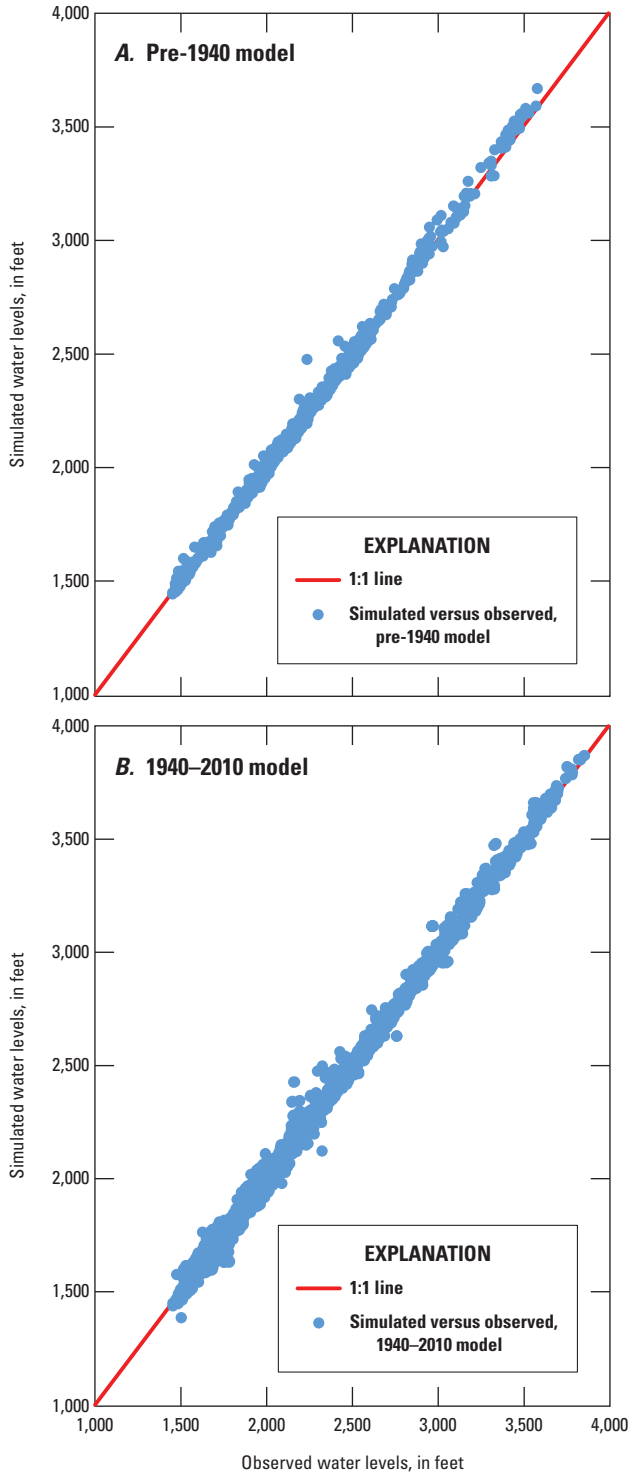

Figure 11. Relation of simulated outputs to calibration targets; *A*, for groundwater levels, pre-1940; and *B*, for groundwater levels, 1940–2010.

the preceding 7 days. It is assumed that these low-flow values are stream base flow. The average base flow for the specific month of the period of record for each streamgage was used as a calibration target in the model.

Stream base-flow targets for the pre-1940 period were estimated from 38 streamgages in the study area, as done by Stanton and others (2010). The pre-1940 base-flow targets were the average of the April and October base-flow values for the earliest 10 years of record for each streamgage. The April and October values were selected to represent the months when the stream was least likely to be affected by anthropogenic uses, ice accumulation, and evapotranspiration. No targets were zero-weighted during the pre-1940 simulation.

Stream base-flow targets for the 1940–2010 period were obtained from 51 streamgages in the study area (appendix, locations shown in fig. 1.1), plus 184 single measurements of low flow (Peterson and Strauch, 2007), for a total of 22,169 calibration targets for the 1940–2010 simulation. Some base-flow targets were affected by either flooding, diversions, or high reservoir releases, which last for several days. These affected base-flow targets were apparent in the base-flow record and, because they were not indicative of normal flows, were excluded from the calibration by zero weighting the related stream base-flow targets. A total of 189 stream base-flow targets were zero weighted in the 1940–2010 period.

The estimated and simulated base-flow values and average residuals are shown in table 4. Average differences by streamgage ranged from about 1 percent (Snake River above Merritt Reservoir, USGS streamgage 06459200, 228 calibration points) to about 93 percent (Wood River near Alda, USGS streamgage 06772000, 417 calibration points). A summary of base-flow target values is shown in table 4. The average percent difference between estimated and simulated base-flow values is 6 percent, compared to 4 percent from the phase two simulation (Stanton and others, 2010). The phase three simulation used monthly base-flow estimates as calibration targets, whereas the phase two simulation used annual base-flow estimates. The phase three simulation was not able to reproduce extreme monthly variations that would not have been apparent in an annual base-flow estimation, resulting in a higher average percent difference.

Graphs of simulated and observed stream base flows for selected streamgages in the study area are shown in figure 13. Similar graphs for the remaining streamgages are in the appendix. These graphs show that the simulation reproduced the observed temporal trends in base flow, as shown by the local weighted regression (LOWESS) curves on the graphs (Cleveland, 1979; Cleveland and Devlin, 1988). LOWESS curves were used to visually compare the trends of simulated and estimated base flow to ensure the model was properly capturing groundwater discharge to streams. The simulations were not able to reproduce extreme monthly variations, especially in areas affected by reservoir releases and canal diversions.

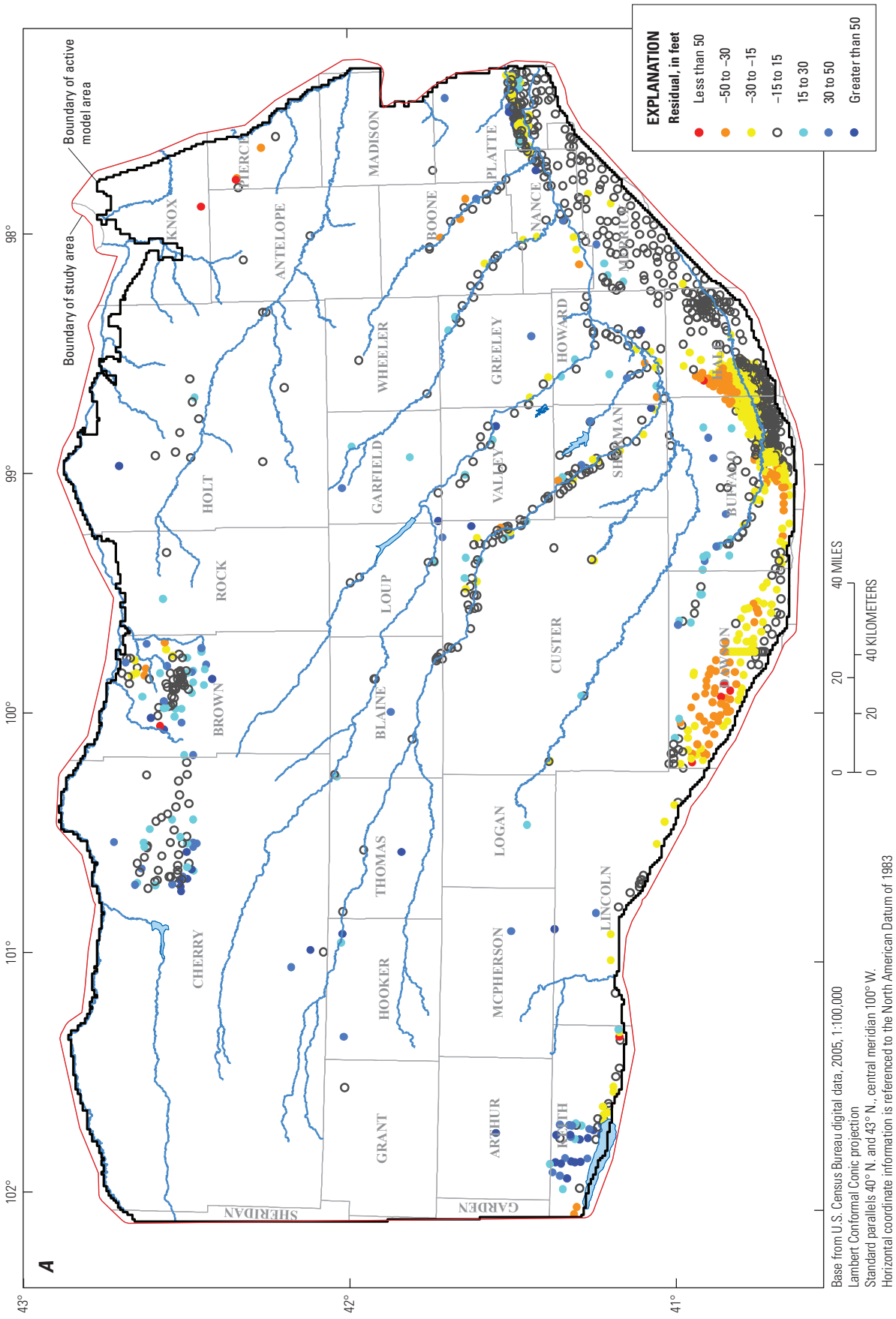

Figure 12. Residuals, in feet, for calibrated water-level measurements, Elkhorn and Loup River Basins, central Nebraska; *A*, pre-1940; and *B*, average 1940–2010 period.

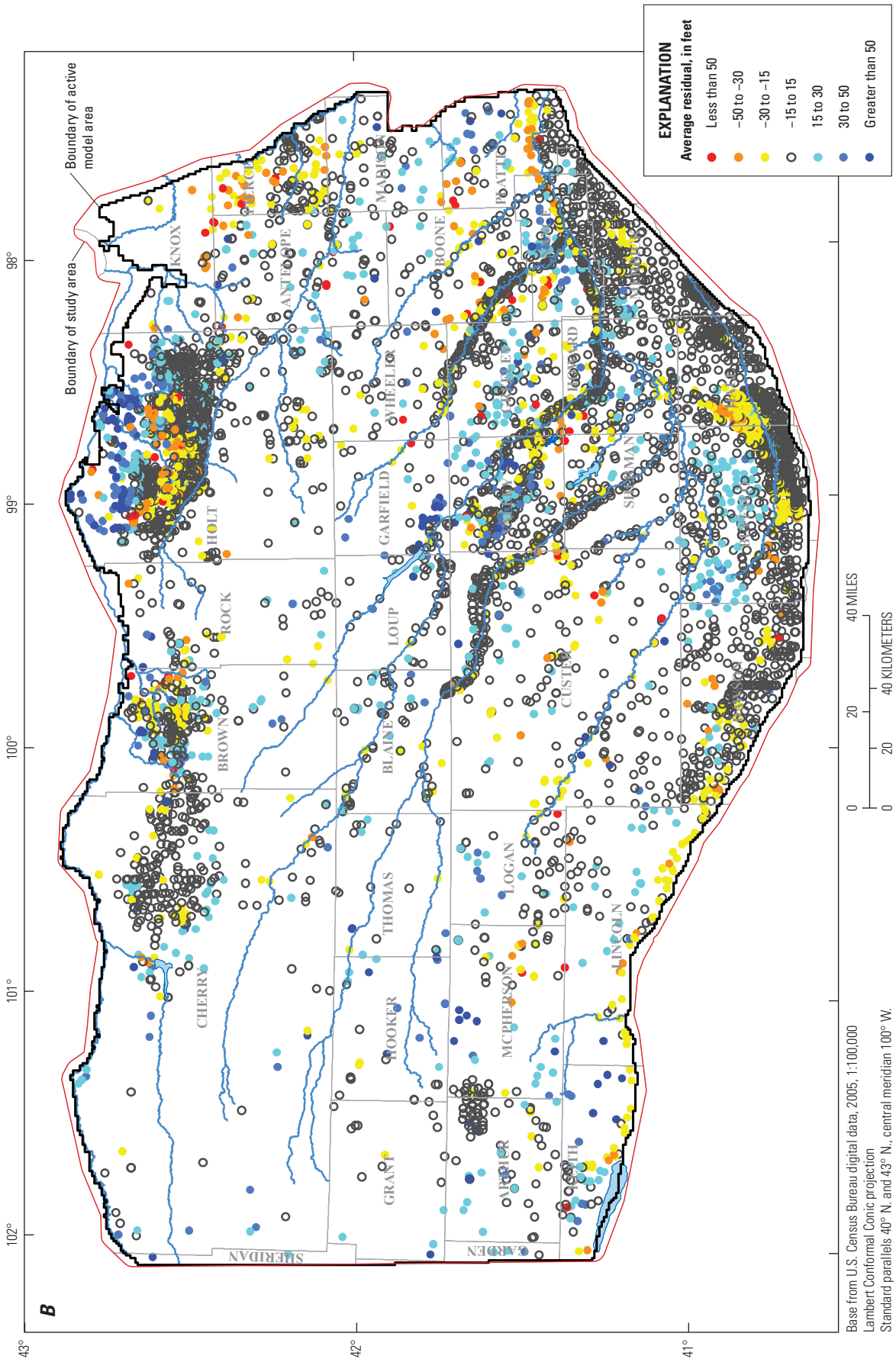

Figure 12. Residuals, in feet, for calibrated water-level measurements, Elkhorn and Loup River Basins, central Nebraska; *A*, pre-1940; and *B*, average 1940–2010 period.—Continued

Table 4. Stream base-flow analysis for streamgages with multiple measurements, 1940–2010, Elkhorn and Loup River Basins, central Nebraska.

[USGS, U.S. Geological Survey; ID, identifier; R., River; Ne., Nebraska; abv., above; Nebr., Nebraska; nr., near; Br., Branch; Cr., Creek; Riv., River; C., Creek]

USGS streamgage ID	USGS streamgage name	Period of record	Number of monthly mean base-flow estimates	Estimated mean monthly base flow, in cubic feet per second, for period of record, calculated using Wahl and Wahl (2007)			Simulated mean monthly base flow, in cubic feet per second, for period of record			Average residual, in cubic feet per second
				Mean	Minimum	Maximum	Average	Minimum	Maximum	
06459175	Snake R. at Doughboy, Ne.	10/1993–9/2010	204	160	130	200	190	170	220	−30
06459200	Snake River abv. Merritt Reservoir, Nebr.	10/1962–9/1981	228	190	130	240	190	170	260	0
06459500	Snake River near Burge, Nebr.	10/1947–9/2004	684	150	10	300	210	20	930	−60
06461500	Niobrara River near Sparks, Nebr.	10/1945–8/2010	779	640	220	1,170	590	380	1,260	50
06462000	Niobrara River nr. Norden, Nebr.	10/1952–9/1986	384	690	330	1,170	620	430	1,020	70
06463080	Long Pine Creek nr. Long Pine, Ne.	10/1979–3/1991	138	100	80	120	80	60	110	20
06465680	North Br. Verdigre Cr. nr. Verdigre, Ne.	10/1979–9/1992	156	20	0	50	30	20	40	−10
06466400	Bazile Creek at Center, Nebr.	10/2002–8/2010	95	50	20	130	30	20	30	20
06466500	Bazile Creek near Niobrara, Nebr.	6/1952–8/2010	615	50	0	290	40	30	50	10
06692000	Birdwood Creek near Hershey, Ne.	1/1940–11/2006	739	140	90	180	110	80	170	30
06771000	Wood River near Riverdale, Nebr.	7/1946–9/1973	311	2	0	10	2	0	0	0
06771500	Wood River near Gibbon, Ne.	4/1949–9/1995	354	2	0	30	2	0	10	0
06772000	Wood River near Alda, Nebr.	2/1954–9/2004	417	3	0	80	0	0	0	3
06775000	Middle Loup River at Seneca, Ne.	5/1948–11/2006	66	190	160	230	150	150	200	40
06775500	Middle Loup River at Dunning, Nebr.	10/1945–4/2008	751	410	230	560	360	250	650	50
06775900	Dismal River near Thedford, Nebr.	10/1966–8/2010	527	200	170	250	260	210	390	−60
06776000	Dismal R nr. Gem, Nebr.	10/1946–9/1953	84	260	110	300	290	260	350	−30
06776500	Dismal River at Dunning, Ne.	10/1945–9/1995	600	310	170	400	350	260	640	−40
06777000	Middle Loup River near Milburn, Nebr.	11/1951–9/1964	121	690	380	850	610	540	720	80

Table 4. Stream base-flow analysis for streamgages with multiple measurements, 1940–2010, Elkhorn and Loup River Basins, central Nebraska.—Continued

[USGS, U.S. Geological Survey; ID, identifier; R., River; Ne., Nebraska; abv., above; Nebr., Nebraska; nr., near; Br., Branch; Cr., Creek; Riv., River; C., Creek]

USGS streamgage ID	USGS streamgage name	Period of record	Number of monthly mean base-flow estimates	Estimated mean monthly base flow, in cubic feet per second, for period of record, calculated using Wahl and Wahl (2007)			Simulated mean monthly base flow, in cubic feet per second, for period of record			Average residual, in cubic feet per second
				Mean	Minimum	Maximum	Average	Minimum	Maximum	
06779000	Middle Loup R. at Arcadia, Nebr.	1/1940–12/1994	660	790	150	1,510	770	540	1,440	20
06780000	Middle Loup River at Rockville, Nebr.	10/1955–9/1975	204	640	170	1,070	700	550	950	−60
06782000	South Loup River nr. Cumro, Nebr.	6/1946–9/1953	88	130	80	190	100	90	110	30
06782500	South Loup River at Ravenna, Ne.	10/1940–11/2006	313	130	20	270	130	110	160	0
06783500	Mud Creek near Sweetwater, Ne.	8/1946–8/2004	697	20	0	70	20	10	60	0
06784000	South Loup River at Saint Michael, Nebr.	10/1943–8/2010	803	150	10	410	190	140	330	−40
06784500	Oak Creek nr. Dannebrog, Nebr.	8/1949–9/1957	90	1	0	0	1	0	0	0
06785000	Middle Loup River at Saint Paul, Nebr.	1/1940–8/2010	848	790	150	1,950	1,050	670	1,790	−260
06785500	North Loup River at Brewster, Nebr.	10/1945–7/2010	75	320	140	510	370	310	710	−50
06786000	North Loup River at Taylor, Nebr.	1/1940–4/2008	820	410	100	760	540	350	1,030	−130
06786500	North Loup R. at Burwell, Nebr.	10/1952–9/1960	96	400	190	610	440	400	560	−40
06787000	Calamus River nr. Harrop, Ne.	1/1998–9/2010	153	250	160	430	250	220	350	0
06787500	Calamus River near Burwell, Nebr.	1/1995–9/2010	189	200	20	430	310	40	1,020	−110
06788500	North Loup River at Ord, Ne.	7/1952–11/2006	628	780	260	1,440	880	600	1,700	−100
06789000	North Loup River at Scotia, Ne.	1/1940–11/2006	361	660	150	1,230	730	570	1,090	−70
06790000	North Loup Riv. nr. Cotesfield, Nebr.	7/1950–9/1956	75	740	270	1,210	710	640	810	30
06790500	North Loup River near Saint Paul, Nebr.	1/1940–8/2010	848	770	150	1,580	920	580	1,780	−150

Table 4. Stream base-flow analysis for streamgages with multiple measurements, 1940–2010, Elkhorn and Loup River Basins, central Nebraska.—Continued

[USGS, U.S. Geological Survey; ID, identifier; R., River; Ne., Nebraska; abv., above; Nebr., Nebraska; nr., near; Br., Branch; Cr., Creek; Riv., River; C., Creek]

USGS streamgage ID	USGS streamgage name	Period of record	Number of monthly mean base-flow estimates	Estimated mean monthly base flow, in cubic feet per second, for period of record, calculated using Wahl and Wahl (2007)			Simulated mean monthly base flow, in cubic feet per second, for period of record			Average residual, in cubic feet per second
				Mean	Minimum	Maximum	Average	Minimum	Maximum	
06791500	Cedar River near Spalding, Ne.	10/1944–9/2004	720	130	0	340	100	60	160	30
06791800	Cedar R. at Belgrade, Ne.	10/1959–11/2006	73	170	90	400	120	110	180	50
06792000	Cedar River near Fullerton, Nebr.	10/1940–9/2004	736	180	40	480	150	90	240	30
06793000	Loup River near Genoa, Nebr.	11/1943–8/2010	802	1,840	180	3,640	2,240	1,470	3,800	−400
06793500	Beaver Cr. at Loretto, Ne.	10/1944–11/2006	409	60	20	180	60	30	100	0
06794000	Beaver Creek at Genoa, Nebr.	10/1940–8/2010	839	80	0	290	120	60	230	−40
06796973	Elkhorn River nr. Atkinson, Ne.	1/1992–9/2010	225	50	0	380	50	30	80	0
06796978	Holt Creek nr. Emmet, Nebr.	10/1978–9/1989	132	20	0	140	0	0	10	20
06797500	Elkhorn River at Ewing, Nebr.	8/1947–8/2010	757	100	10	1100	100	40	190	0
06798000	South Fork Elkhorn River near Ewing, Ne.	8/1947–9/2004	544	40	20	220	40	20	90	0
06798300	Clearwater C. nr. Clearwater, Ne.	7/1961–11/2006	247	30	10	130	30	20	90	0
06798500	Elkhorn River at Neligh, Ne.	1/1940–9/2004	755	200	30	1,480	210	90	440	−10
06799000	Elkhorn River at Norfolk, Nebr.	10/1945–8/2010	779	330	50	2,050	270	110	550	60
06799080	Willow Creek near Foster, Nebr.	10/1975–11/2006	349	10	0	50	10	0	30	0
06799100	North Fork Elkhorn River near Pierce, Nebr.	8/1960–8/2010	601	60	0	440	40	0	130	20

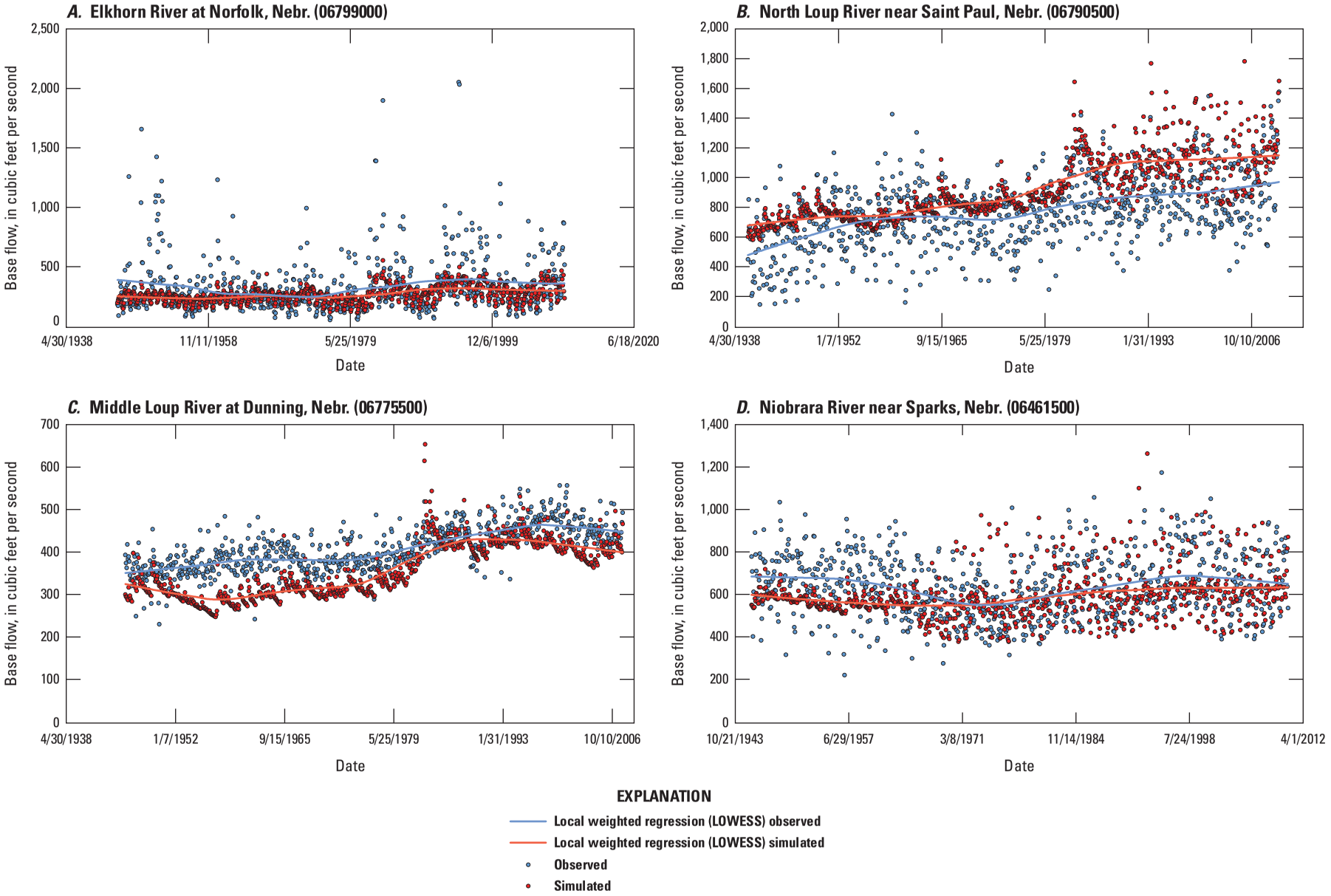

Figure 13. Selected observed and simulated calibrated base flow for streams used in the Elkhorn and Loup, and River Basin model, phase three, central Nebraska.

Simulated Groundwater Budget

For 1940 through 2010, almost all water entering the aquifer was from recharge (table 5). The largest aquifer outflows were, in decreasing order, stream base flow (52 percent), groundwater outflows to aquifer storage (19 percent), irrigation well withdrawal (15 percent), evapotranspiration (11 percent), fixed water-level boundaries (2 percent), and municipal well withdrawal (1 percent). These results were generally consistent with the phase two model. Average annual recharge and stream base flow were larger in the phase three model than in the phase two model, which could be attributed at least in part to the addition of canal seepage as a component of recharge for the phase three model. For the phase two model, irrigation-return flow was accounted for using a net irrigation withdrawal term that represented only the amount of withdrawal that needed to satisfy evapotranspiration demands rather than a total pumping volume that included irrigation-return flow. The phase three model produced about half the evapotranspiration volume as the phase two model, which is likely because the phase three model grid cells were smaller, resulting in an active evapotranspiration area that was smaller and could be represented more precisely. Reductions in the amount of groundwater in storage were larger (more groundwater-level declines) for the phase three model.

Groundwater-budget terms varied with time. Recharge and evapotranspiration vary climatically, and well withdrawal increased substantially starting in the 1980s, corresponding to increased conversion of dryland agriculture to irrigated agriculture (Stanton and others, 2010). In addition, two periods (1950s and 1970s) with lower precipitation amounts resulted in less recharge.

Sensitivity Analysis

Parameter sensitivity was analyzed to determine which parameter groups have the greatest potential to affect the model residuals. The analysis of parameter sensitivity followed a similar approach to that described in the "Composite Parameter Sensitivity" section of Peterson and others (2016). The responses of the model to changes in the parameters were extracted from the Jacobian matrix generated using the PEST automated calibration process (Doherty, 2016). Each residual generated from the model then was multiplied by the weight of the corresponding observation target. The sensitivities were summed for each parameter group: K_h (layer 1 and layer 2), recharge (precipitation and canal seepage), and streambed conductivity. Larger composite sensitivities indicate the changes in those groups had a larger effect in the magnitude of residuals.

Sensitivities were analyzed for the following calibration targets: pre-1940 groundwater levels (1,462 targets), pre-1940 base flows (38 targets), 1940–2010 groundwater levels (149,902 targets), and 1940–2010 base flows (22,169 targets). Because the 1940–2010 groundwater levels had the largest number of targets, they had the greatest effect on all parameter groups (fig. 14).

The calibration targets for pre-1940 and 1940–2010 were most sensitive to modifications in the recharge parameter group (fig. 14), which could be due to the temporal setup of the model. The calibration targets varied by month, and, therefore, the recharge parameters were most likely to respond to target variation.

Simulation of Effect of Additional Groundwater Withdrawals on Future Stream Base-Flow, Evapotranspiration, and Storage Depletion

The calibrated phase three model was used to calculate future stream base flow, evapotranspiration and storage depletion. Depletion maps are used to make water-resources management decisions within the ELM study area (Tylr Naprstek, Lower Loup NRD, written commun, 2012). Base-flow depletions are a combination of induced recharge from the stream and captured groundwater discharge to the stream. Water pumped from a well initially draws water from storage in the aquifer, depleting water from all sides of the aquifer around the well. Over time the aquifer depletion expands further and further from the well, and can intercept other sources of water into and out of the aquifer, such as streams and ET (Barlow and Leake, 2012). Previous studies in the area (Peterson and others, 2008; Stanton and others, 2010) have shown the primary source of water being pumped by a hypothetical well in the ELM area was captured groundwater discharge that would have otherwise become stream base flow.

Depletion exists when a pumping well reduces groundwater discharge to other aquifer outputs, such as storage, streams, or evapotranspiration (Jenkins, 1968). It is a function of time, location of the pumping well, storage coefficient and aquifer transmissivity, and the geometry of the aquifer and streams. When a well begins to pump water, the source of the water typically is storage, resulting in groundwater declines near the well (Theis, 1940). As pumping continues, the effect of the pumping well can expand, potentially causing increased inflow to the aquifer and decreased outflow from the aquifer (Stanton and others, 2010). The base-flow depletion calculations are generated by determining the percentage of water that was intercepted by pumping the additional hypothetical well in each model cell, therefore indicating simulated depletion as a function of pumping-well location and duration of pumping.

Table 5. Simulated water budgets for the pre-1940 model and the 1940–2010 model, Elkhorn and Loup River Basins, central Nebraska.

[Components may not sum to totals because of rounding. SWB, soil water balance; N/A, not applicable; %, percent]

Water budget component	Pre-1940 period		1940–2010 period															
			1940–1949		1950–1959		1960–1969		1970–1979		1980–1989		1990–1999		2000–2010		1940–2010	
	Thousands of acre-feet per year	Budget percent	Thousands of acre-feet per year	Budget percent	Thousands of acre-feet per year	Budget percent	Thousands of acre-feet per year	Budget percent	Thousands of acre-feet per year	Budget percent	Thousands of acre-feet per year	Budget percent	Thousands of acre-feet per year	Budget percent	Thousands of acre-feet per year	Budget percent	Thousands of acre-feet per year	Budget percent
Inflows																		
Recharge (total)	2,435	97	4,931	100	2,761	84	4,939	100	4,604	100	7,174	100	7,212	100	6,601	100	5,460	100
Recharge from SWB	N/A	N/A	4,673	95	2,467	89	4,628	94	4,261	93	6,831	95	6,857	95	6,253	95	5,139	94
Recharge from canal seepage	N/A	N/A	257	5	294	11	311	6	343	7	343	5	354	5	348	5	321	6
Reservoir seepage	N/A	N/A	3	0	5	0	7	0	8	0	8	0	8	0	5	0	6	0
Groundwater storage	67	3	0	N/A	507	15	0	N/A	0	N/A	0		0	N/A	0	N/A	0	N/A
Total inflow		**100%**		**100%**		**99%**		**100%**		**100%**		**100%**		**100%**		**100%**		**100%**
Outflows																		
Groundwater storage	0	N/A	1,675	34	0	N/A	1,189	24	218	5	1,627	23	1,228	17	453	7	913	16
Stream base flow	1,993	80	2,426	49	2,424	74	2,709	55	2,740	59	3,327	46	3,578	50	3,398	51	2,943	53
Irrigation wells	N/A	N/A	148	3	167	5	289	6	904	20	1,314	18	1,398	19	1,815	27	862	16
Municipal wells	N/A	N/A	23	0	28	1	36	1	43	1	46	1	47	1	48	1	39	1
Evapotrans-piration	447	18	510	10	528	16	580	12	592	13	736	10	828	11	803	12	654	12
Fixed-water level boundaries	63	2	152	3	127	4	143	3	115	2	132	2	141	2	89	1	128	2
Total outflow		**100%**		**100%**		**100%**		**100%**		**100%**		**100%**		**100%**		**100%**		**100%**

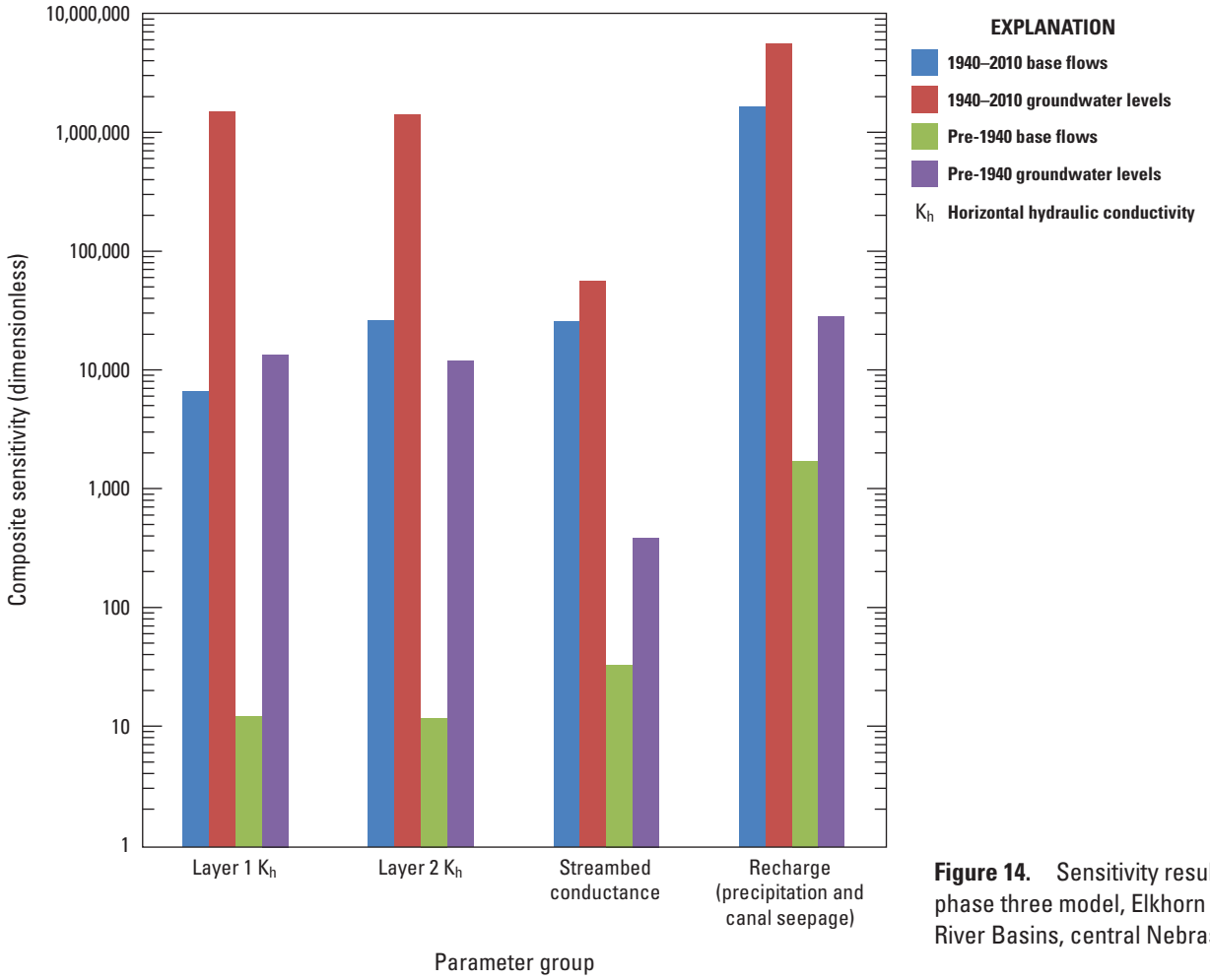

Figure 14. Sensitivity results for the phase three model, Elkhorn and Loup River Basins, central Nebraska.

Future Baseline Simulation, 2011–60

The future baseline simulation represents the estimated future conditions without any changes after 2010 to the number and location of groundwater-irrigated acres, groundwater pumping, or canal seepage recharge. The baseline simulation continues the conditions at the end of the 1940–2010 simulation period into the 2011–60 simulation period using the same spatial discretization as the 1940–2010 period. The calibrated aquifer properties from the pre-1940 and 1940–2010 periods were used as the aquifer properties in the future baseline simulation. The simulated water levels from the end of the 1940–2010 calibration period were used as starting water levels for the future simulation. Calibrated streambed conductivity was used as the streambed conductivity for the future analysis streams. Input values for the future simulation period were the monthly 2009 inflows from the 1940–2010 calibrated simulation. These values were recharge from both precipitation and canal seepage, and evapotranspiration. The 2009 values were chosen to represent the future conditions because they most closely represented the average climatic conditions for 1900–2010 during the 2000–10 period. It was important to select a year within 2000–10 period to replicate for the future simulation inflows because land use and surface-water diversions have not varied greatly during the final decade of the 1940–2010 period.

The temporal discretization of the future baseline simulation initially was set to monthly stress periods for the 2011–60 period using the monthly values from 2009. The future simulation was converted to a single stress period model, using an average 2009 rate for each input, which produced similar results in the budget terms of the model and base-flow depletion. The monthly stress period model completed a single model run in about 4 hours. A single stress period model completed a model run in about half an hour. The conversion to a single stress period model drastically reduced computation time for the future period model. A comparison of the net budget terms for the monthly stress period model and single stress period model is shown in table 6, which shows that the mass balance and individual budget components are not greater than 1 percent between each model. The base-flow depletion for selected cells in the model simulation comparing monthly stress periods to a single stress period simulation is shown in figure 15. This figure illustrates the depletion rates follow the same patterns. The cells were chosen at random. The cells were assigned a unique cell code by combining the row and column placement of the cell. The cell locations are highlighted in figure 2.

Table 6. Comparison of single stress period and monthly stress period budgets for the 2011–60 future baseline simulation, phase three, Elkhorn and Loup groundwater-flow model, central Nebraska.

Single stress period			
Inflows, in thousands of acre-feet per year		Outflows, in thousands of acre-feet per year	
Groundwater storage	794	Constant heads	42
Reservoirs	12	Wells	2,372
Recharge	6,312	Evapotranspiration	886
		Streams	3,818
Total	**7,118**		**7,118**

Monthly stress periods			
Inflows, in thousands of acre-feet per year)		Outflows, in thousands of acre-feet per year	
Groundwater storage	792	Constant heads	42
Reservoirs	12	Wells	2,372
Recharge	6,286	Evapotranspiration	866
		Streams	3,808
Total	**7,090**		**7,090**

Depletion Analysis and Maps

A base-flow depletion map for 2011–60 was generated by simulating an additional hypothetical well in each cell within the model area; each additional well is assumed to withdraw water at a continuous rate throughout the entire simulation period. The future simulation for the phase three model was developed to update the base-flow depletion map from Stanton and others (2010). The purpose of recalculating the base-flow depletion map for phase three was to reanalyze the depletion percentages with the decreased cell size and additional layer used in the phase three model. The phase two depletion analysis focused on the Elkhorn and Loup River Basins (fig. 1), approximately 17,700 mi^2. The phase three depletion analysis calculated depletion for additional areas outside of the Elkhorn and Loup River Basins, yet still within the model boundary, which was approximately 29,000 mi^2.

Depletion was determined by pumping a single well in the designated pumping layer from the calibrated model in each active cell at a continuous rate of 1 cubic foot per second (ft^3/s) for 2011–60. Base-flow depletion was calculated for 117,814 cells. Of these cells, approximately 1,800 were excluded from depletion mapping because of their proximity to the Niobrara, Platte, or Platte tributaries, or they were located in areas with little saturated thickness close to the model boundary. The Niobrara River is the northern-most boundary of the model, and simulation results could be affected by the model boundary conditions in the immediate area. Depletion analysis was not included on the figure for the cells adjoining and including the Platte River and the Platte River tributaries because the Platte River was simulated as fixed water-level cells in the model, and the stream cells for the tributaries were assumed to contribute to Platte River depletion which was outside the scope of the project. The percentage of hypothetical well withdrawal corresponding to simulated base-flow depletion in the Elkhorn and Loup River Basins for 2011 through 2060 is shown in figure 16.

The base-flow depletion analysis for the phase three model indicated that the base-flow depletion from pumping a hypothetical well for 50 years was greatest in areas closest to the stream (fig. 16). Base-flow depletions more than 10 to 12 mi from a stream usually were less than 10 percent (fig. 16). Areas of stream base-flow depletion percentages greater than 80 percent were generally within 1 mi from the stream (fig. 16). The distance increased to 6 mi near the confluence of the Dismal and Middle Loup Rivers, and the North Loup and Calamus Rivers (fig. 16). The percentage of stream base-flow depletion decreased as the distance from the stream increased. Base-flow depletion was not uniform along streams because depletion was affected by the heterogeneity of the simulated aquifer system.

The results of the base-flow depletion analysis for the phase three model followed similar patterns to that of Stanton and others (2010); however, some differences are worth noting. Base-flow depletion was similar in most areas, and the highest depletion took place in areas adjacent to streams; however, more depletion resulted from simulated pumping wells in areas north of the Elkhorn River near the Niobrara tributaries, which were not included in Stanton and others (2010). Additionally, depletion in the phase three model was not as high along many streams as it was in Stanton and others (2010), which is due to the adjustments in calibration from grid discretization and boundary conditions. This allows for depletion effects to be restrained to smaller areas. Base-flow depletion (fig. 16) in the phase three model was lower along the dissected plains rivers (fig. 10). The calibrated phase three model performed best when the dissected plains streambed conductivity was decreased to 0.06 ft/d, limiting the amount of interchange between the groundwater and surface-water systems. Additionally, base-flow depletion in the phase three model decreased along the South Fork Elkhorn River (fig. 1). Depletion is lower in this area because more evapotranspiration was simulated in the area in the phase three model. The pumping well affected both the stream base-flow depletion and evapotranspiration depletion in this area.

Not all water intercepted by the additional hypothetical wells was stream base flow. Groundwater withdrawals by the additional hypothetical wells also resulted in depletions to evapotranspiration (fig. 17*A*) and depletions from storage (fig. 17*B*).

The evapotranspiration depletion map from hypothetical well withdrawal for 2011–60 (fig. 17*A*) from the phase three model is slightly different from the similar map in Stanton and others (2010). The spatial distribution of percentage of

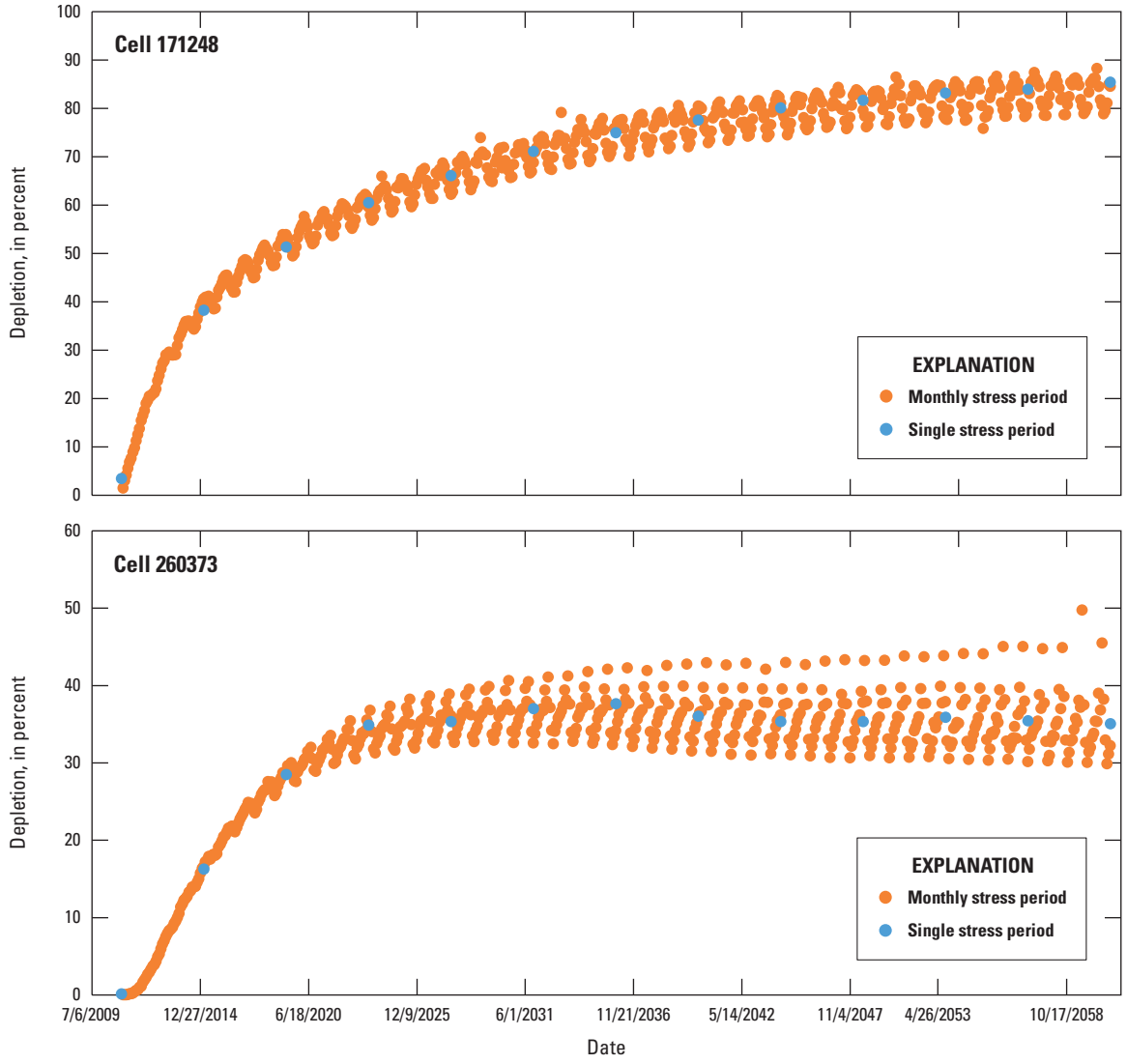

Figure 15. Base-flow depletion comparisons between a monthly stress period model and a single stress period model, 2011–60, Elkhorn and Loup River Basins, central Nebraska.

depletion of evapotranspiration in the phase three model indicates similar patterns as Stanton and others (2010), but the phase three future simulation extent is greater because the hypothetical additional wells were across a larger model area, as opposed to only in the Elkhorn and Loup River Basins as in Stanton and others (2010). In addition, the overall evapotranspiration extent was not as great for phase two because of the discretization changes between the models. Evapotranspiration depletion was largest in areas closest to streams, specifically in the Elkhorn River watershed. It was also larger in areas of interdunal wetlands within the Sand Hills. Evapotranspiration depletion was negligible in areas greater than 5 mi from a stream, with the exception of interdunal areas in Cherry, Grant, and Arthur Counties. The areas of higher evapotranspiration depletion in the phase three model coincide with areas of concentrated evapotranspiration cells, which reflect areas of interdunal wetlands (U.S. Fish and Wildlife Service, 2017; Mitsch and Gosselink, 2007). These wetlands were better represented in the phase three model because of the smaller grid cell sizes.

The groundwater storage depletion from hypothetical well withdrawal for 2011–60 (fig. 17*B*) for the phase three model is more widespread than that of Stanton and others (2010), which might be because of the extra model area that was analyzed and the difference in distribution associated with evapotranspiration in the phase three model compared to Stanton and others (2010). The storage depletion percentage increased as the distance from a stream increased. Storage depletion was largest in areas between streams (fig 17*B*). Areas experiencing the smallest amount of storage depletion were adjacent to streams, as most of the depletion in those areas occurred to streamflow and evapotranspiration.

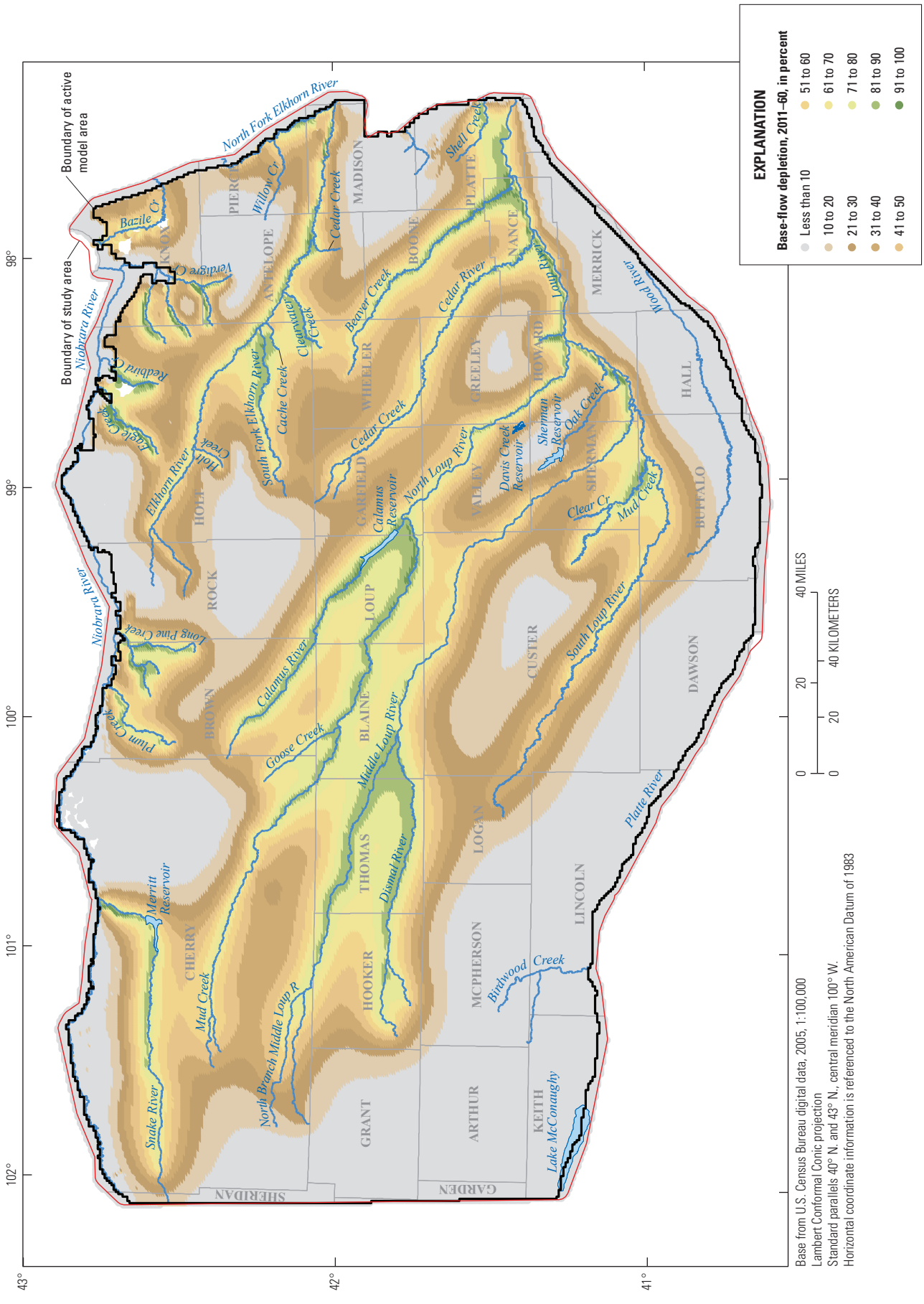

Figure 16. Percentage of hypothetical well withdrawal corresponding to simulated base-flow depletion, 2011–60, Elkhorn and Loup River Basins, central Nebraska.

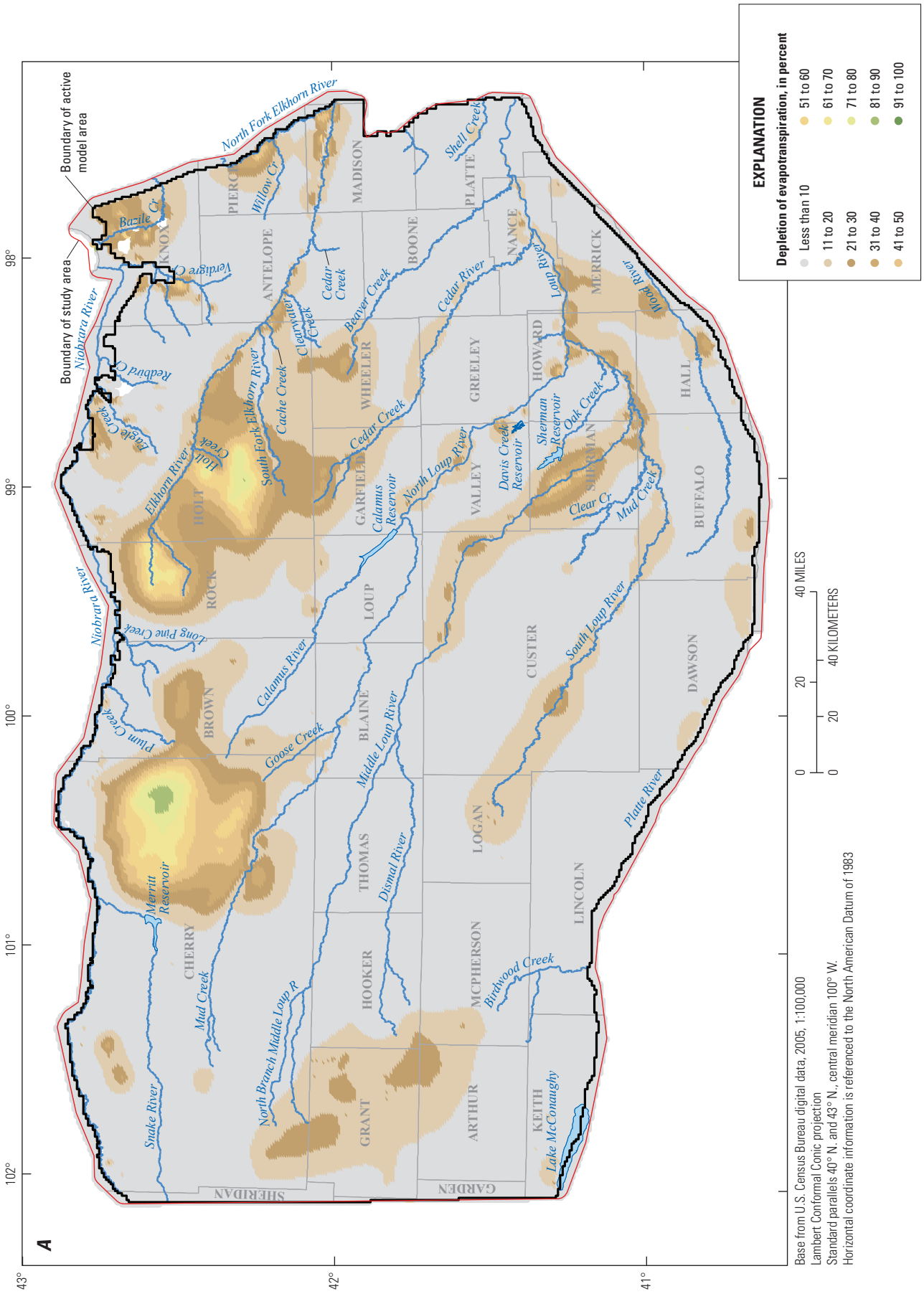

Figure 17. Percentage of hypothetical well withdrawal for 2011–60, Elkhorn and Loup River Basins, central Nebraska; *A*, corresponding to simulated depletion of evapotranspiration from groundwater; and *B*, corresponding to simulated depletion of groundwater storage.

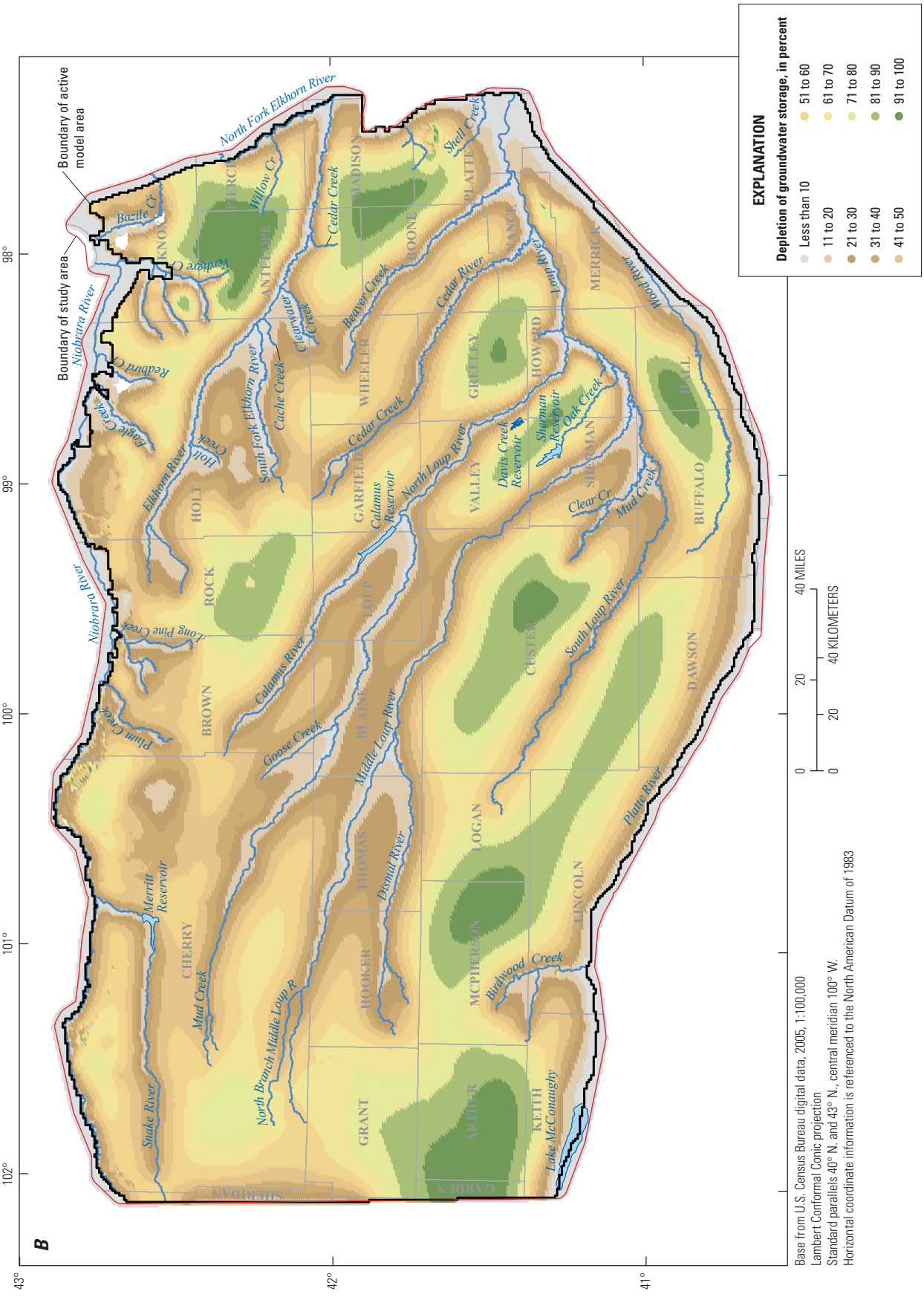

Figure 17. Percentage of hypothetical well withdrawal for 2011–16, Elkhorn and Loup River Basins, central Nebraska; *A*, corresponding to simulated depletion of evapotranspiration from groundwater; and *B*, corresponding to simulated depletion of groundwater storage.—Continued

Model Assumptions

Using MODFLOW to simulate groundwater-flow systems through finite-difference solution techniques implies many assumptions (Harbaugh, 2005). Several specific assumptions related to the ELM study objectives are presented here. It is assumed that the aquifer and its sources and sinks of water, such as streams, withdrawal, and recharge, can be appropriately simulated using grid cells that are one-half mile by one-half mile in size, and aquifer properties are uniform within the area of each grid cell. Some aquifer properties are known to change for distances of less than half a mile, but this assumption is appropriate for the model because it is meant to be used for regional management scenarios. It also is assumed that the groundwater-flow system, before major anthropogenic effects, was in long-term equilibrium, which can be approximated using a 1,000-year transient stress period. Because no substantial anthropogenic effects would have been present in the system before major groundwater development before 1940, groundwater levels from pre-1940 would have represented the integration of climate effects of the previous decades or centuries.

Model Limitations

The phase three model represents a simplification of a complex natural system and, despite improvements since Stanton and others (2010), it is limited by data availability, discretization of the system in space and time, and the assumptions made as part of the finite-difference model approach (Harbaugh, 2005). Daily precipitation and temperature data used for estimating recharge and irrigation well withdrawal were distributed between weather stations using a simple interpolation method (Westenbroek and others, 2010). Simulated recharge from the SWB code is highly sensitive to changes in precipitation (Stanton and others, 2011). Therefore, better methods for defining daily climate data or adjusting interpolated precipitation values within the expected range of uncertainty between weather stations for the modeled period could improve calibration results.

A limitation of the phase three model is that the SWB and MODFLOW-NWT programs used for the phase three model do not represent the complete hydrologic system because the programs do not fully couple landscape, surface-water, and groundwater processes to allow feedback between all components of the hydrologic system during the simulation. For example, neither the SWB nor MODFLOW packages used in the phase three model represent unsaturated zone properties or processes between the root zone and the water table; instead, the phase three model assumed recharge simulated by the SWB code reaches the water table immediately.

The SWB code provides estimated well pumping based on crop type, soil type, and precipitation. An assumption in the SWB code is that an irrigator will use only the amount of water required for the crop. It is likely that pumping was over or underestimated by SWB compared to what the irrigator actually used.

The phase three model is designed to simulate regional-scale hydrologic conditions and cannot represent local-scale processes. Future simulation periods depend on the representation of hydrologic conditions that were simulated for historical periods. Future simulations are a representation of how the resources could behave under defined stress conditions and should not be considered a forecast of future conditions.

This model was constructed to simulate groundwater flow in the central Nebraska region from pre-groundwater and surface water development through 2010 and should be used only as a tool to inform readers on groundwater flow. The future conditions are hypothetical and developed only to determine the effect of additional groundwater withdrawals for irrigation on stream base flow. Using these models for any other purpose, such as contaminant transport or individual well response analysis, is not advised.

Summary

The U.S. Geological Survey designed and completed the phase three modeling study in cooperation with the Lewis and Clark, Lower Elkhorn, Lower Loup, Lower Platte North, Middle Niobrara, Upper Elkhorn, and Upper Loup Natural Resources Districts. The phase three model area is a 30,000-square mile area of the High Plains aquifer in central Nebraska. This study was an enhancement of the regional groundwater-flow model documented in the previous phase two model; the enhancements were an increase in the spatial and temporal discretization of the previous model to improve understanding of the stream-aquifer conditions and to quantify the effects of groundwater withdrawal from 2011 to 2060 by hypothetical additional wells on future stream base flow in the Elkhorn and Loup River Basins. The model documented in this report incorporated new spatial and temporal discretization and used the Soil-Water Balance code to estimate recharge and groundwater withdrawals for irrigation. This model incorporated newly collected data, which were not included in the previous model, to aid in the expansion of the temporal discretization. The publication of the base of the Plio-Pleistocene sediments allowed for the expansion of the model into two layers. This report summarizes the refinements to the previous model, the components of the phase three model, and the phase three model results.

The phase three groundwater-flow model was constructed for the study area using half-mile grid cell spacing horizontally and two layers vertically. The active model extent was the same size as the previous model. The active model domain for the phase three model was divided into of 235,643 active grid cells. The model was calibrated to match groundwater level and base-flow data from the stream-aquifer system from pre-1940 through 2010 (including predevelopment [pre-1895],

early development [1895–1940], and historical development [1940 through 2010] conditions) using an automated parameter-estimation method.

The calibration results of the pre-1940 period indicated that 83 percent of the simulated groundwater levels were within 30 feet of the measured groundwater levels. Calibration results using 1940 through 2010 groundwater levels indicated that 75 percent of the simulated groundwater levels were within 15 feet from measured groundwater levels. Stream base-flow trends generally were reproduced by the model at most sites.

The calibrated model was used to develop a future simulation based on the 2009 inputs and 1940–2010 calibrated data. This future simulation was developed to determine possible effects of groundwater withdrawals on stream base flow, similar to the previous model simulation. A map of simulated stream base-flow depletion as a percentage of water pumped from an additional hypothetical well from 2011 through 2060 was generated. Simulated base-flow depletion results indicate depletions of less than 10 percent of withdrawal in 50 years in areas that are about 10 miles or farther from the Elkhorn and Loup Rivers and their tributaries. Evapotranspiration depletion was largest in areas closest to streams, specifically in the Elkhorn River watershed. It was also larger in areas of interdunal wetlands within the Sand Hills. Evapotranspiration depletion was negligible in areas greater than 5 miles from a stream, with the exception of interdunal areas in Cherry, Grant, and Arthur Counties. The groundwater storage depletion percentage increased as the distance from a stream increased. Areas experiencing the smallest amount of storage depletion were adjacent to streams. Calibrated model outputs and streamflow depletion analysis is publicly available online.

The model documented in this report has limitations, as do all tools used to analyze complex natural systems. The model reflects the input-data limitations, system simplifications, simulation assumptions, and computer resources available at the time of construction and calibration. Development of this regional model focused on generalized hydrogeologic characteristics within the study area and did not attempt to describe variations important to local-scale conditions. The regional model is most appropriate for analyzing groundwater-management scenarios for large areas and during long periods and is not reliable for analyzing small areas or periods shorter than those used in building the model.

References Cited

Barlow, P.M., and Leake, S.A., 2012, Streamflow depletion by wells—Understanding and managing the effects of groundwater pumping on streamflow: U.S. Geological Survey Circular 1376, 84 p. [Also available at https://pubs.usgs.gov/circ/1376/.]

Cannia, J.C., Woodward, D., and Cast, L.D., 2006, Cooperative hydrology study COHYST hydrostratigraphic units and aquifer characterization report: Cooperative Hydrology Study report, February 24, 2006, 96 p., accessed December 14, 2017, at http://cohyst.nebraska.gov/document/dc012hydro_aquifer_022406.pdf.

Center for Advanced Land Management Information Technologies, 2007, 2005 Nebraska land use patterns: Lincoln, Nebr., Center for Advanced Land Management Information Technologies, remote-sensing image, scale 1:100,000, accessed July 18, 2018, at https://calmit.unl.edu/2005.

Cleveland, W.S., 1979, Robust locally weighted regression and smoothing scatterplots: Journal of American Statistical Association, v. 74, no. 368, p. 829–836.

Cleveland, W.S., and Devlin, S.J., 1988, Locally weighted regression—An approach to regression analysis by local fitting: Journal of American Statistical Association, v. 83, no. 403, p. 596–610.

Condra, G.E., and Reed, E.C., 1943, The geological section of Nebraska: Conservation and Survey Division, University of Nebraska–Lincoln, Nebraska Geological Survey Bulletin 14, 82 p.

Conservation and Survey Division, 2003, 1995 water table contours: Lincoln, University of Nebraska, Institute of Agriculture and Natural Resources, digital data, file watertable95.e00, accessed February 28, 2003, at http://snr.unl.edu/data/geographygis/NebrGISdata.asp.

Conservation and Survey Division, University of Nebraska-Lincoln, 2005a, Geology related GIS data—Till: University of Nebraska-Lincoln, School of Natural Resources, digital data, accessed September 26, 2017, at http://snr.unl.edu/data/geographygis/geology.aspx.

Conservation and Survey Division, University of Nebraska-Lincoln, 2005b, Geology related GIS data—Topographic regions: University of Nebraska-Lincoln, School of Natural Resources, digital data, accessed March 3, 2017, at http://snr.unl.edu/data/geographygis/geology.aspx.

Conservation and Survey Division, University of Nebraska-Lincoln, 2017, Historic Nebraska Statewide Groundwater Level Program—Data retrieval: University of Nebraska-Lincoln, School of Natural Resources, digital data, accessed March 3, 2017, at http://snr.unl.edu/data/water/groundwater/NebGW_Levels.aspx.

Cronshey, R.G., McCuen, R.H., Miller, N., Rawls, W., Robbins, S., and Woodward, D., 1986, Urban hydrology for small watersheds—TR-55 (2d ed.): Washington, D.C., U.S. Department of Agriculture, Soil Conservation Service, Engineering Division, Technical Release 55, 164 p.

Doherty, J., 2016, PEST, model independent parameter estimation—User manual part 1—PEST, SENSAN and Global Optimisers (6th ed.): Brisbane, Australia, Watermark Numerical Computing, accessed March 29, 2017, at http://pesthomepage.org/Downloads.php.

Environmental Simulations, Inc., 2009, Groundwater Vistas version 6: Environmental Simulations, Inc., software release March 3, 2015, accessed March 29, 2017, at http://www.groundwatermodels.com.

Esri, 2017, About ArcGIS, flow path tool: Esri web page, accessed September 29, 2017, at http://www.esri.com/software/arcgis/.

Esri, 2018, World imagery with metadata: Esri web page, accessed August 3, 2018, at http://www.arcgis.com/home/item.html?id=c1c2090ed8594e0193194b750d0d5f83.

Flynn, A.T., 2018, Water-level and digital data for the Elkhorn and Loup River Basins, central Nebraska, phase three groundwater flow model: U.S Geological Survey data release, https://doi.org/10.5066/P9UA3UUD.

Flynn, A.T., and Stanton, J.S., 2018, MODFLOW–NWT groundwater-flow model used to evaluate groundwater flow in the Elkhorn and Loup River Basins, central Nebraska, phase three: U.S. Geological Survey data release, https://doi.org/10.5066/P9RITFNL.

Gutentag, E.D., Heimes, F.J., Krothe, N.C., Luckey, R.R., and Weeks, J.B., 1984, Geohydrology of the High Plains aquifer in parts of Colorado, Kansas, Nebraska, New Mexico, Oklahoma, South Dakota, Texas, and Wyoming: U.S. Geological Survey Professional Paper 1400–B, 63 p. [Also available at https://pubs.er.usgs.gov/publication/pp1400B.]

Harbaugh, A.W., 2005, MODFLOW–2005, the U.S. Geological Survey modular ground-water model—The ground-water flow process: U.S. Geological Survey Techniques and Methods, book 6, chap. A16, [variously paged]. [Also available at https://pubs.usgs.gov/tm/2005/tm6A16/.]

Hill, M.C., and Tiedeman, C.R., 2007, Effective groundwater model calibration with analysis of data, sensitivities, predictions, and uncertainty: Hoboken, N.J., Wiley-Interscience, 455 p.

Hobza, C.M., Bedrosian, P.A., and Bloss, B.R., 2012, Hydrostratigraphic interpretation of test-hole and surface geophysical data, Elkhorn and Loup River Basins, Nebraska, 2008 to 2011: U.S. Geological Survey Open-File Report 2012–1227, 95 p. [Also available at https://pubs.usgs.gov/of/2012/1227/of2012-1227.pdf.]

Houston, N.A., Gonzales-Bradford, S.L., Flynn, A.T., Qi, S.L., Peterson, S.M., Stanton, J.S., Ryter, D.W., Sohl, T.L., and Senay, G.B., 2013, Geodatabase compilation of hydrogeologic, remote sensing, and water-budget-component data for the High Plains aquifer, 2011: U.S. Geological Survey Data Series 777, 12 p., accessed March 7, 2017, at https://pubs.usgs.gov/ds/777/.

Jenkins, C.T., 1968, Computation of rate and volume of stream depletion by wells: U.S. Geological Survey Techniques of Water-Resources Investigations, book 4, chap. D1, 17 p. [Also available at https://pubs.usgs.gov/twri/twri4d1/pdf/twri_4-D1_a.pdf.]

Johnston, K., Ver Hoef, J.M., Krivoruchko, K., and Lucas, N., 2001, Using ArcGIS Geostatistical Analyst: Redlands, Calif., Esri ArcGIS manual, 278 p.

Konikow, L.F., Hornberger, G.Z., Halford, K.J., and Hanson, R.T., 2009, Revised multi-node well (MNW2) package for MODFLOW ground-water flow model: U.S. Geological Survey Techniques and Methods, book 6, chap. A30, 67 p. [Also available at https://pubs.usgs.gov/tm/tm6a30/.]

McGuire, V.L., and Peterson, S.M., 2009, Base of principal aquifer for the Elkhorn-Loup model area, north-central Nebraska: U.S. Geological Survey Scientific Investigations Map 3042, 1 sheet. [Also available at https://pubs.usgs.gov/sim/3042.]

Mehl, S.W., and Hill, M.C., 2010, MODFLOW–LGR—Modifications to the Streamflow-Routing Package (SFR2) to Route Streamflow through Locally Refined Grids: U.S. Geological Survey Techniques and Methods book 6, chap. A34, 15 p. [Also available at https://water.usgs.gov/nrp/gwsoftware/modflow2005_lgr/tm6a34.pdf]

Mitsch, W.J., and Gosselink, J.G., 2007, The Nebraska Sandhills and Great Plains Playas *in* Wetlands (4): Hoboken, NJ., Wiley, 256p.

Multi-Resolution Land Characteristics Consortium, 2001, National Land Cover Database 2001: U.S. Geological Survey digital data, accessed August 22, 2011, at https://www.mrlc.gov/nlcd01_data.php.

Musgrave, G.W., 1955, How much of the rain enters the soil?: Washington, D.C., U.S. Department of Agriculture, Yearbook of Agriculture, p. 151–159. [Also available at https://naldc.nal.usda.gov/download/IND43894552/PDF.]

National Climatic Data Center, 2012, Locate weather observation station record: National Oceanic and Atmospheric Administration web page, accessed May 5, 2012, at https://www.ncdc.noaa.gov/cdo-web/search.

Nebraska Department of Natural Resources, 1998, 7.5 Digital elevation models—DEM—10 meter—Index for the State of Nebraska: Nebraska Department of Natural Resources, digital data, accessed July 9, 2017, at https://dnr.nebraska.gov/sites/dnr.nebraska.gov/files/doc/data/elevation/DEM.html.

Nebraska Department of Natural Resources, 2002, Natural Resources District Boundary: Nebraska Department of Natural Resources, digital data, accessed October 2, 2017, at https://dnr.nebraska.gov/sites/dnr.nebraska.gov/files/doc/data/boundaries/nrdbnd2.pdf.

Nebraska Department of Natural Resources, 2003, County Boundaries—TIGER 2010: Nebraska Department of Natural Resources, digital data, accessed October 2, 2017, at https://dnr.nebraska.gov/sites/dnr.nebraska.gov/files/doc/data/boundaries/cntybnd.pdf.

Nebraska Department of Natural Resources, 2012, Registered groundwater wells data retrieval: Nebraska Department of Water Resources, digital data, accessed July 19, 2017, at http://nednr.nebraska.gov/dynamic/wells/Menu.aspx.

Nebraska Department of Natural Resources, 2017, Active NeDNR and USGS stream gages/links to gage data: Nebraska Department of Natural Resources, accessed March 3, 2017, at https://nednr.nebraska.gov/RealTime/Gage/Index.

Niswonger, R.G., Panday, S., and Ibaraki, M., 2011, MODFLOW–NWT, A Newton formulation for MODFLOW–2005: U.S. Geological Survey Techniques and Methods, book 6, chap. A37, 44 p. [Also available at https://pubs.usgs.gov/tm/tm6a37/.]

Niswonger, R.G., and Prudic, D.E., 2005, Documentation of the Streamflow-Routing (SFR2) Package to include unsaturated flow beneath streams—A modification to SFR1: U.S. Geological Survey Techniques and Methods, book 6, chap. A13, 47 p. [Also available at https://pubs.usgs.gov/tm/2006/tm6A13/.]

Peterson, S.M., Flynn, A.T., and Traylor, J.P., 2016, Groundwater flow model of the Northern High Plains aquifer in Colorado, Kansas, Nebraska, South Dakota, and Wyoming: U.S. Geological Survey Scientific Investigations Report 2016–5153, 88 p. [Also available at https://doi.org/10.3133/sir20165153.]

Peterson, S.M., Stanton, J.S., Saunders, A.T., and Bradley, J.R., 2008, Simulation of ground-water flow and effects of ground-water irrigation on base flow in the Elkhorn and Loup River Basins, Nebraska: U.S. Geological Survey Scientific Investigations Report 2008–5143, 65 p. [Also available at https://pubs.usgs.gov/sir/2008/5143/.]

Peterson, S.M., and Strauch, K.R., 2007, Streamflow measurements in north-central Nebraska, November 2006: U.S. Geological Survey Data Series 332, 29 p. [Also available at https://pubs.usgs.gov/ds/332/.]

Stanton, J.S., 2013, Base of the upper layer of the phase-three Elkhorn-Loup groundwater-flow model, north-central Nebraska: U.S. Geological Survey Scientific Investigations Map 3259, 1 sheet. [Also available at https://doi.org/10.3133/sim3259.]

Stanton, J.S., Peterson, S.M., and Fienen, M.N., 2010, Simulation of groundwater flow and effects of groundwater irrigation on stream base flow in the Elkhorn and Loup River Basins, Nebraska, 1895–2055—Phase two: U.S. Geological Survey Scientific Investigations Report 2010–5149, 78 p. with app. [Also available at https://pubs.usgs.gov/sir/2010/5149/].

Stanton, J.S., Qi, S.L., Ryter, D.W., Falk, S.E., Houston, N.A., Peterson, S.M., Westenbroek, S.M., and Christenson, S.C., 2011, Selected approaches to estimate water-budget components of the High Plains, 1940 through 1949 and 2000 through 2009: U.S. Geological Survey Scientific Investigations Report 2011–5183, 79 p. [Also available at https://pubs.usgs.gov/sir/2011/5183/.]

Stanton, J.S., Ryter, D.W., and Peterson, S.M., 2012, Effects of linking a soil-water-balance model with a groundwater-flow model: Groundwater, v. 51, no. 4, p. 613–622. [Also available at https://doi.org/10.1111/j.1745-6584.2012.01000.x.]

Strauch, K.R., and Linard, J.I., 2009, Streamflow simulations and percolation estimates using the Soil and Water Assessment Tool for selected basins in North-Central Nebraska, 1940–2005: U.S. Geological Survey Scientific Investigations Report 2009–5075, 20 p. [Also available at https://pubs.usgs.gov/sir/2009/5075/.]

Teeple, A.P., Vrabel, J., Kress, W.H., and Cannia, J.C., 2009, Apparent resistivity and estimated interaction potential of surface water and groundwater along selected canals and streams in the Elkhorn-Loup Model study area, north-central Nebraska, 2006–07: U.S. Geological Survey Scientific Investigations Report 2009–5171, 66 p. [Also available at https://pubs.usgs.gov/sir/2009/5171/.]

Theis, C.V., 1940, The source of water derived from wells: Civil Engineering, v. 10, no. 5, p. 277–280.

Thornthwaite, C.W., and Mather, J.R., 1957, Instructions and tables for computing potential evapotranspiration and the water balance: Philadelphia, Penn., Drexel Institute of Technology, Publications in Climatology, v. 10, no. 3, p. 185–311.

University of Nebraska, 2017, Nebraska statewide test-hole database: University of Nebraska, Institute of Agriculture and Natural Resources, digital data, accessed September 28, 2017, at http://snr.unl.edu/data/geologysoils/NebraskaTestHole/NebraskaTestHoleIntro.aspx.

U.S. Bureau of Reclamation, 2017, Hydromet—RES070 monthly values for period of record: Bureau of Reclamation digital database, accessed March 6, 2017, at https://www.usbr.gov/gp/hydromet/res070.html.

U.S. Department of Agriculture, 2004, Hydrologic soil-cover complexes, chap. 9 *of* Hydrology—National Engineering Handbook, part 630: Washington, DC, U.S. Department of Agriculture, 14 p.

U.S. Department of Agriculture, 2006, United States General Soil Map (STATSGO2): Natural Resources Conservation Service digital data, accessed April 12, 2017, at https://www.nrcs.usda.gov/wps/portal/nrcs/detail/soils/survey/geo/?cid=nrcs142p2_053629.

U.S. Fish and Wildlife Service, 2017, National Wetlands Inventory: U.S. Fish and Wildlife Service digital data, accessed March 7, 2017, at https://www.fws.gov/wetlands/Data/Data-Download.html.

U.S. Geological Survey, 2016a, USGS groundwater data for Nebraska: U.S. Geological Survey database, accessed August 1, 2016, at https://waterdata.usgs.gov/ne/nwis/gw.

U.S. Geological Survey, 2016b, USGS surface-water data for Nebraska: U.S. Geological Survey database, accessed July 30, 2008, at https://waterdata.usgs.gov/ne/nwis/sw.

Wahl, K.L., and Wahl, T.L., 2007, BFI—A computer program for determining an index to base flow (ver. 4.15): Bureau of Reclamation software release, accessed July 23, 2008, at http://www.usbr.gov/pmts/hydraulics_lab/twahl/bfi/.

Watermolen, J., 2005, 1:2,000,000-scale hydrologic unit boundaries (ver. 2.4): Reston, Va., National Atlas of the United States, digital data, accessed December 12, 2017, at https://nationalmap.gov/small_scale/atlasftp.html?openChapters=chpwater#chpwater.

Westenbroek, S.M., Kelson, V.A., Dripps, W.R., Hunt, R.J., and Bradbury, K.R., 2010, SWB—A modified Thornthwaite-Mather Soil-Water-Balance code for estimating groundwater recharge: U.S. Geological Survey Techniques and Methods, book 6, chap. A31, 60 p. [Also available at https://pubs.usgs.gov/tm/tm6-a31/.]

Appendix Figures

Graphs of estimated and simulated stream base flows for four streamgages were included in the "Calibration Targets and Results, Stream Base Flows" section (fig. 13). Data from 235 streamgages were used as calibration targets. Of these streamgages, 184 were single-measurement stations. A total of 51 of the streamgages contained a record of more than two measurements. The locations of the 51 streamgages are shown on figure 1.1. The multi-measurement streamgage graphs are presented herein for additional detail (figs. 1.2 to 1.52). These graphs show that the simulation reproduced the observed temporal trends in base flow, as shown by the local weighted regression (LOWESS) curves on the graphs (Cleveland, 1979; Cleveland and Devlin, 1988). LOWESS curves were used to visually compare the trends of simulated and estimated base flow to ensure the model was properly capturing groundwater discharge to streams.

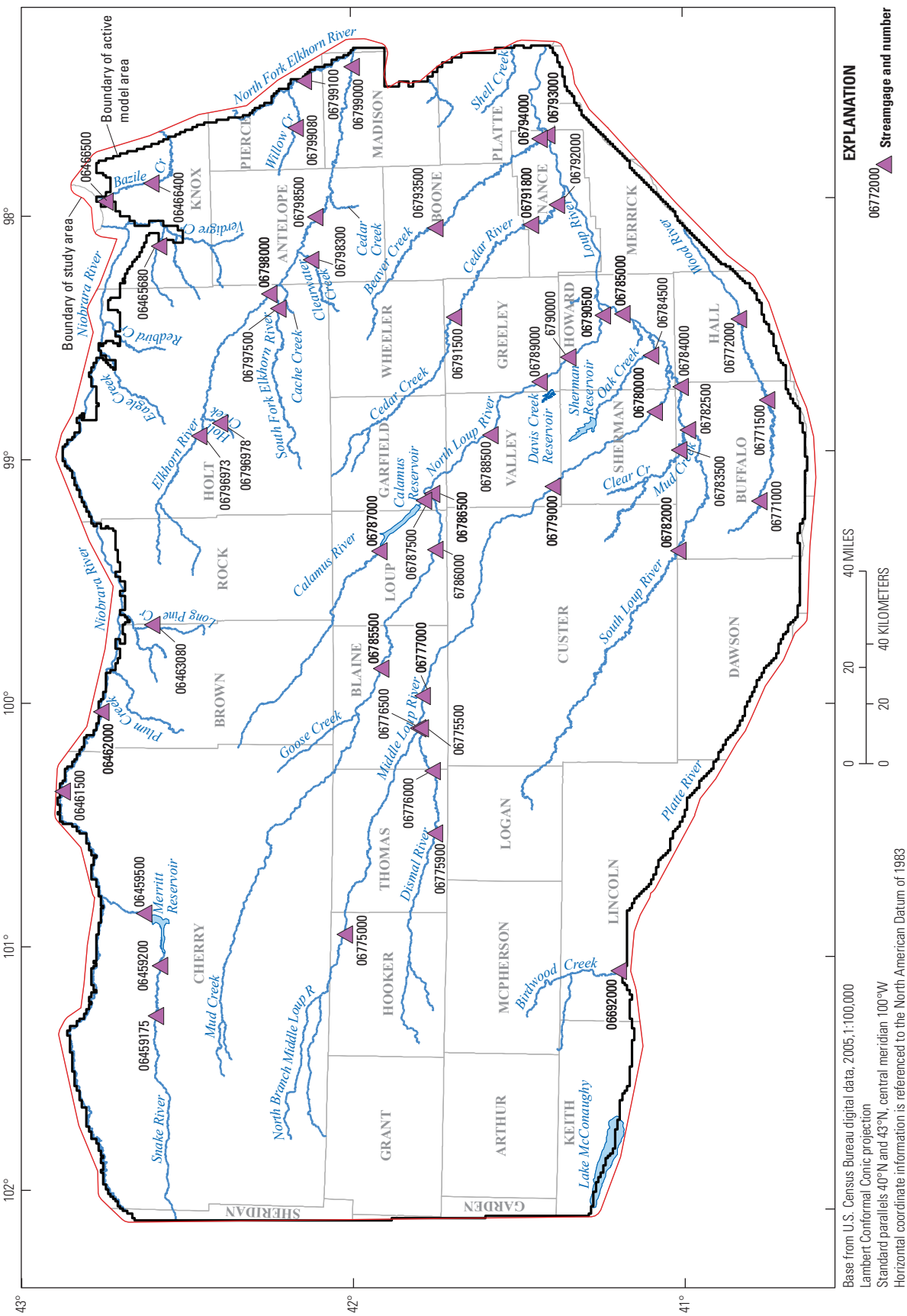

Figure 1.1. Location of multimeasurement streamgages used for calibration in phase three, Elkhorn and Loup River Basins, Nebraska.

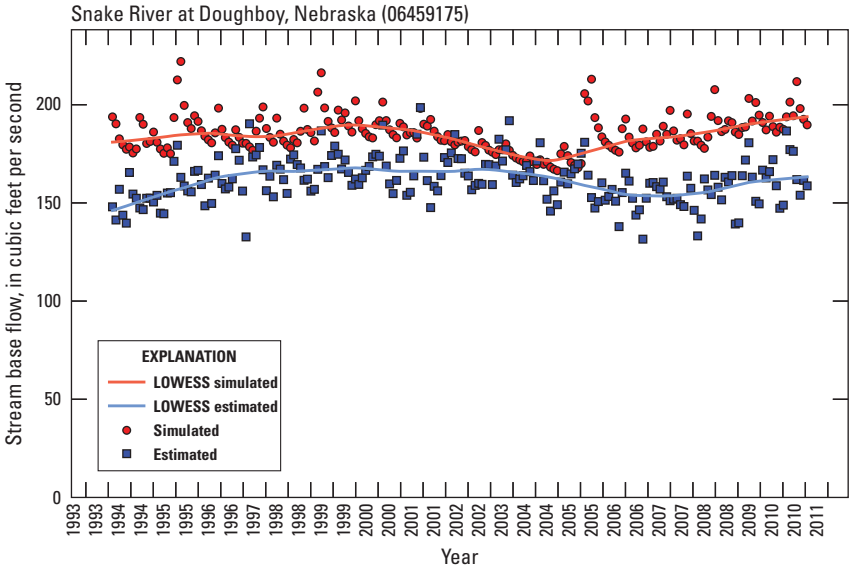

Figure 1.2. Snake River at Doughboy, Nebraska (U.S. Geological Survey streamgage 06459175).

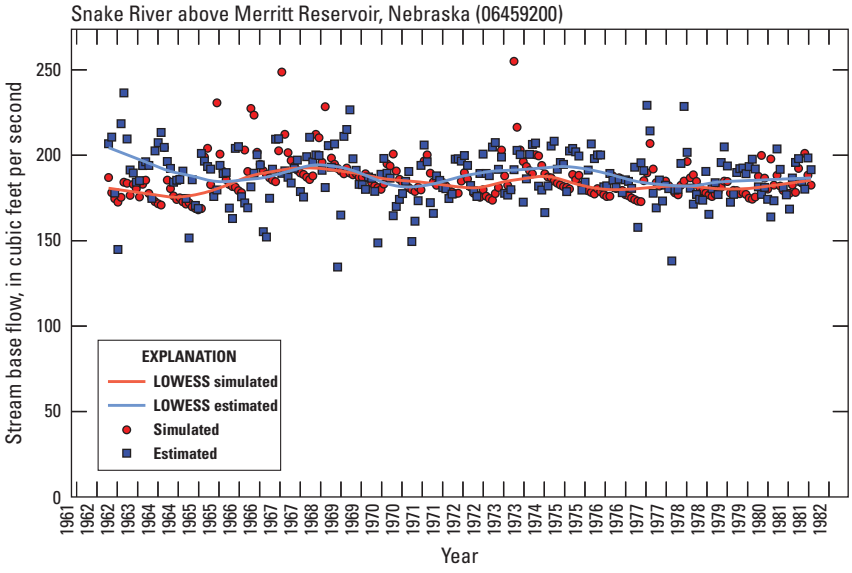

Figure 1.3. Snake River above Merritt Reservoir, Nebraska (U.S. Geological Survey streamgage 06459200).

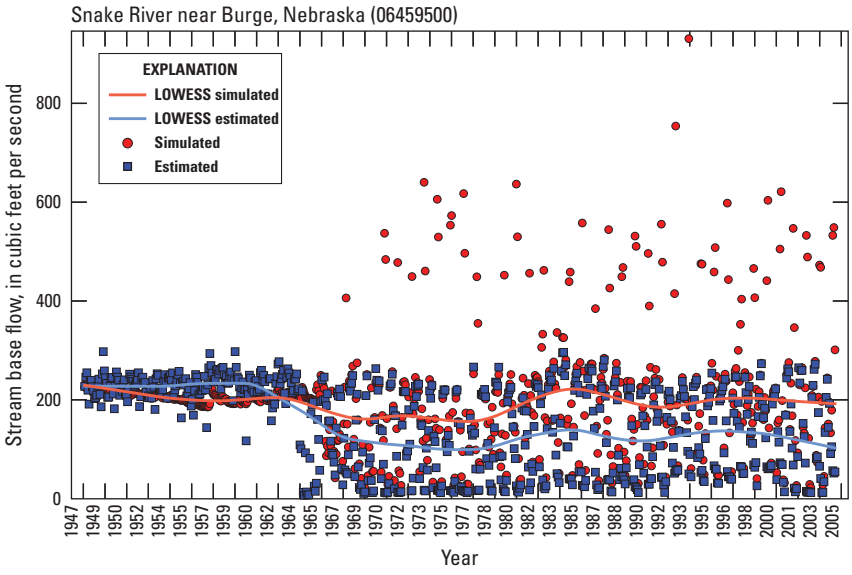

Figure 1.4. Snake River near Burge, Nebraska (U.S. Geological Survey streamgage 06459500).

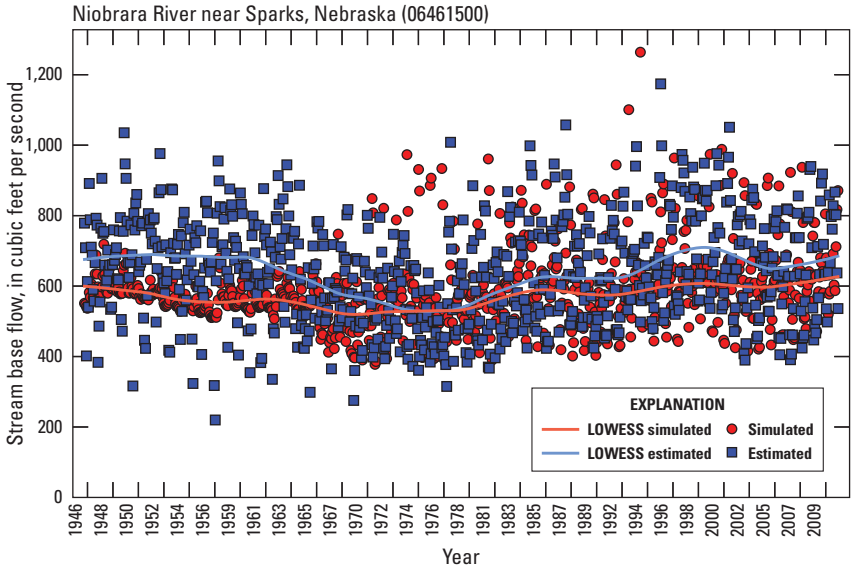

Figure 1.5. Niobrara River near Sparks, Nebraska (U.S. Geological Survey streamgage 06461500).

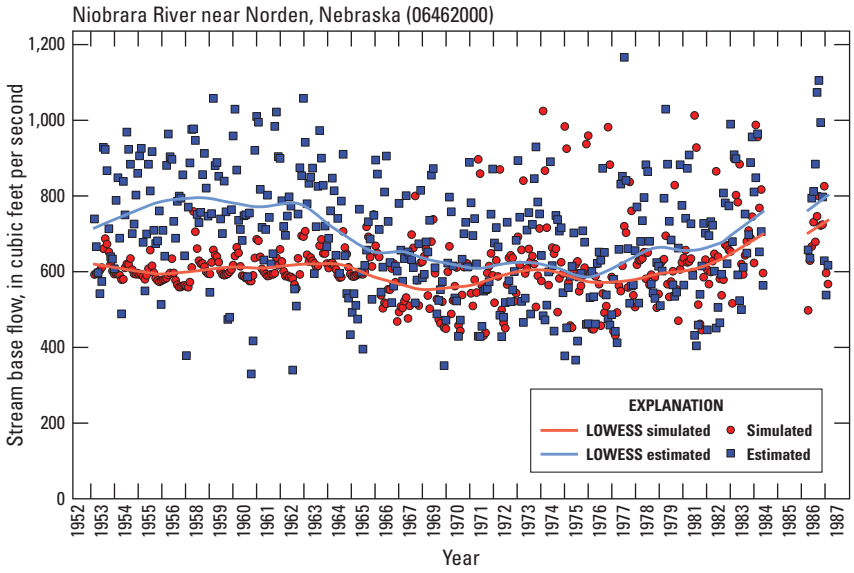

Figure 1.6. Niobrara River near Norden, Nebraska (U.S. Geological Survey streamgage 06462000).

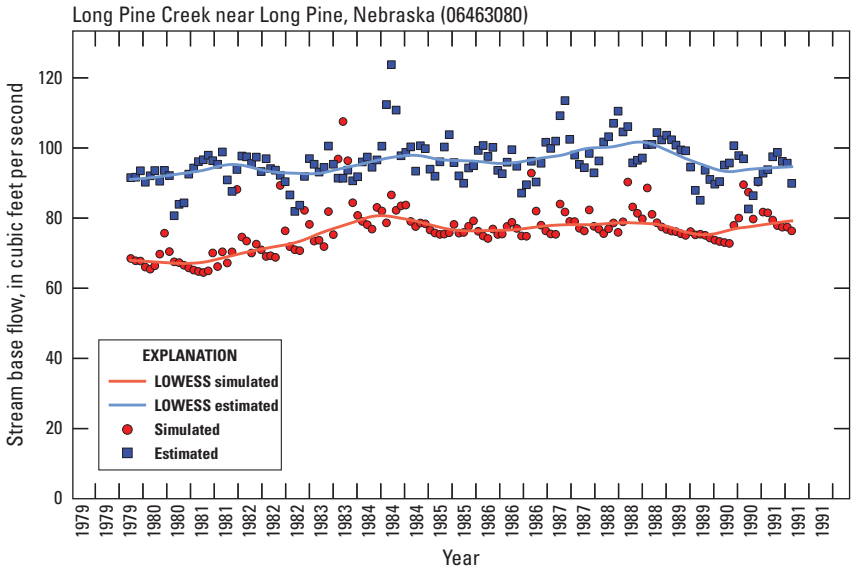

Figure 1.7. Long Pine Creek near Long Pine, Nebraska (U.S. Geological Survey streamgage 06463080).

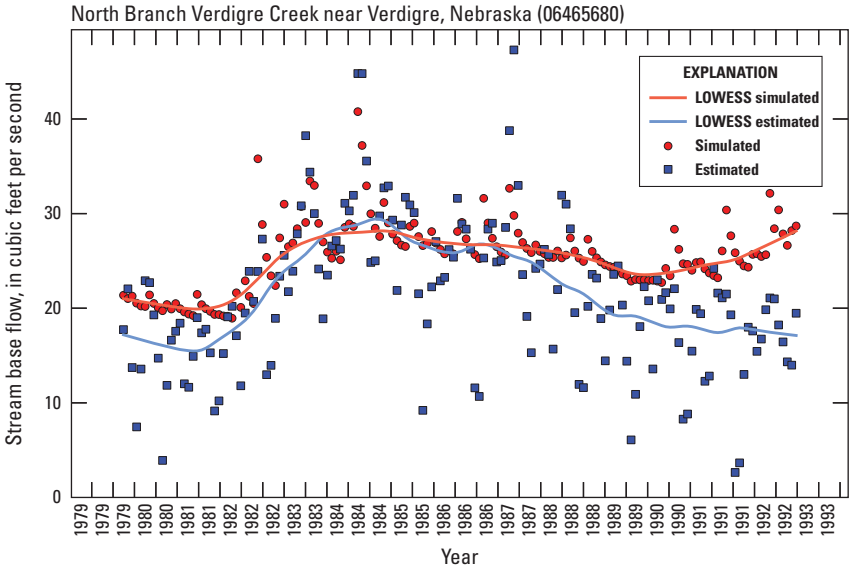

Figure 1.8. North Branch Verdigre Creek near Verdigre, Nebraska (U.S. Geological Survey streamgage 06465680).

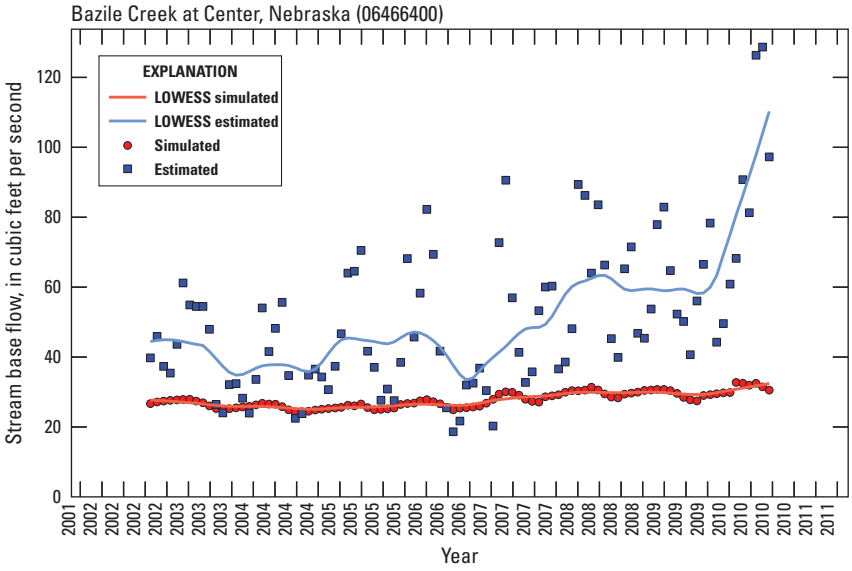

Figure 1.9. Bazile Creek at Center, Nebraska (U.S. Geological Survey streamgage 06466400).

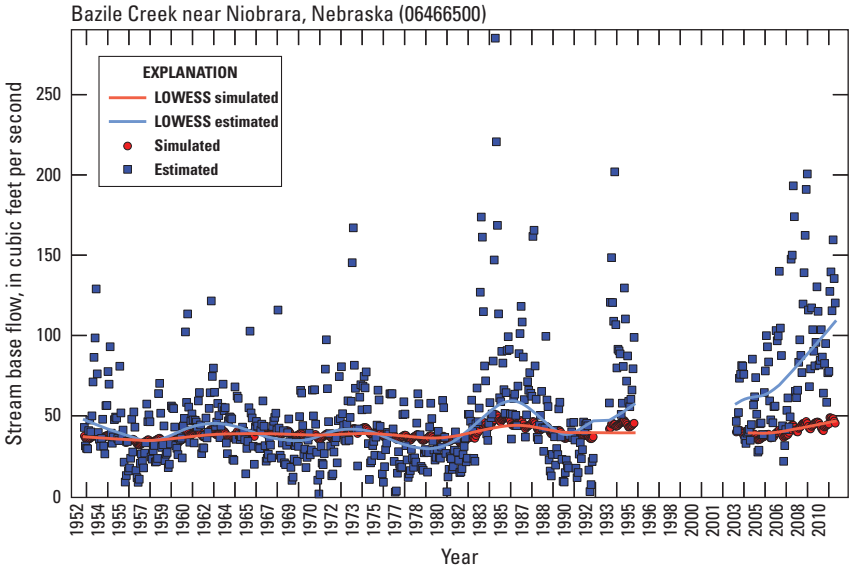

Figure 1.10. Bazile Creek near Niobrara, Nebraska (U.S. Geological Survey streamgage 06466500).

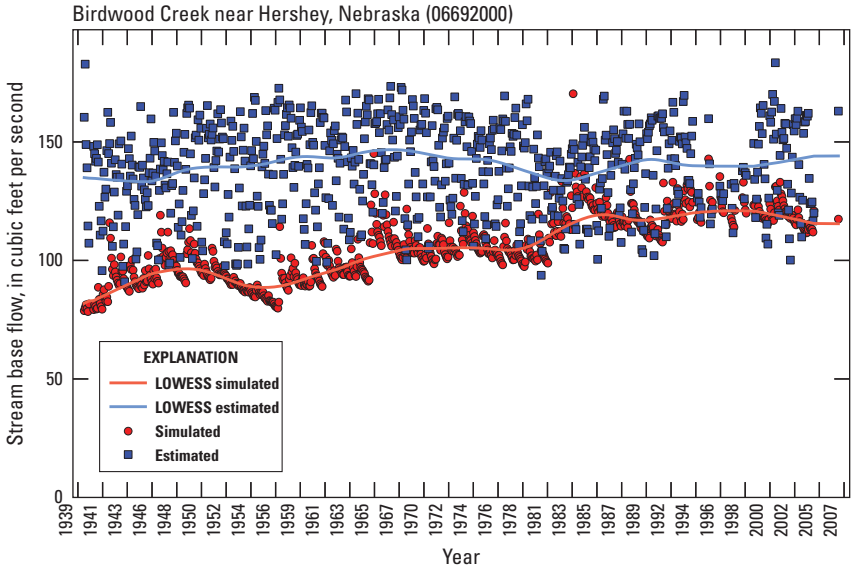

Figure 1.11. Birdwood Creek near Hershey, Nebraska (U.S. Geological Survey streamgage 06692000).

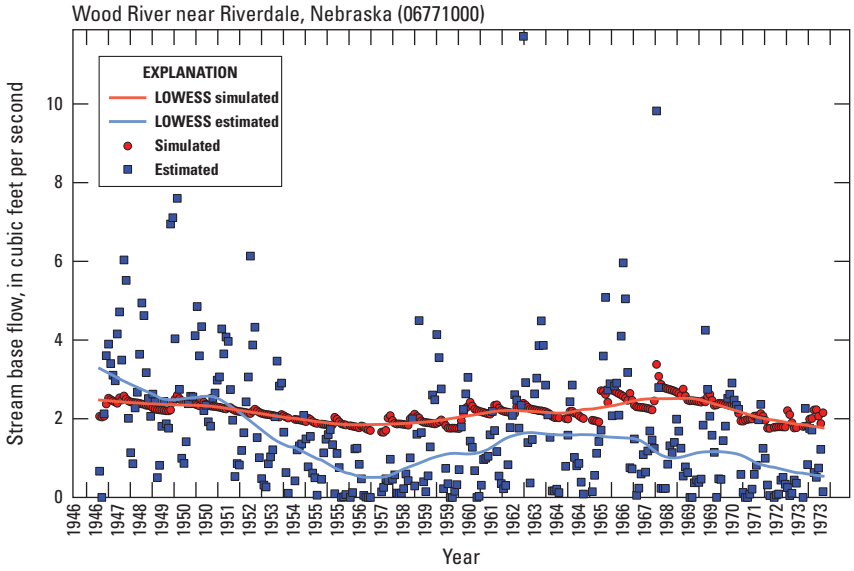

Figure 1.12. Wood River near Riverdale, Nebraska (U.S. Geological Survey streamgage 06771000).

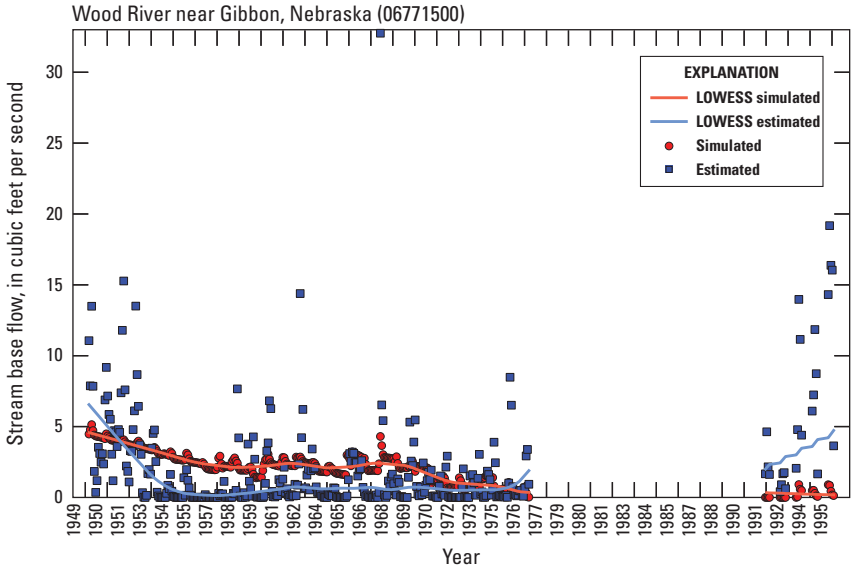

Figure 1.13. Wood River near Gibbon, Nebraska (U.S. Geological Survey streamgage 06771500).

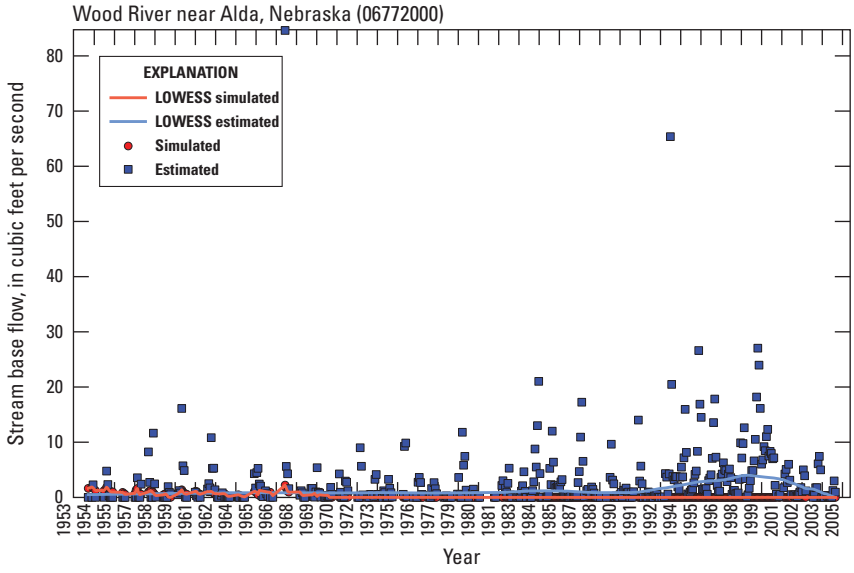

Figure 1.14. Wood River near Alda, Nebraska (U.S. Geological Survey streamgage 06772000).

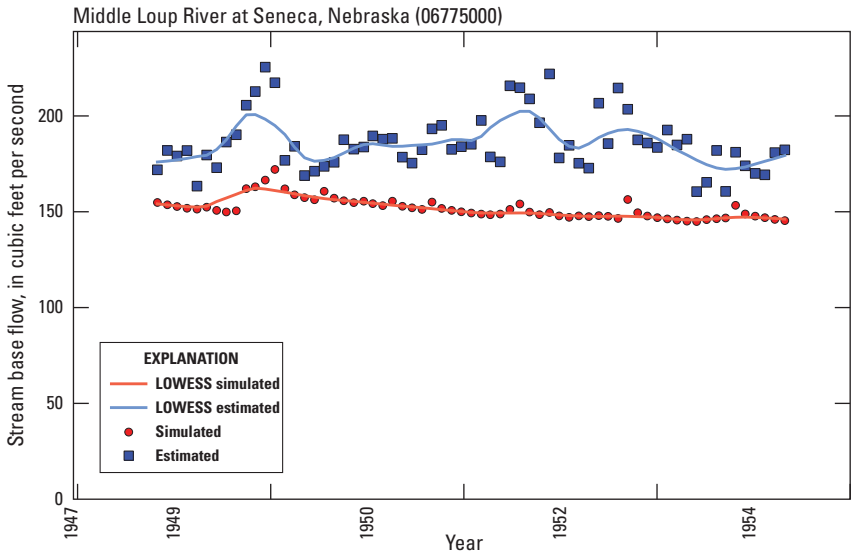

Figure 1.15. Middle Loup River at Seneca, Nebraska (U.S. Geological Survey streamgage 06775000).

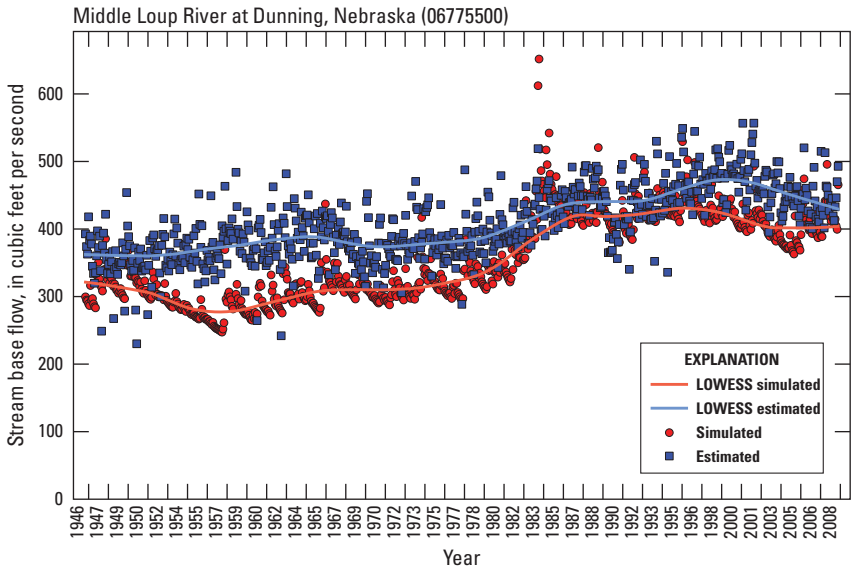

Figure 1.16. Middle Loup River at Dunning, Nebraska (U.S. Geological Survey streamgage 06775500).

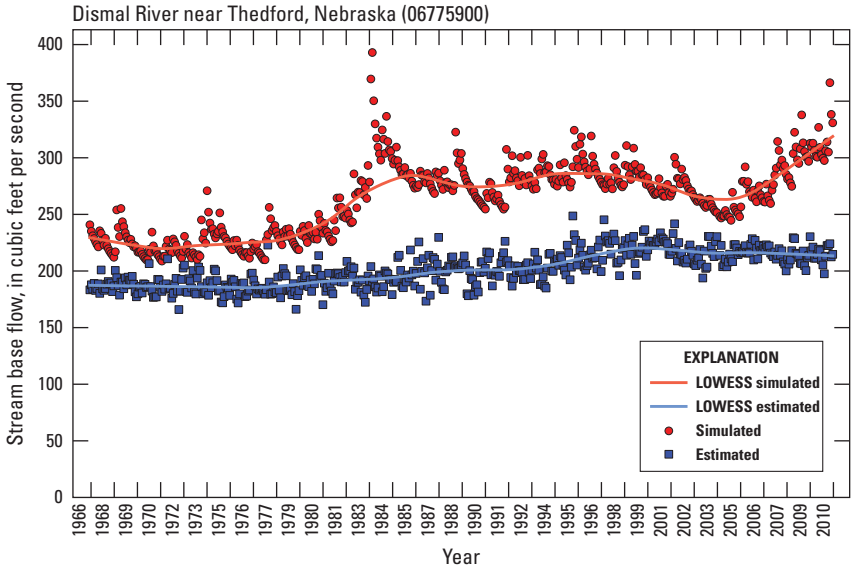

Figure 1.17. Dismal River at Thedford, Nebraska (U.S. Geological Survey streamgage 06775900).

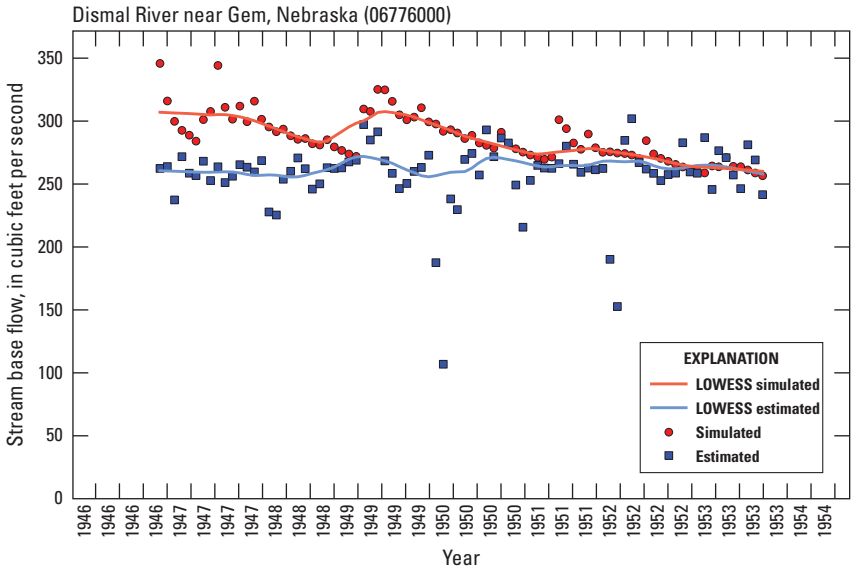

Figure 1.18. Dismal River near Gem, Nebraska (U.S. Geological Survey streamgage 06776000).

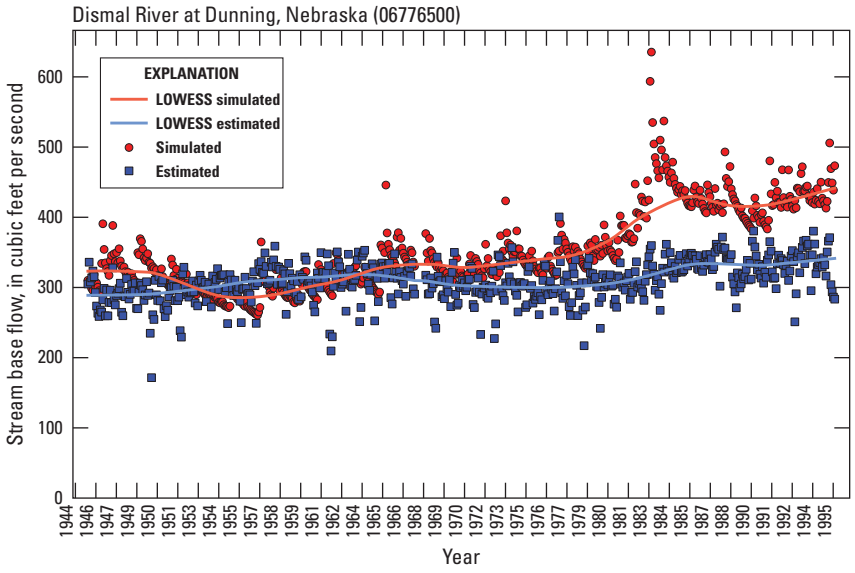

Figure 1.19. Dismal River at Dunning, Nebraska (U.S. Geological Survey streamgage 06776500).

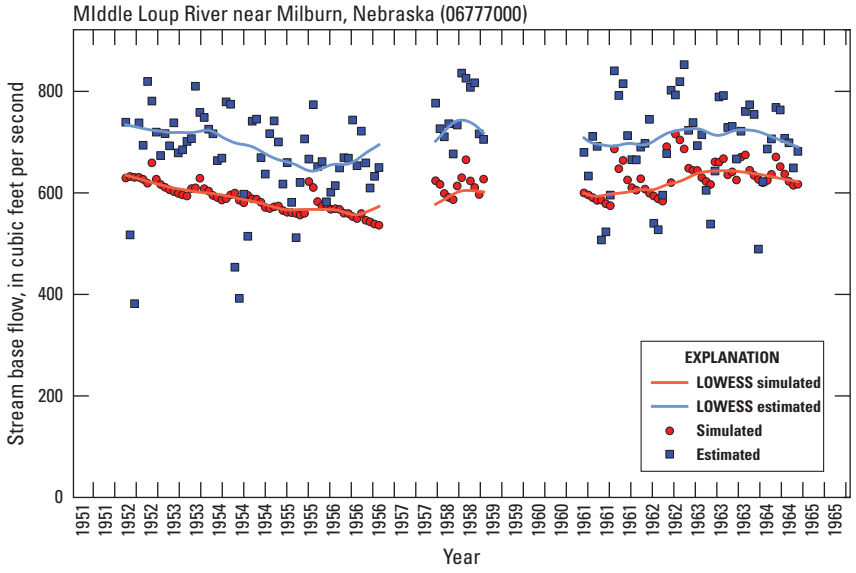

Figure 1.20. Middle Loup River near Milburn, Nebraska (U.S. Geological Survey streamgage 06777000).

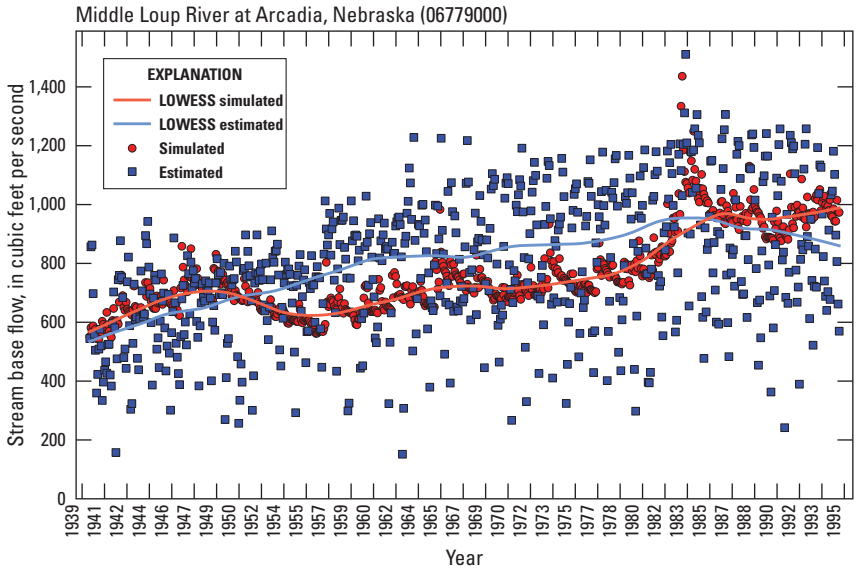

Figure 1.21. Middle Loup River at Arcadia, Nebraska (U.S. Geological Survey streamgage 06779000).

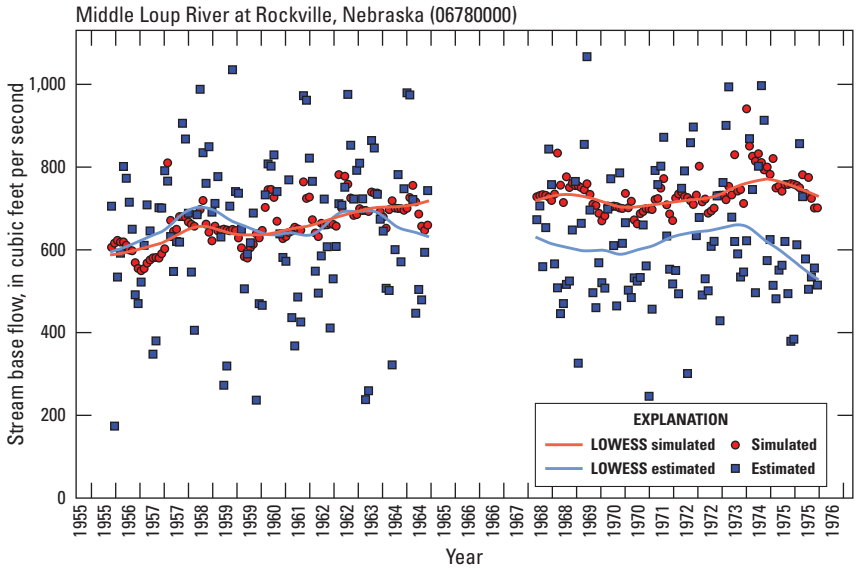

Figure 1.22. Middle Loup River at Rockville, Nebraska (U.S. Geological Survey streamgage 06780000).

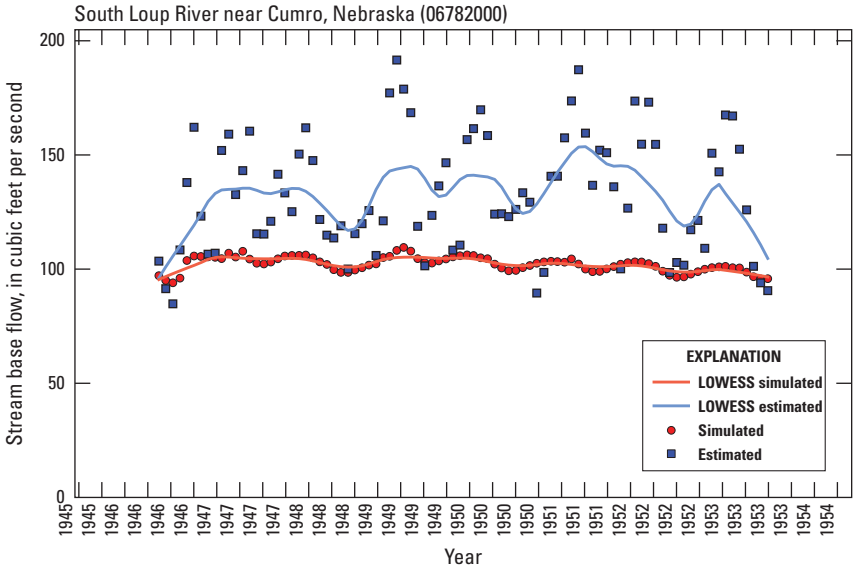

Figure 1.23. South Loup River near Cumro, Nebraska (U.S. Geological Survey streamgage 06782000).

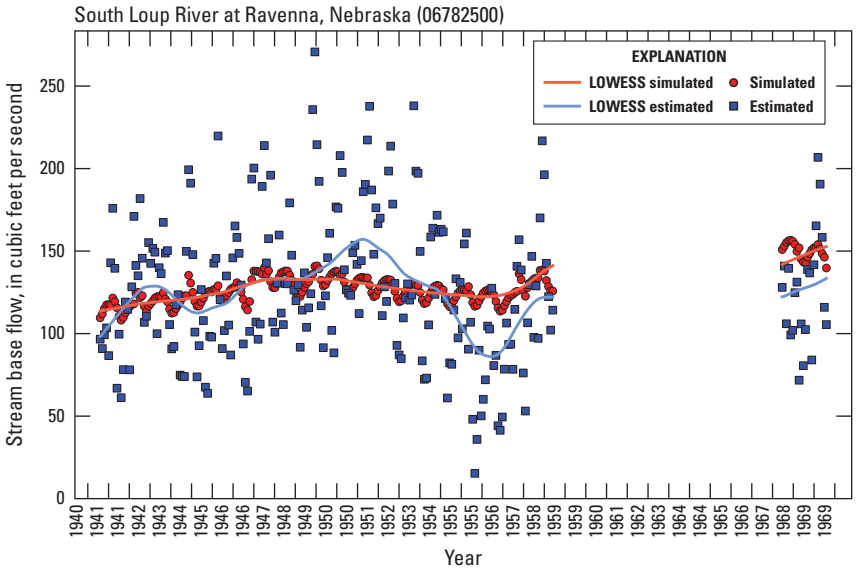

Figure 1.24. South Loup River at Ravenna, Nebraska (U.S. Geological Survey streamgage 06782500).

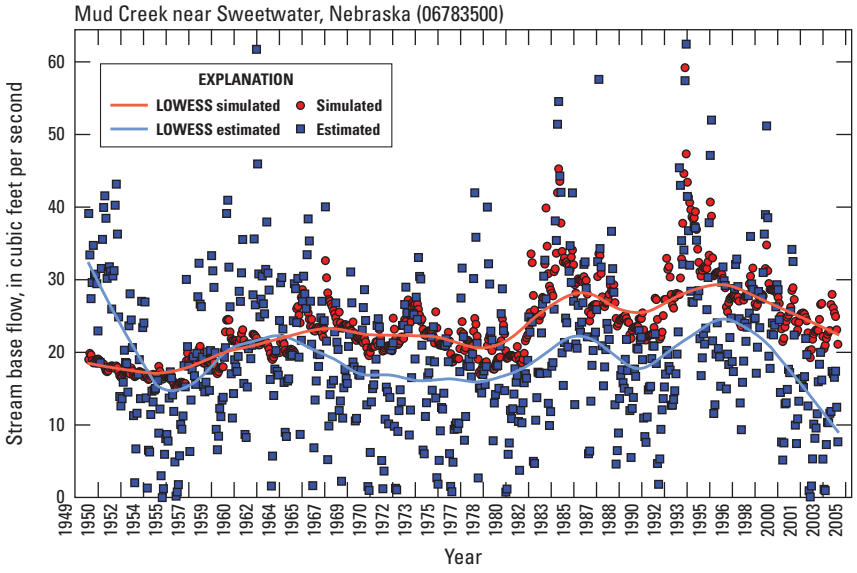

Figure 1.25. Mud Creek near Sweetwater, Nebraska (U.S. Geological Survey streamgage 06783500).

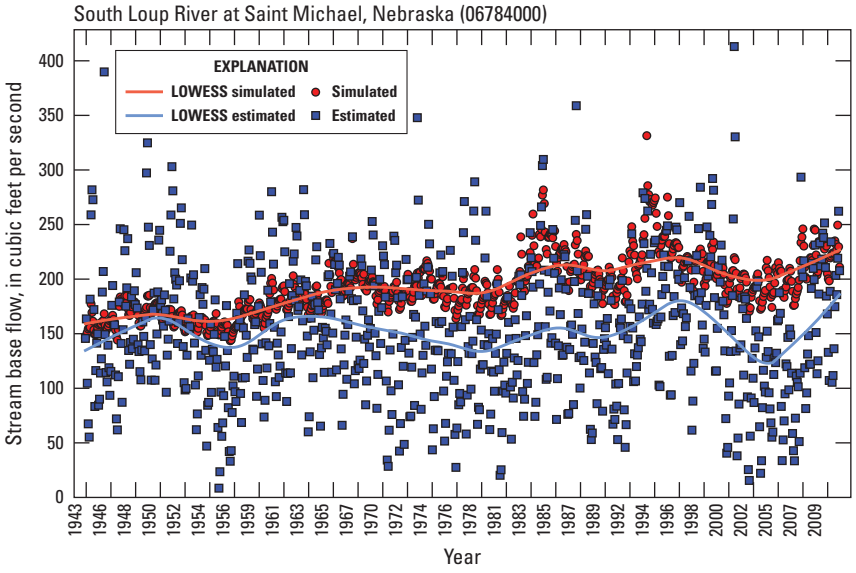

Figure 1.26. South Loup River at Saint Michael, Nebraska (U.S. Geological Survey streamgage 06784000).

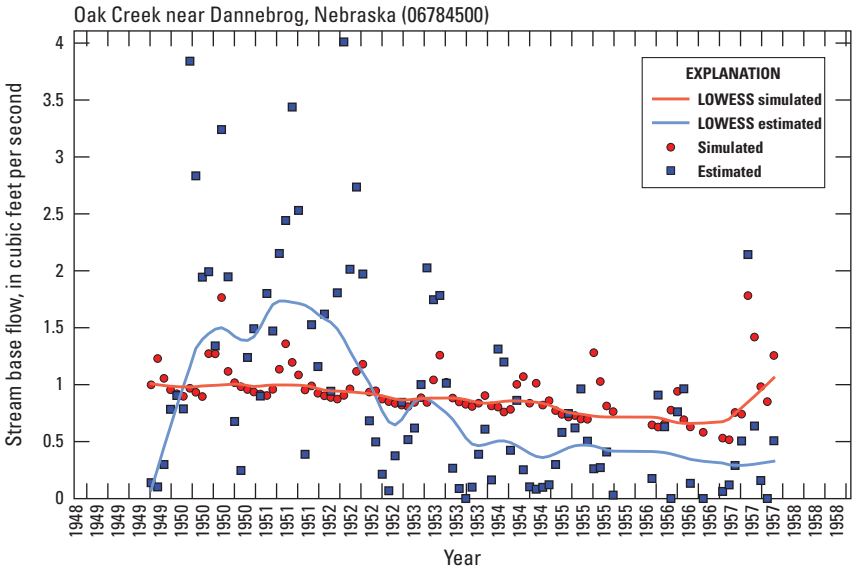

Figure 1.27. Oak Creek near Dannebrog, Nebraska (U.S. Geological Survey streamgage 06784500).

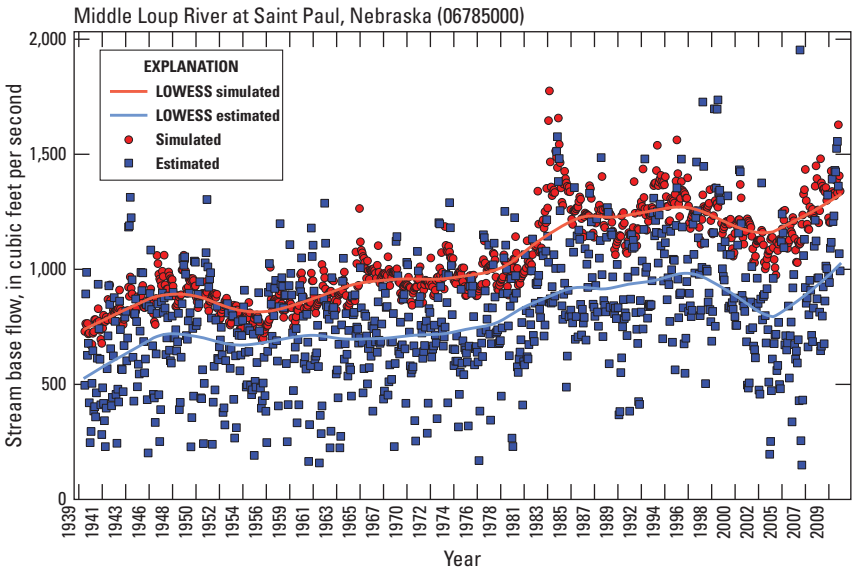

Figure 1.28. Middle Loup River near Saint Paul, Nebraska (U.S. Geological Survey streamgage 06785000).

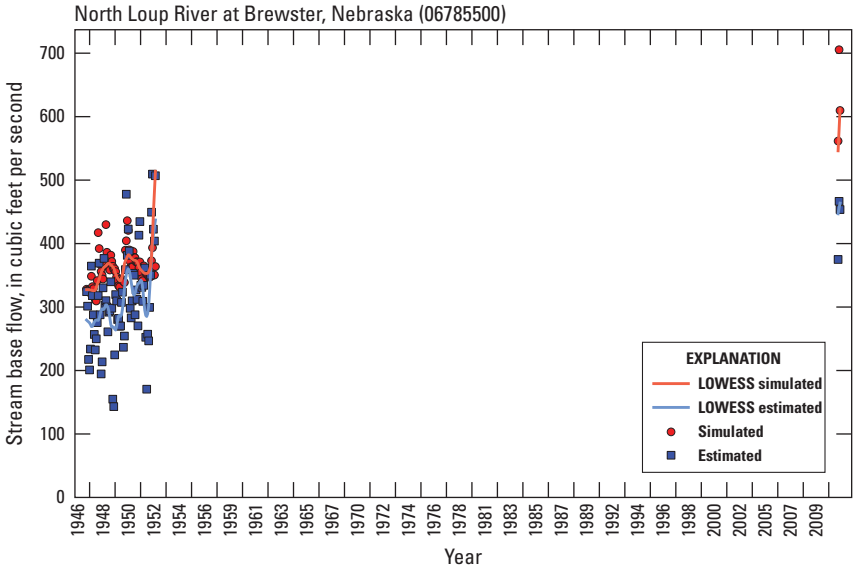

Figure 1.29. North Loup River near Brewster, Nebraska (U.S. Geological Survey streamgage 06785500).

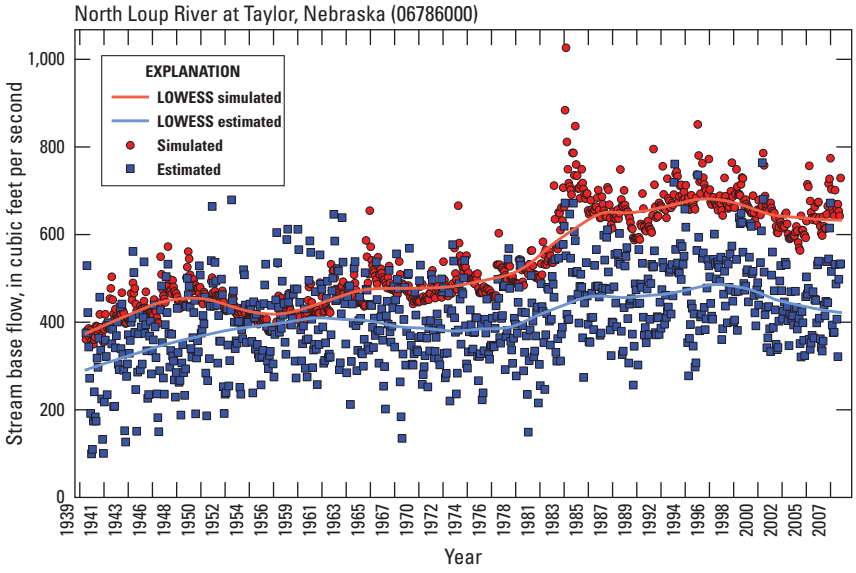

Figure 1.30. North Loup River at Taylor, Nebraska (U.S. Geological Survey streamgage 06786000).

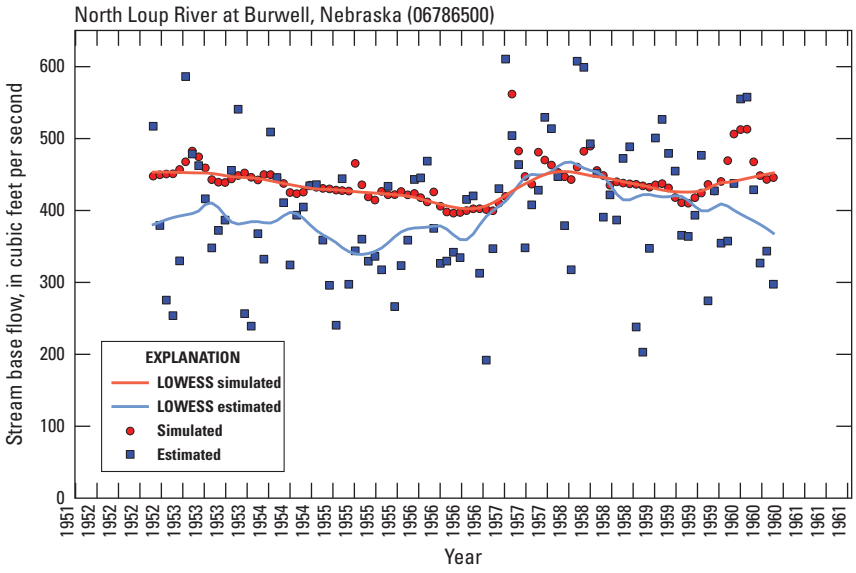

Figure 1.31. North Loup River at Burwell, Nebraska (U.S. Geological Survey streamgage 06786500).

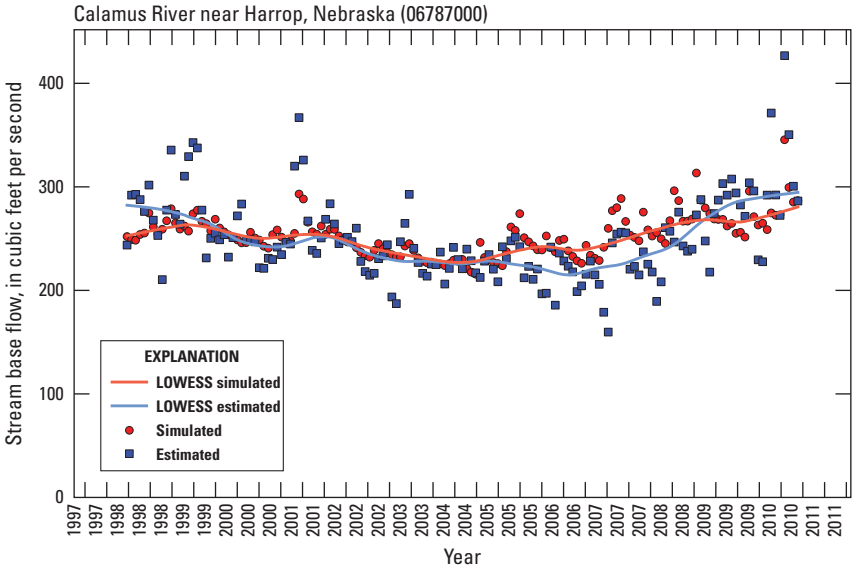

Figure 1.32. Calamus River near Harrop, Nebraska (U.S. Geological Survey streamgage 06787000).

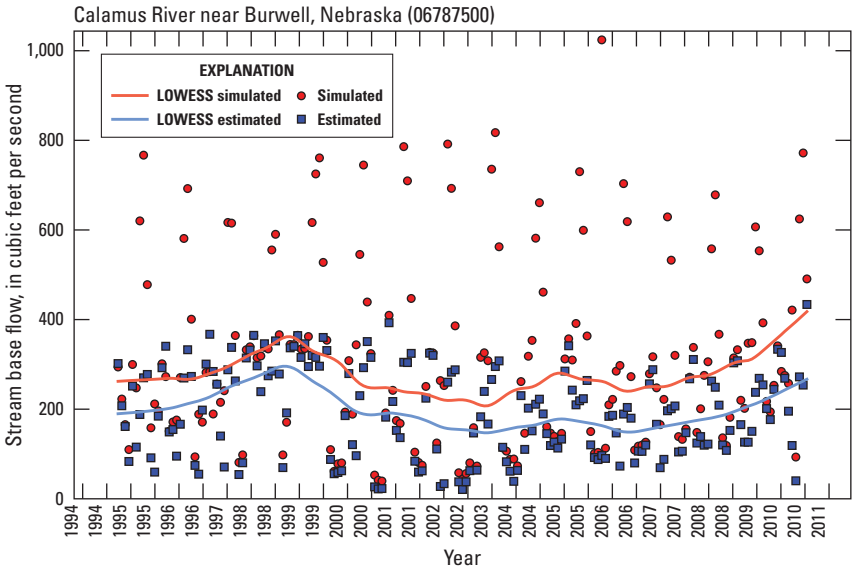

Figure 1.33. Calamus River near Burwell, Nebraska (U.S. Geological Survey streamgage 06787500).

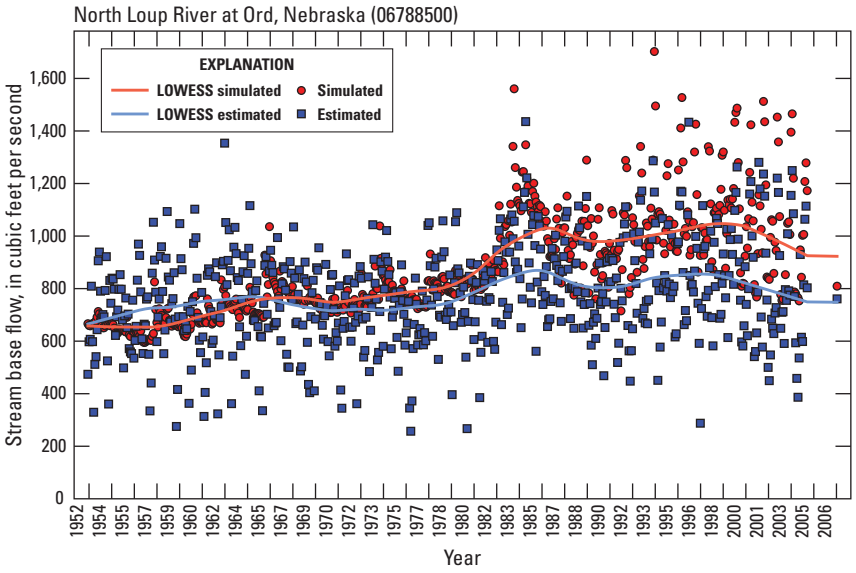

Figure 1.34. North Loup River at Ord, Nebraska (U.S. Geological Survey streamgage 06788500).

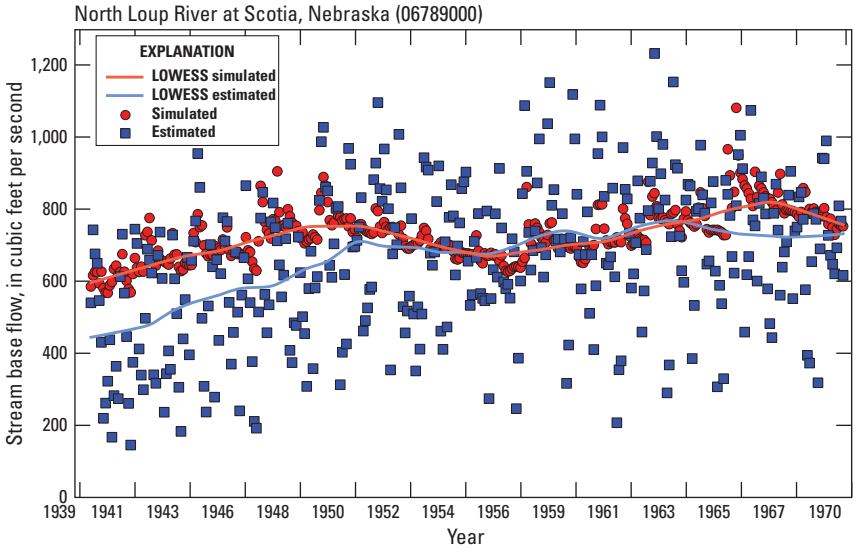

Figure 1.35. North Loup River at Scotia, Nebraska (U.S. Geological Survey streamgage 06788500).

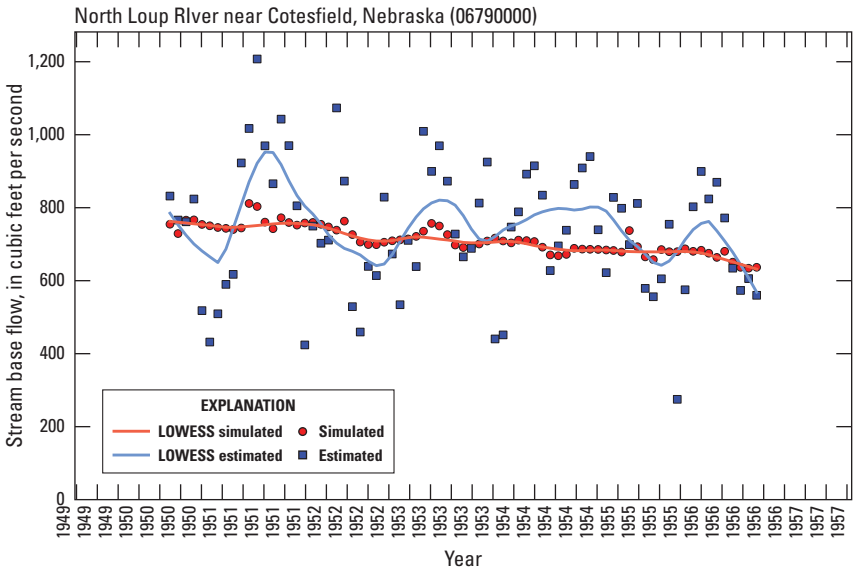

Figure 1.36. North Loup River near Cotesfield, Nebraska (U.S. Geological Survey streamgage 06790000).

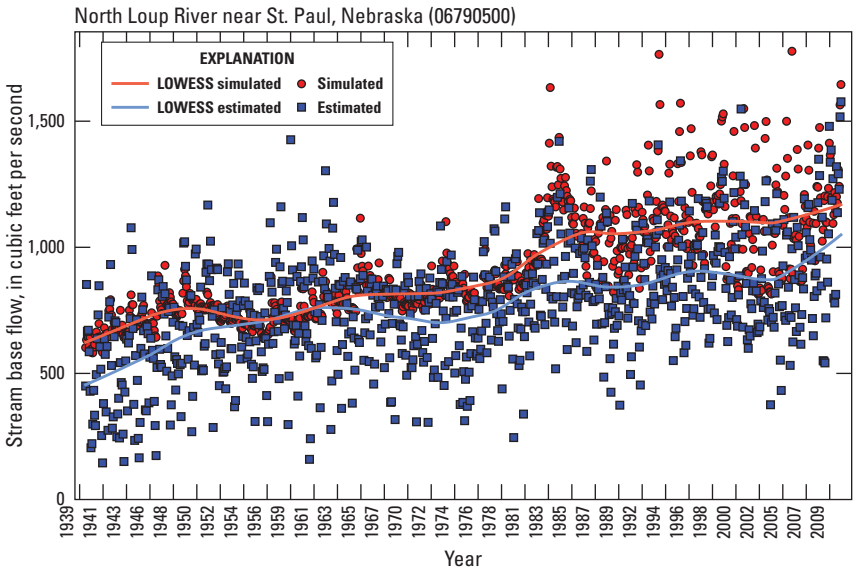

Figure 1.37. North Loup River near Saint Paul, Nebraska (U.S. Geological Survey streamgage 06790500).

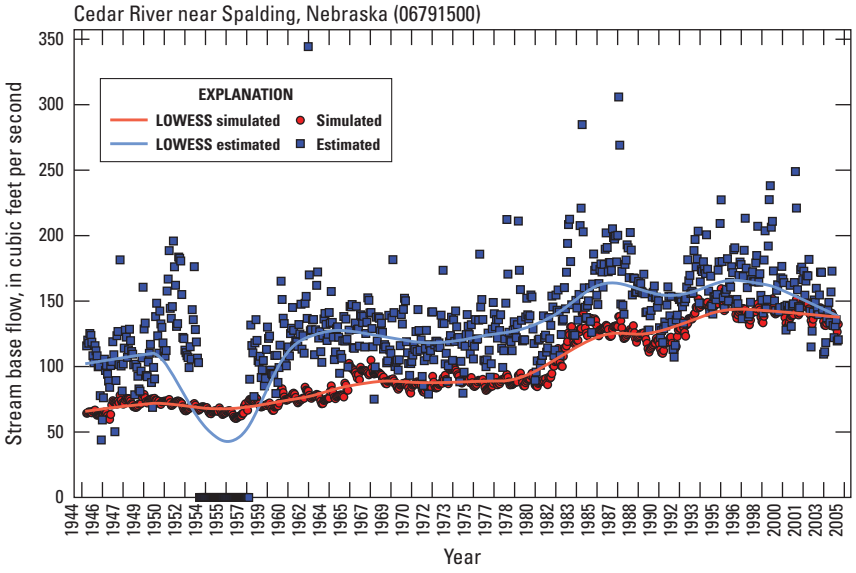

Figure 1.38. Cedar River near Spaulding, Nebraska (U.S. Geological Survey streamgage 06791500).

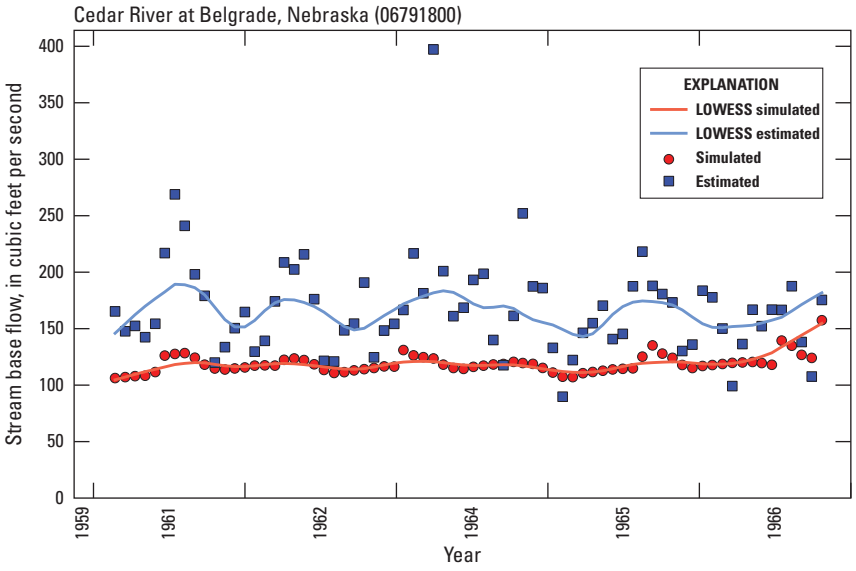

Figure 1.39. Cedar River at Belgrade, Nebraska (U.S. Geological Survey streamgage 06791800).

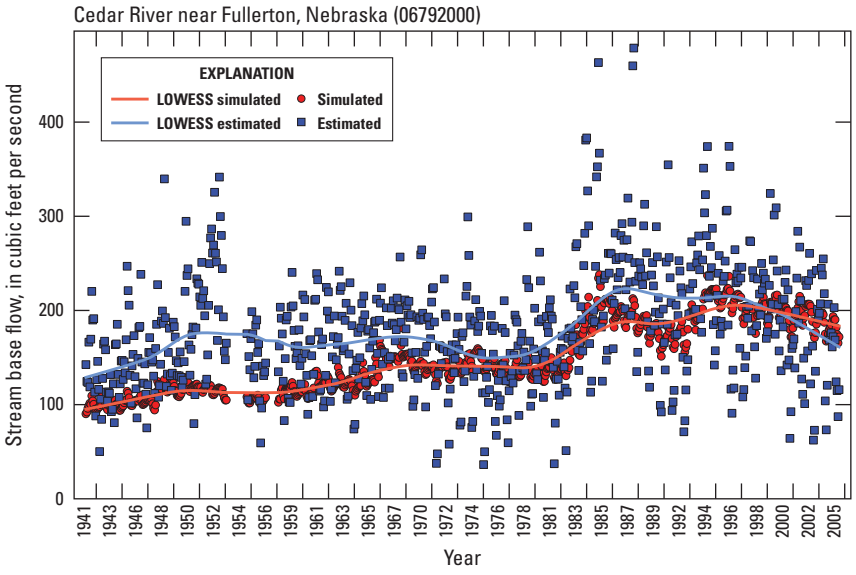

Figure 1.40. Cedar River near Fullerton, Nebraska (U.S. Geological Survey streamgage 06792000).

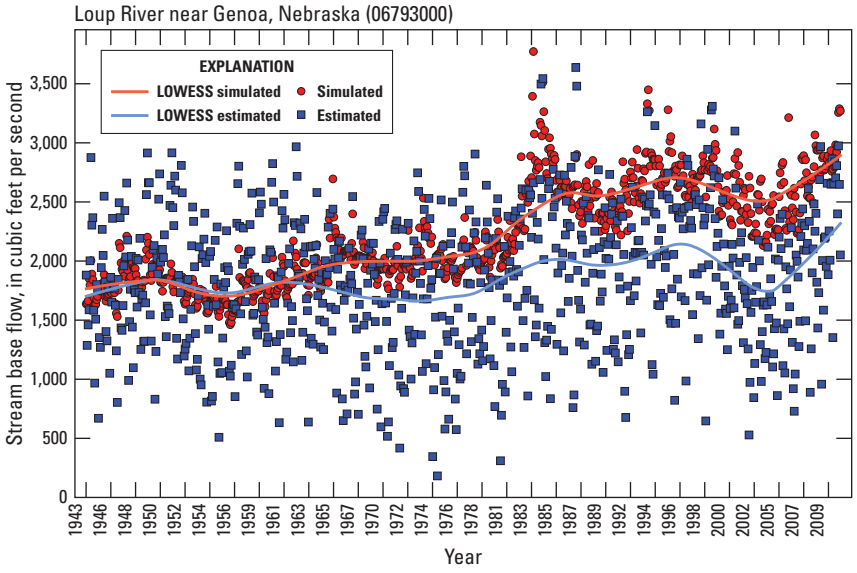

Figure 1.41. Loup River near Genoa, Nebraska (U.S. Geological Survey streamgage 06793000).

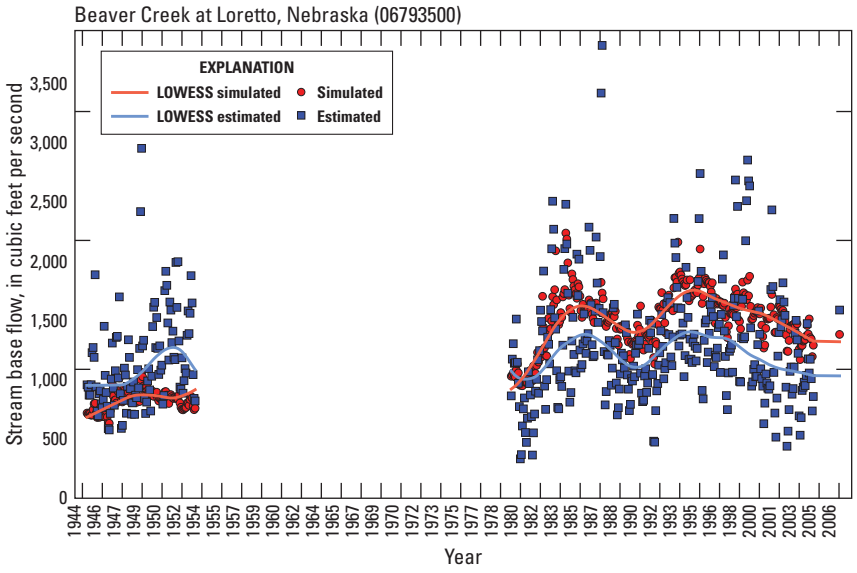

Figure 1.42. Beaver Creek at Loretto, Nebraska (U.S. Geological Survey streamgage 06793500).

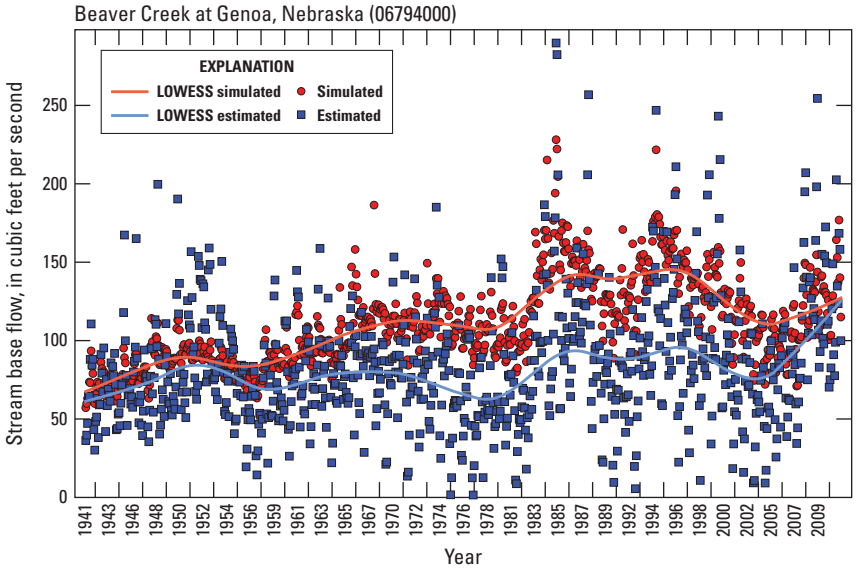

Figure 1.43. Beaver Creek at Genoa, Nebraska (U.S. Geological Survey streamgage 06794000).

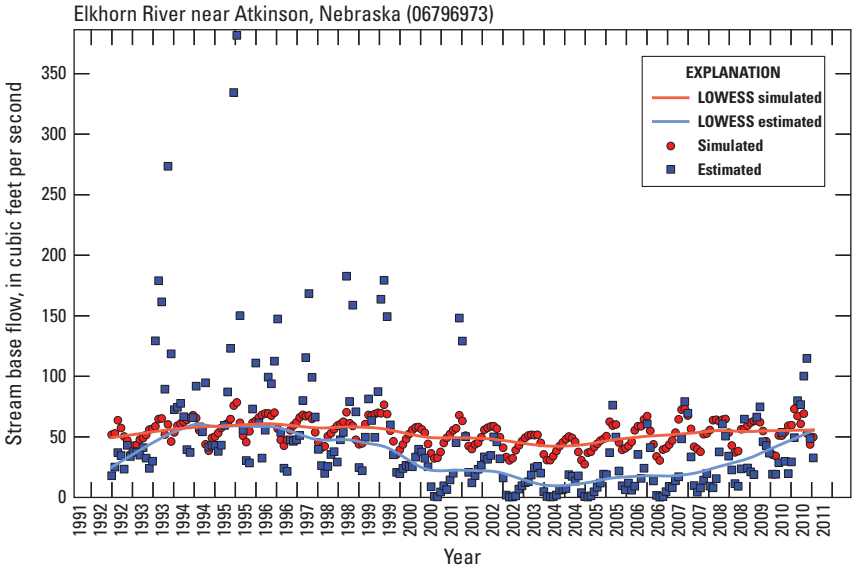

Figure 1.44. Elkhorn River near Atkinson, Nebraska (U.S. Geological Survey streamgage 06796973).

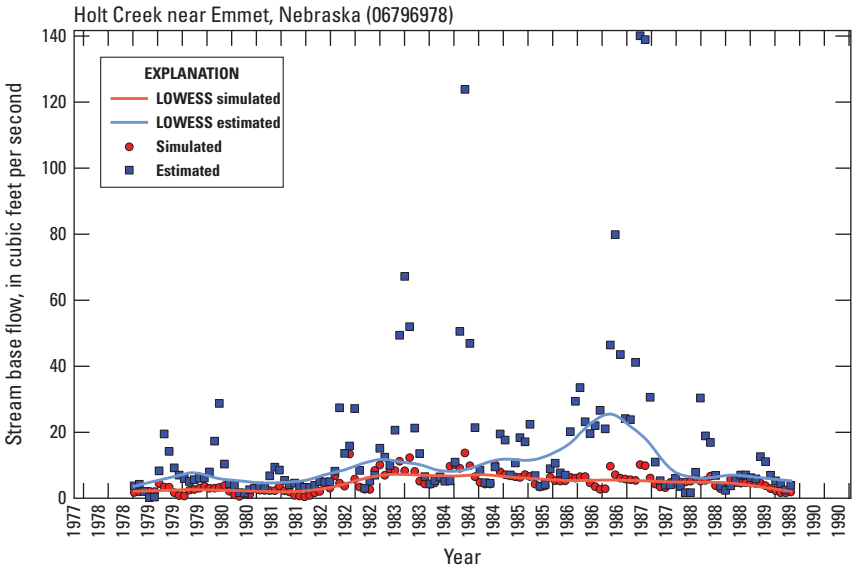

Figure 1.45. Holt Creek near Emmet, Nebraska (U.S. Geological Survey streamgage 06796978).

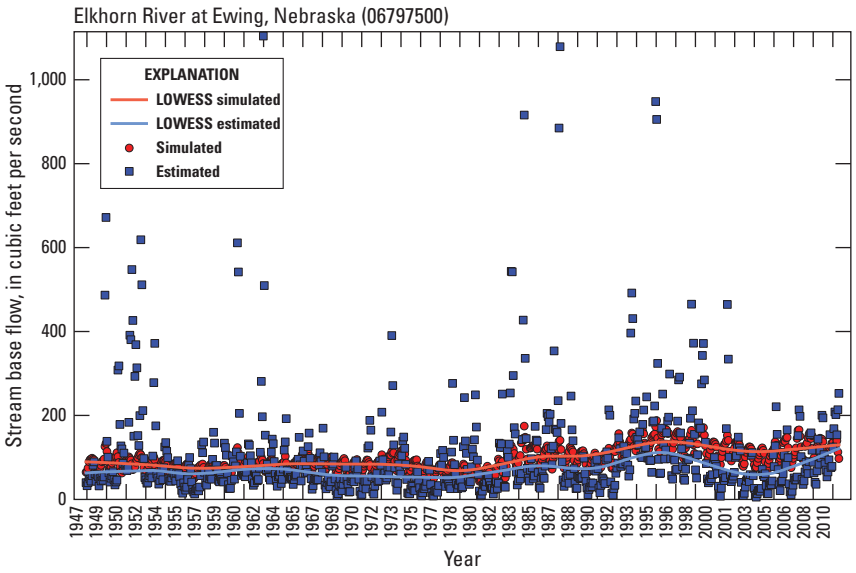

Figure 1.46. Elkhorn River at Ewing, Nebraska (U.S. Geological Survey streamgage 06797500).

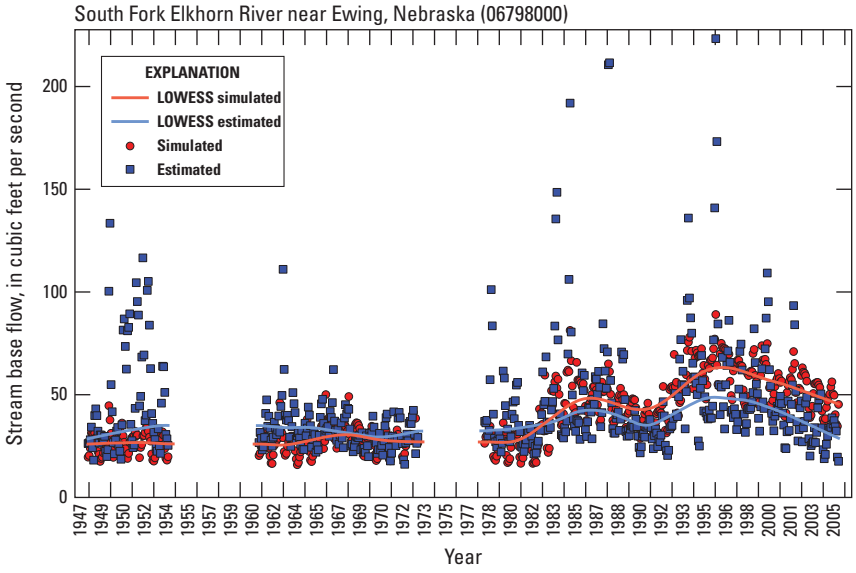

Figure 1.47. South Fork Elkhorn River near Ewing, Nebraska (U.S. Geological Survey streamgage 06798000).

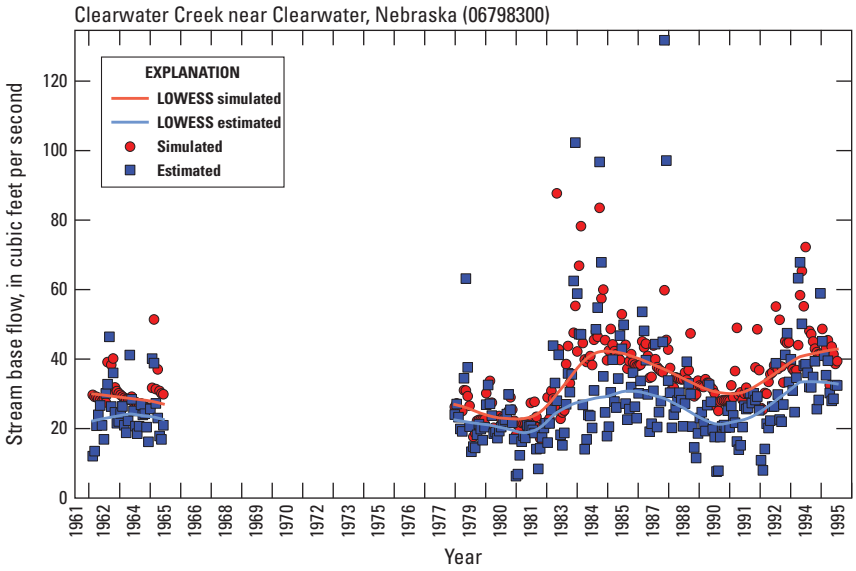

Figure 1.48. Clearwater Creek near Clearwater, Nebraska (U.S. Geological Survey streamgage 06798300).

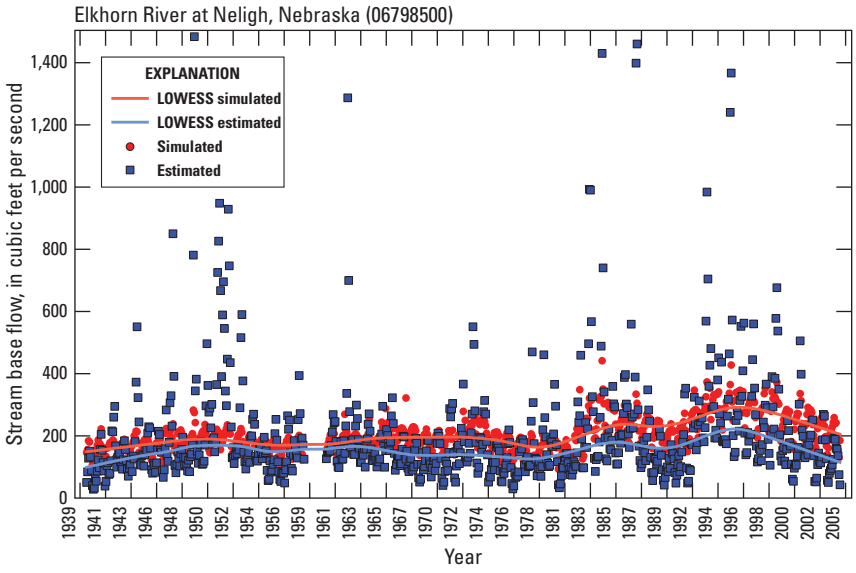

Figure 1.49. Elkhorn River at Neligh, Nebraska (U.S. Geological Survey streamgage 06798500).

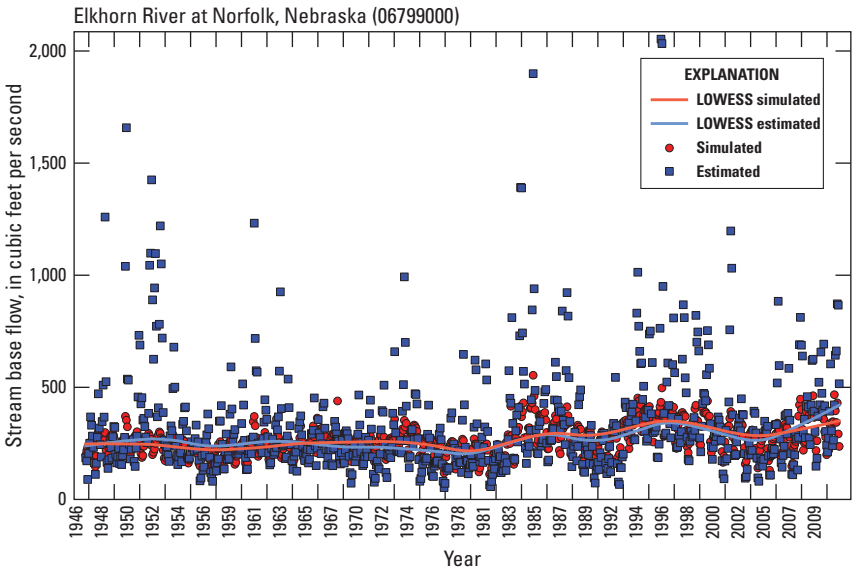

Figure 1.50. Elkhorn River at Norfolk, Nebraska (U.S. Geological Survey streamgage 06799000).

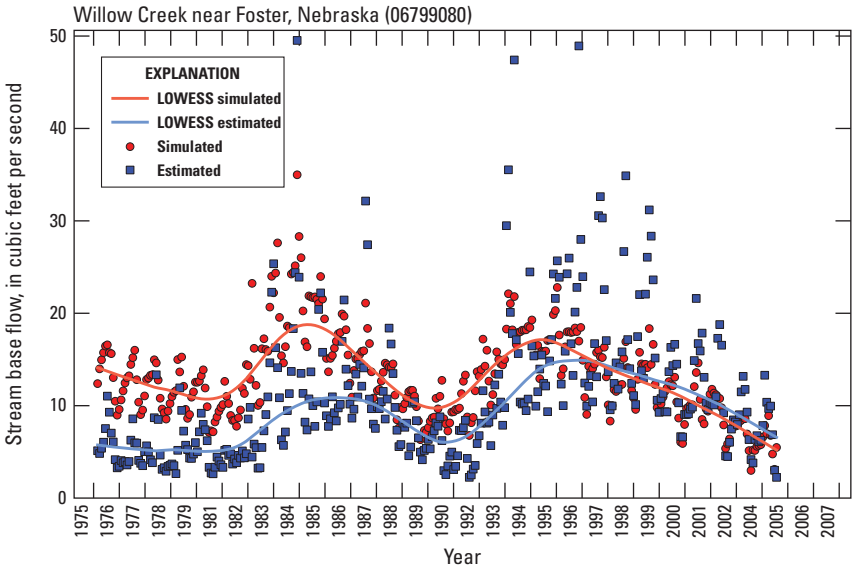

Figure 1.51. Willow Creek near Foster, Nebraska (U.S. Geological Survey streamgage 06799080).

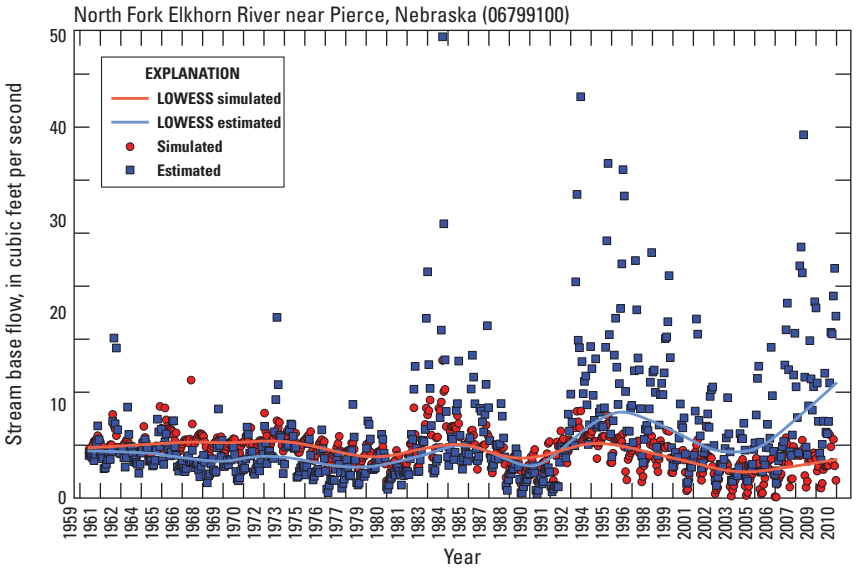

Figure 1.52. North Fork Elkhorn River near Pierce, Nebraska (U.S. Geological Survey streamgage 06799100).

For more information about this publication, contact
Director, USGS Nebraska Water Science Center
5231 South 19th Street
Lincoln, NE 68512
(402) 328–4100

For additional information visit https://www.usgs.gov/centers/ne-water

Publishing support provided by the
Rolla Publishing Service Center

ISSN 2328-0328 (online)
https://doi.org/10.3133/sir20185106